Joseph Nkengele

Determination of Dogleg Severity and Side Force for Stuck Pipe Prevention

Master's thesis in Petroleum Engineering
Supervisor: Pål Skalle
August 2019

Master's thesis

■ NTNU

Norwegian University of Science and Technology

NTNU

Norwegian University of Science and Technology

Master's Thesis (TPG 4920)

On

Determination of Dogleg Severity and Side Force for Stuck Pipe Prevention.

Joseph Nkengele

Supervisor: Pål Skalle

Co-supervisors: Godwin Nsemwa & Fred Mkuyi

Abstract

A drill pipe is said to get stuck if it cannot be pulled out of the hole without damaging it and exceeding the maximum allowable hook load. Stuck pipe results from various causes such as excessive dogleg severity (DLS) and side force (SF). Dogleg severity refers to the measure of change of inclination and or direction of the borehole expressed in degrees per 30 meters of course length. When the DLS increases the wellbore becomes tight and may create keyseats which result into high side forces on the drill string during tripping operation. The stuck pipe incidence interferes with drilling schedule and results in non-productive time (NPT) and added drilling and rig cost.

The main objective of the present work was to create a Matrix Laboratory (MATLAB) data agent that was used to calculate and give report whenever allowable limit of DLS and side force is exceeded. This was necessary for minimization of the possibility of stuck pipe incidence during tripping operation. The objective was met by selecting mathematical models from literatures based on their accuracy and usability. The models were incorporated with the real time drilling data (RTDD) and survey data using the data agent generated to perform computations of DLS and side force. The outputs were then validated using the base case data given.

It was generally observed that the data agent generated performed well and from the computations it was seen that the highest value of DLS by the model was 7. 7 ^{o}/ 30 m seen from 34/10-C-47 wellbore at around 3556 mMD. This value deviated for more than 156 % from the recommended and allowable value of DLS. The maximum value of computed side force was 1.3 ton observed at 3788 mMD of the 34/10-C-47 wellbore. This force was seen to increase by 30% of the recommended and acceptable value.

The present work was very significant because it produced data agent using MATLAB that was used to compute DLS and side force, this agent was also used to locate the areas in the well with acceptable and non-acceptable DLS and side force. However, the model selected for calculation of side force was not realistically validated due to lack of effective and efficient side force base case data. The main recommendation on the work was to make an improvement of the model used to compute DLS by considering the effect of survey interval between two points. This can be done by including a specific scale factor for taking into account such an effect

Dedication

I dedicate this work to my family, relatives and friends for their strong support towards completion of this thesis.

Acknowledgement

Table of Contents

1 Introduction

Doglegs are common in wellbores. They are in general a threat to drillers as some of them are difficult to avoid and to resolve. Excessive doglegs have a great influence on occurrence of wellbore troubles such as mechanical stuck pipe. This is because, high doglegs pose difficulty in tripping and running casing or liner (Brechan, et al., 2017). This problem results from generation of keyseats that impose strong bending, compressional and friction forces on drill string during tripping.

1.1 Problem description

Stuck pipe is one of the major problems while drilling, that interferes with the drilling schedule. This results into non-productive time (NPT) and added drilling and rig cost worldwide. Muqeem, et al., (2012) claim that stuck pipe contributes about 25% of total NPT. Moreover Bailey, et al., (1991) stipulate that, stuck pipe costs the oil industry between $200 and $500 million each year and it occurs in every 15% of the wells drilled. An investigation done by Brechan, et al., (2017) showed that the root cause of stuck pipe used to be 65% due to planning, 25% operational errors and 10% other. The main cause of stuck pipe focused on in this work is keyseating as a result of poor minimization of doglegs resulting into high side force, torque and drag as well.

1.2 State-of-the-art

Principally and most often, best practice is the most likely applied strategy in different parts of the world to mitigate stuck pipe incidences. In most cases proper planning and training on the problem has reduced NPT. Muqeem, et al., (2012) stipulate that, the best practices include documentations that express how to prevent stuck pipe incidents pertaining to drilling, mud rheology, tripping, well path trajectory, torque and drag as well as hole cleaning and casing wear. Therefore, reduction of stuck pipe requires close monitoring of early warning signs such as: increased torque and drag, excessive cuttings loading and loss of circulation during drilling.

The strategy used in this work was to monitor DLS and side force by generating a data agent that was used to calculate and give report whenever allowable limit of DLS and side force is exceeded.

1.3 Objectives

The main objective of this work was to prevent the possibility of stuck pipe in wellbores by creating a Matrix Laboratory (MATLAB) data agent that was used to calculate and give report whenever allowable limit of DLS and side force is exceeded. It was supported by specific objective, which was to select DLS and side force mathematical models that were incorporated with the RTDD and survey data using the data agent generated for computations of DLS and side force.

1.4 Approach to meet the objectives

The objectives set up were achieved through the following stepwise approaches, that were followed based on the structure of this project.

i.   Learning from previous experience on doglegs and its consequences particularly stuck pipe by studying related previous literatures

ii.   Selection of mathematical models to calculate both DLS and side forces

iii. Implementation of the models using MATLAB data agents by incorporating the RTDD and survey data

iv.   Use of different base case data particularly real time drill data (RTDD) and survey data to test the models selected and data agent generated

v.   Validation of results; to check obtained result against base case data to verify

2 Literature Review

This chapter lies on presentation of relevant information required to meet the objectives of this work. The chapter consists of studies from previous experience or relevant published literature and summary of comments from the review.

2.1 Previous experience and relevant published literature

The most focused literatures reviewed were based on doglegs, side force and their consequences in inclined wellbores. The main consequence that is stuck pipe is also presented in this chapter. A summary of all literatures reviewed has been presented in Table 2.1. From that table, the study was divided into two parts; part A as primary and part B as secondary. The primary study (part A) focused mainly on inclined wellbore, dogleg (DLS) and side force, while the secondary study (part B) was presented for related literatures.

Table 2-1: Comments from the literatures and details of prioritized references

Author(s)	Title	Part	Relevance
(Menand, Mills, & Suarez, 2016)	Micro Dogleg Detection with Continuous Inclination Measurements and Advanced BHA Modeling	A	Most relevant
(Gaynor, Hamer, Chen, & Stuart, 2002)	Quantifying Tortuosities by Friction Factors in Torque and Drag Model	A	Most relevant
(Bang, Jegbefume, Ledroz, & Thompson, 2015)	Wellbore Tortuosity Analysed by a Novel Method May Help to Improve Drilling, Completion, and Production Operations	A	Most relevant
(Gaynor, Chen, Stuart, & Comeaux, 2001)	Tortuosity versus Micro-Tortuosity - Why Little Things Mean a Lot	A	Most relevant
(Gharib & Kirkhope, 2017)	A Modified Three-Point Contact Approach for Dogleg Severity Modeling	A	Most relevant
(Brechan, Corina, Gjersvik, Sangesland, & Skalle, 2017)	Compendium; TPG4215 Drilling Engineering, Drilling, Completion, Intervention and P&A –design and operations	A	Most relevant
(Muqeem, et al., 2012)	Stuck Pipe Best Practices - A Challenging Approach to Reducing Stuck Pipe Costs	B	Medium relevant
(Hess, 2016)	Pipe Sticking Prediction Using LWD Real-Time Measurements	B	Medium relevant
(Aadnoy, Larsen, & Berg, 1999)	Analysis of Stuck Pipe in Deviated Boreholes	B	Medium relevant

(Salminen, Cheatham, Smith, & Valiulin, 2016)	Stuck Pipe Prediction Using Automated Real-Time Modeling and Data Analysis	B	Least relevant
(Ahmed A. Elgibaly, 2016)	A study of friction factor model for directional wells	B	Most relevant

2.2 Comments from literatures

Based on the comments from the literatures and their applicability on this work, further presentation was done as per following focal points;

- Doglegs in inclined wellbores.
    - o Causes of doglegs.
    - o Quantification of doglegs.
    - o Consequences of doglegs
- Side force in inclined wellbore
    - o Causes of side force.
    - o Quantification of side force.
    - o Consequences of side force.
- Maximum allowable DLS and side force
- Stuck pipe in inclined wellbores
- MATLAB data agents
- Testing of data agents

2.2.1 Doglegs and dogleg severity in inclined wellbores

Doglegs

Doglegs refer to a more rapid change of direction of the trajectory of the wellbore than anticipated or desired. This change can either be intentional or non-intentional, the non-intentional deviations can lead to drilling problems such as stuck pipe. This change of wellbore trajectory is due to tendency of the drill bit to walk away from the desired well path, as seen in figure 2-1. The departure of the drill bit from the planned wellbore trajectory can be due to the combination of effects from the following factors;

- Heterogeneous nature of the formation and dip angle

- Drill string characteristics and dynamic behavior

- Applied WOB

- Hydraulics at the bit

- Improper hole cleaning

- Drill bit type and basic mechanical and hydraulic design
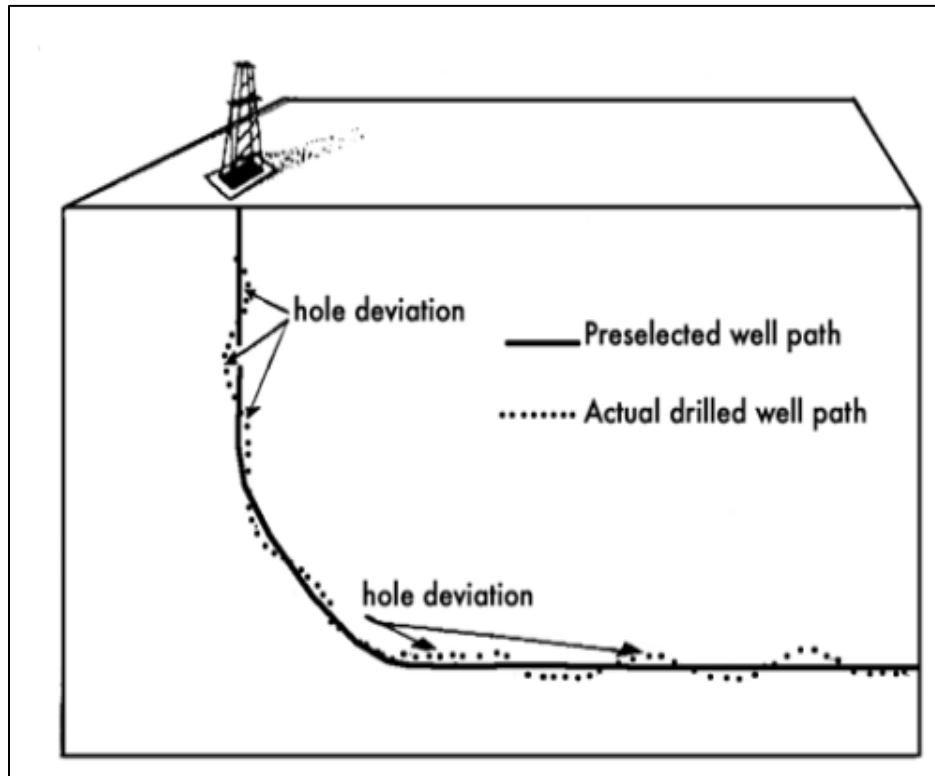
Figure 2-1: Wellbore deviation from planned trajectory (Mitchell, 2006)

Dogleg severity (DLS)

Dogleg severity refers to the measure of change of inclination and or direction of the borehole expressed in degrees per 100 ft of course length (oil field units) or 30 m of course length (metric units). The knowledge of DLS can be used to estimate/predict; stress fatigue in drill pipe (DP), casing wear and casing design loads, and stuck pipe. The DLS can be classified basing on the path angle, Skalle, (2018) grouped DLS severity into light, medium and severe as seen in Table 2-2

Table 2-2: Classification of DLS (Skalle, P. 2018)

DLS (deg/30 m)	Implication
Change in PA < 1	Light DLS
1 < Change in PA < 2	Medium DLS
Change in PA > 3	Severe DLS

According Eastman Oil Well Co.'s, the wellbore curvature of DLS less than 3 º/30 m never causes any problem (Lubinski, 1960). Severe DLS (greater than 3 º/30 m) cause effect and problems during drilling, completion and production phase of the wellbore thus reducing the drilling efficiency.

From the article presented by Schlumberger, (2018) on their website, the consequences of excessive doglegs result into;

- Improper wellbore location as per plan.
- Planned casing string may no longer easily fit through the curved section.
- Repeated abrasion by the drill string in a location of the dogleg results in a worn spot called a keyseat, in which the bottom hole assembly components may become stuck during tripping.
- Casing successfully cemented through the dogleg may wear unusually quickly due to higher contact forces between the drill string and the inner diameter (ID) of the casing through the dogleg.
- Increase the overall friction to the drill string, that can result into increasing the likelihood of getting stuck or not reaching the planned total depth.
- Possibility that a planned casing string may no longer easily fit through the curved section.

These problems are manageable and the mostly used remedial actions are reaming or underreaming through the dogleg, or even sidetracking in extreme situations.

Quantification of doglegseverity

From the literatures reviewed, there are several mathematical models that are used to calculate and quantify DLS. Every model is used by the author basing on the available data (inputs) to the model in order to comply with the functionality, reliability and usability of the model selected. Some of the models prioritized are shown in the lists below.

- Radius of curvature method as presented by Drilling Templates, (2015)

$$DLS = 100\sqrt{a^2 \sin^2 \phi + b^2} \qquad (2-1)$$

Where a = rate of change in direction angle in degrees/ft

　　b = rate of change in inclination angle in degrees/ft

　　ϕ = inclination angle in degrees

- Model presented by Choudhany, (2011)

$$DLS = \frac{100}{\Delta MD} \cos^{-1}\{(sinI_1 sinI_2)[(sinA_1 sinA_2) + (cosA_1 cosA_2) + (cosI_1 cosI_2)]\} \qquad (2-2)$$

　　Where ΔMD = Change in measured depth

　　$I_1 \& I_2$ = Inclination in degrees

　　$A_1 \& A_2$ = Azimuth in degrees

- Another model, presented by Brechan, et al., (2017) is as shown in equation 2-3

$$DLS = \frac{\phi \; x \; 30}{CL} \qquad (2-3)$$

- Furthermore, another equation wad developed by Lubinski, (1960)

$$DLS = \frac{2}{L_2 - L_1} \sin^{-1}\sqrt{\sin^2(\frac{A_2 - A_1}{2}) \sin(I_1) \sin(I_2) + \sin^2(\frac{I_2 - I_1}{2})} \qquad (2-4)$$

Referring to the functionality, reliability and usability of the models to this thesis, the model presented by Brechan, et al., (2017) is selected and used in the present work. This model is very simple to implement, and it very accurate compared to other survey methods. It will in this case be used for estimation of DLS in this work. The details of this model are presented in chapter 3.

2.2.2   Side force in inclined wellbores

Side force is normal force acting laterally on the drill string as the result of either compression, tension or bending of the drill pipe (DP) as portrayed in figure 2-2. In inclined wellbores the side force is common in sections with build up or drop off situation. Side force is caused by either a dogleg in the bore hole, buckling of the bottom hole assembly (BHA), centrifugal orbiting the

BHA, or the inclination of the bore hole. If the tool joint is within a dogleg, then the lateral load will be concentrated at the tool joint and the drill pipe will not contact the wall (Brechan, et al., 2017).

The side force can cause different incidences during drilling, some of these problems are;

- Stuck pipe
- Wearing of tool joint and drill pipe
- Keyseats in the well wall
- Grooves in the casing made by tool joint during tripping (Arthur, 1961)
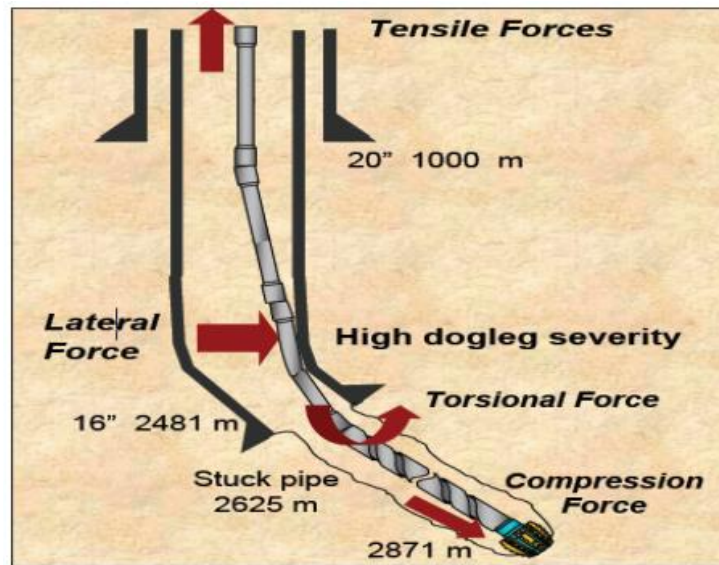
Figure 2-2: Side/lateral force acting on DP in inclined well (Asadi, et al., 2011)

List of prioritized models to quantify side forces

The authors have presented a number of models to estimate side force, the prioritized models are listed below

- The model by Ansari, (2018).

$$\boldsymbol{S_F = T sin\phi} \qquad\qquad (2-5)$$

where S_F is the side force (N), T is the tension (N) in the drill string just above the key-seat area, and ϕ is the dogleg angle in degrees.

- The model by Brechan, et al., (2017)

$$S_F = 2W_{DP-String} \sin\left(DLS * \frac{S}{2}\right) \qquad (2-5)$$

where S_F is the side force (N), $W_{DP-String}$ is the average buoyed weight of the drill string in the center of the dogleg (N), DLS is the dogleg severity (º/m) and S is the length of the dogleg or course length (m).

- Another model is presented by the same authors Brechan, et al., (2017). This model computes side force by considering the effect of inclination of the wellbore

$$S_F = BW\sin(I) \qquad (2-6)$$

From the model above, S_F is the side force (lbs), BW is linear buoyed weigh of tubular DP (ppf) and I is the inclination of the well (º)

The model in equation 2-6 is accepted and used to estimate the side force in this work. More explanations are presented in chapter 3.

2.3 Maximum allowable DLS and side force

There are many researches and surveys done by different oil and gas companies to analyze the maximum allowable DLS and side force. Eastman Oil Well Survey Co. is one of the companies that experienced that, hole curvature of less than 3º / 100 ft (30 m) never cause any trouble during drilling (Arthur, 1961)

It is difficult to assign maximum allowable side force since, the quantity of force depends on different factors such as abrasiveness of the borehole wall, abrasiveness of the tool joint surface, drilling rate and number of round trips (Arthur, 1961). Under assumptions and neglection of these factors, the side force of 2000 lbs causes no harm to both tool joint and wellbore wall Brechan, et al., (2017).

2.4 Stuck pipe in inclined wellbores

Various studies indicate that stuck pipe occurs in every 15% of the wells drilled worldwide. DP is said to get stuck if it cannot be pulled out of the hole without damaging it and exceeding the maximum allowable hook load. There are generally two kinds of stuck pipe namely, mechanical

pipe sticking and differential pressure sticking. Mechanical pipe sticking is the one that is highly addressed in the present work.

2.4.1.1 Mechanical stuck pipe

An investigation done by Brechan…et al (2017), showed that the general root cause of stuck pipe used to be 65% due to planning, 25% operational errors and 10% other reasons. These causes can individually produce a noticeable effect in inclined boreholes. According to Mitchell (2006) the most common causes of mechanical stuck pipe are;

- Inadequate removal of drilling cuttings from the annulus
- Borehole instabilities
- Key seating

Inadequate removal of drilling cuttings from the annulus: Excessive drilled cuttings in the annulus results into settling of a large number of suspended cuttings to the bottom. These cuttings can park off the BHA or DP on the low side of the wellbore, thus leading into stuck pipe is indicated in figure 2-3.
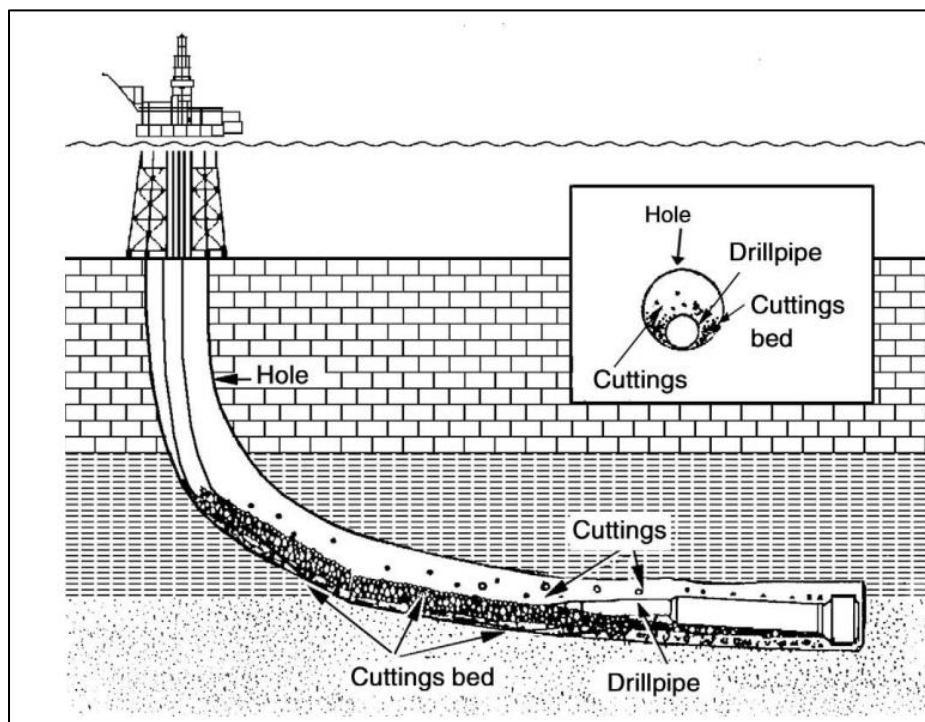
Figure 2-3: Cutting build up in directional wells (Mitchell, 2006)

Borehole instability: This happen mostly in shale formations, basing on the physical and chemical properties of the drilling mud, shales can slough or plastically flow inward therefore causing pipe sticking as shown in figure 2-4.
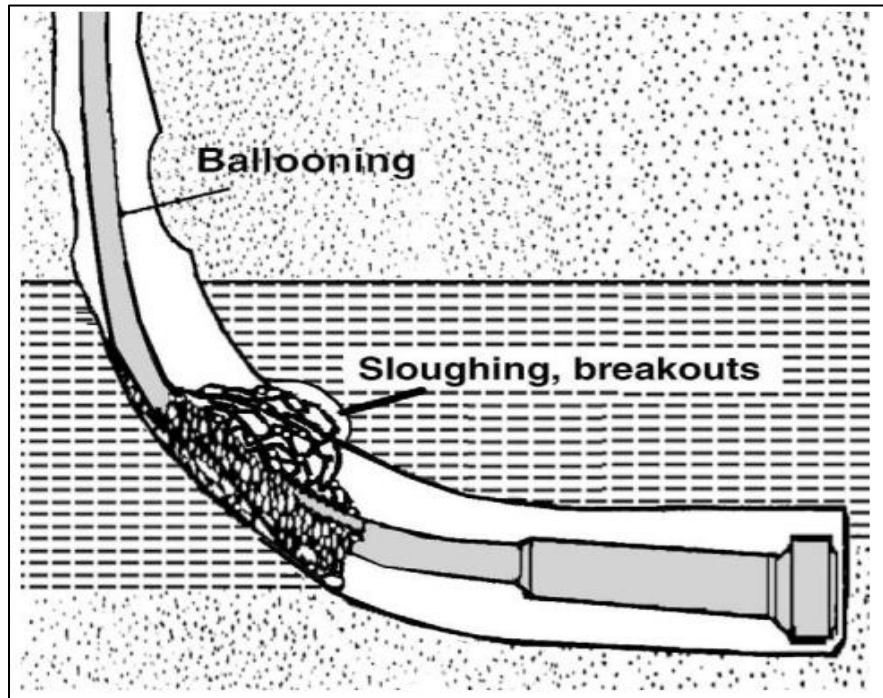
Figure 2-4: Pipe sticking caused by wellbore instability (Mitchell, 2006)

Keyseating: According to Mitchell, (2006) key seating is a major cause of mechanical pipe sticking. The mechanics of key seating involve wearing a small hole (groove) into the side (wall) of a bore hole. This groove is caused by the drill string rotation with side force acting on it as shown in figure 2-5. This condition is created in doglegs or in undetected ledges near the washouts.
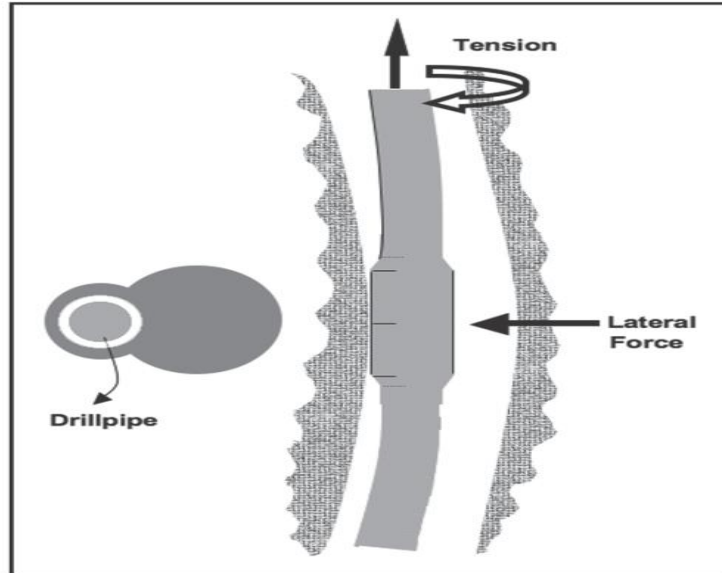
Figure 2-5: Pipe sticking due to keyseating (Azar, et al., 2007)

Effects of stuck pipe

The stuck pipe as one of the major problems while drilling, interferes with the drilling schedule and results in non-productive time and added cost worldwide. Muqeem, et al., (2012) claim that stuck pipe contributes about 25% of total NPT. Moreover Bailey, et al., (1991) stipulate that, stuck pipe costs the oil industry between $200 and $500 million each year. Most of these costs are; recovery costs, replacement costs and additional rig time costs.

Quantification of stuck pipe

The stuck pipe in inclined wellbore is always accessed basing on variation of the following drilling parameters:

- Torque
- Hook load
- Standpipe pressure
- Drill rate

From the parameters above, there is a minimum acceptable value for indication of stuck pipe (Salminen, et al., 2016). In general, stuck pipe in inclined wellbore is associated with drilling problems, Baker, (1995) shows some of the drilling problems and indicators of stuck pipe as presented in table 2-3.

Table 2-3: Stuck pipe problems and indicators (Hughes, 1995)

Indicator Problem	Torque	Pressure	Drill rate
Poor hole cleaning	Increase	Increase	Gradual increase
High overbalance	Gradual increase	No change	Gradual increase
Mobile formation	Gradual increase	Increase	Gradual increase
Fractured and faulted formation	Sudden erratic increase	May be unaffected	Sudden increase
Geo- pressured formation	Increase	Increase	Initial increase with gradual decrease
Reactive formation	Gradual increase	Increase	Gradual decrease
Unconsolidated formation	Increase	Increase	Decrease
Junk	Sudden increase	No change	Sudden decrease
Cement blocks	Sudden increase	No change	Sudden decrease

2.5 Data agents

A data agent is a computer program that collects information or performs a task in the background at a specific schedule (Techopedia, 2019). The term data agent is often thought of as a software abstraction that can act with a certain degree of autonomy to perform a particular task on behalf of the user. Any potential data agent should be effective, efficient and transparent. Example of such software are MATLAB and Microsoft Excel. These software agents offer many benefits to end users by performing complex and repetitive tasks. The agents are applied by making specific codes that traverse data sources and process them in the background as shown in figure 2-6.

Characteristics of data agents

- Self-contained software, and should act as a representative of something or someone
- Must be goal oriented
- Relatively not dependent or autonomy
- Able to communicate with agents, systems or human for its assigned tasks
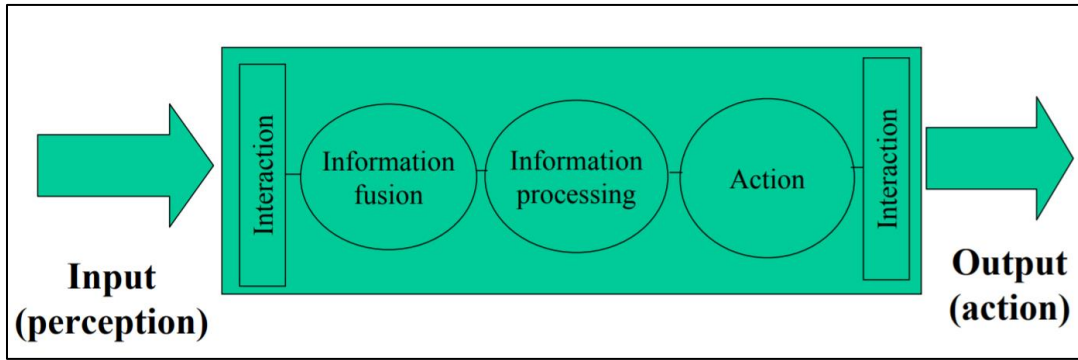- Can interact with other data sources as shown in figure 2-6.

Figure 2-6: A flow sheet showing the interaction of data agent with data sources (Tony, 1999)

3   Methodology of DLS and side force determination

3.1   Hypothesis

The method selected for detecting and preventing stuck pipe during tripping is determination of doglegs and the associated side force. The idea was accomplished by developing models for calculation of these parameters, then implementing the models by constructing data agent using MATLAB. The details of these models are presented from section 3.1.1.

3.1.1   Theoretical determination of DLS and side forces

DLS is determined from the dogleg, the latter is measured using either continuous surveying or computer modelling. The continuous surveying involves measurement while drilling (MWD) done by downhole measuring tools while computer modelling involves analysis of post-drilling data using computer software. In this chapter the idea was to determine the angular deviation of the wellbore from the planned wellbore trajectory as visualized in figure 3-1. The deviations are equivalent to doglegs from which DLS is determined. The doglegs obtained are be used to assess the side force acting on the tool joints of the drill string. This is done basing on the following steps;

- Select, present and explain the model.
- Compute the models using data agent generated by MATLAB.
- Apply a standard input base case data (the RTDD and survey data) to validate the models.
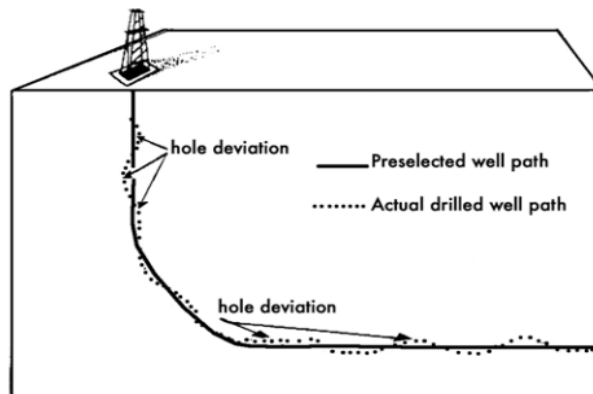

Figure 3-1: A three-dimension representation of deviated wellbore (Mitchell, 2006)

3.2   Development of method

The methodology used based on selection of already existing models as reviewed in chapter 2. The selection focused on the simple models that are easy to implement using existing and affordable software.

3.2.1   Selection of model for projection of the wellbore

Before calculation of DLS, it was important to limit the view of the wellbore into plan view, vertical view and 3D view. These views are very important to present the nature of the profile and direction of the well thus calculation of DLS.

The model used here was adopted from the minimum of curvature survey method as presented in the compendium on Drilling, Completion, Intervention and P&A –design and operations by Bjørn, et al., (2017).

3.2.1.1   Details of the model

Minimum of curvature survey method is the method that is used to calculate the position of a given point of the wellbore in terms of easting, northing and TVD as indicated in figure 3-2. The method resulted from an improvement done to the balanced tangential method by replacing the straight line with an arc. This is only possible by applying the ratio factor *(F)* to correct two tangent lines that are bending. The equations for computation of change in TVD, easting and northing for location of a point on a wellbore are presented from equation 3-1 to 3-3 below. The equation for computation of the ratio factor *(F)* and dogleg angle *(φ)* are shown in equations 3-7 and 3-5 respectively.

$$\Delta TVD = \frac{F.CL}{2}(cos\alpha_n + cos\alpha_{n+1}) \qquad\qquad (3-1)$$

$$\Delta N = \frac{F.CL}{2}(sin\alpha_n cos\beta_n + sin\alpha_{n+1}cos\beta_{n+1}) \qquad\qquad (3-2)$$

$$\Delta E = \frac{F.CL}{2}(sin\alpha_n sin\beta_n + sin\alpha_{n+1}sin\beta_{n+1}) \qquad\qquad (3-3)$$

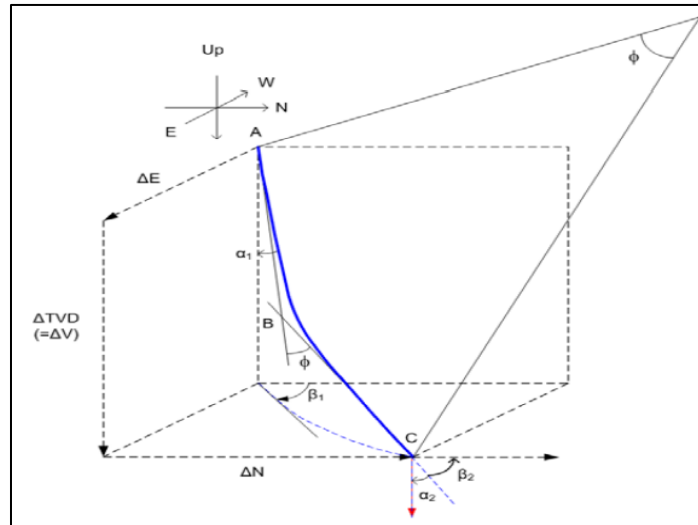$$where\ n = \ 1,2,3 \,...(survey\ measurement\ points)$$

Figure 3-2: Positioning a point of the wellbore by minimum Curvature Wellbore Survey Method (Brechan, et al., 2017)

3.2.2 Selection of DLS mathematical model

Dogleg severity (DLS) refers to the measure of change of inclination or azimuth, mostly expressed in degrees per 100 ft. or 30 m of course length (CL). The DLS describes the smoothness and curvature of the wellbore, it is therefore responsible for side forces such as bending forces to act on the drill string. Most of directional wells are not as smooth as planned, some contain crookedness that are serious to cause drilling problems such as stuck pipe during tripping.

The suggested model to calculate DLS was adopted from the compendium on Drilling, Completion, Intervention and P&A –design and operations by (Brechan, et al., 2017). This method was selected because of its simplicity to implement, and its accuracy as compared to other methods.

3.2.2.1 Details of the DLS model

Even though, most of directional drillers need not perform manual survey calculations due to presence of many software such as COMPASS, WELL PATH, WIN SERVE, mathematical modelling of DLS is important for wellbore planning. The DLS model is used to control the wellbore trajectory, it can also be used to assess the side force in wellbore walls. Based on figure 3-2, doglegs is expressed deviation of inclination, this deviation is then used calculate DLS as it is in equation 3-4

$$DLS = \frac{\phi \, x \, 30}{CL} \qquad\qquad (3-4)$$

3.2.2.1.1 Input parameters of the selected DLS model

i. Dogleg angle (ϕ)

Dogleg angle obtained depends factors such as dip angle, strike, hole inclination, gauge of hole, bit type and length, weight on bit and bottom hole assembly. The dogleg is calculated using a mathematical equation presented in equation 3-5. The equation calculates dogleg by using the current inclination and azimuth at survey point *n* and next inclination and azimuth at survey point *n+1*.

$$\phi = cos^{-1}[cos\alpha_n \, cos\alpha_{n+1} + sin\alpha_n sin\alpha_{n+1} cos(\beta_{n+1} - \beta_n)] \qquad (3-5)$$

$$where \; n = \; 1, 2, 3 \; ...(survey \; measurement \; points)$$

ii. Course length (CL)

Course length is the length of the curved part of the wellbore presented as the difference in measured depth. Basing on figure 3-3, CL is represented by the length of wellbore curve DC. The CL is mathematically obtained by taking the difference of measured depth between two survey points as shown in equation 3-6.

$$CL = DMEA_{n+1} - DMEA_n \qquad\qquad (3-6)$$

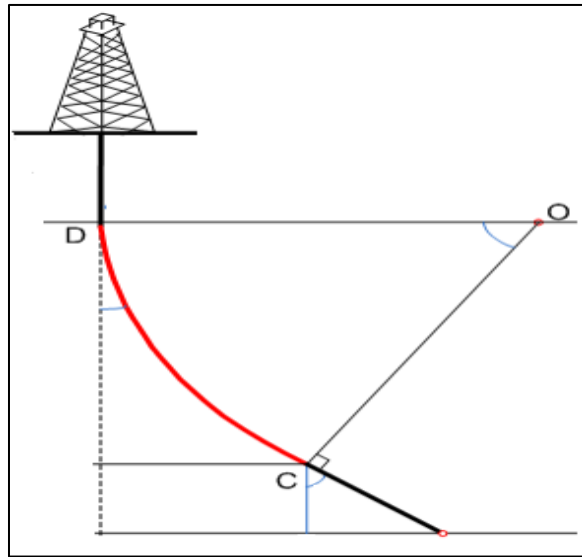$$where \; n = \; 1, 2, 3 \; ...(survey \; measurement \; points)$$

Figure 3-3: Course Length (CL) (Brechan, et al., 2017)

3.2.2.1.2 Assumptions of the model selected

Based on the compendium by Bjørn, et al., (2017), the main assumption upon application of the minimum of curvature survey method is that; two successive survey stations lie on a smooth circular arc by using the angles measured. The arc is obtained by applying the ratio factor (F) to the balanced tangential survey method. The ratio factor (F) is calculated using equation 3-7.

$$F = \frac{2}{\phi}\left(\frac{180}{\pi}\right)\tan\left(\frac{\phi}{2}\right) \qquad\qquad (3-7)$$

3.2.3 Selection of side force model

Side force refers to normal force acting laterally on the drill string as the result of either compression, tension or bending of the drill string. The force acts on the drill string that is in contact with the well wall as seen in figure 3-4. This force is common in inclined wellbores with build up or drop off situation. It is caused by either doglegs, buckling of BHA, centrifugal orbiting of the BHA, or the inclination of the bore hole (Brechan, et al., 2017). When dogleg and crookedness increase the wellbore become tight and may create keyseats which result into high side force on the drill string particularly the tool joint as indicated in figure 3-4. High side forces on the other side, contribute to sticking of the pipe during tripping. The wall force caused by inclination was computed using the mathematical model in equation 3-5 adopted from Brechan…et al (2017).

In this work, the idea was to compute side force from inclinations and evaluate string tension from side force and friction coefficient. The computation began from the BHA towards the subintervals based on the following procedures:

- The wellbore distance was divided into subintervals starting from the bottom and estimate the azimuth and inclination at each subinterval

- Buoyed weight of string was computed at each subinterval

- Side force was computed at each interval

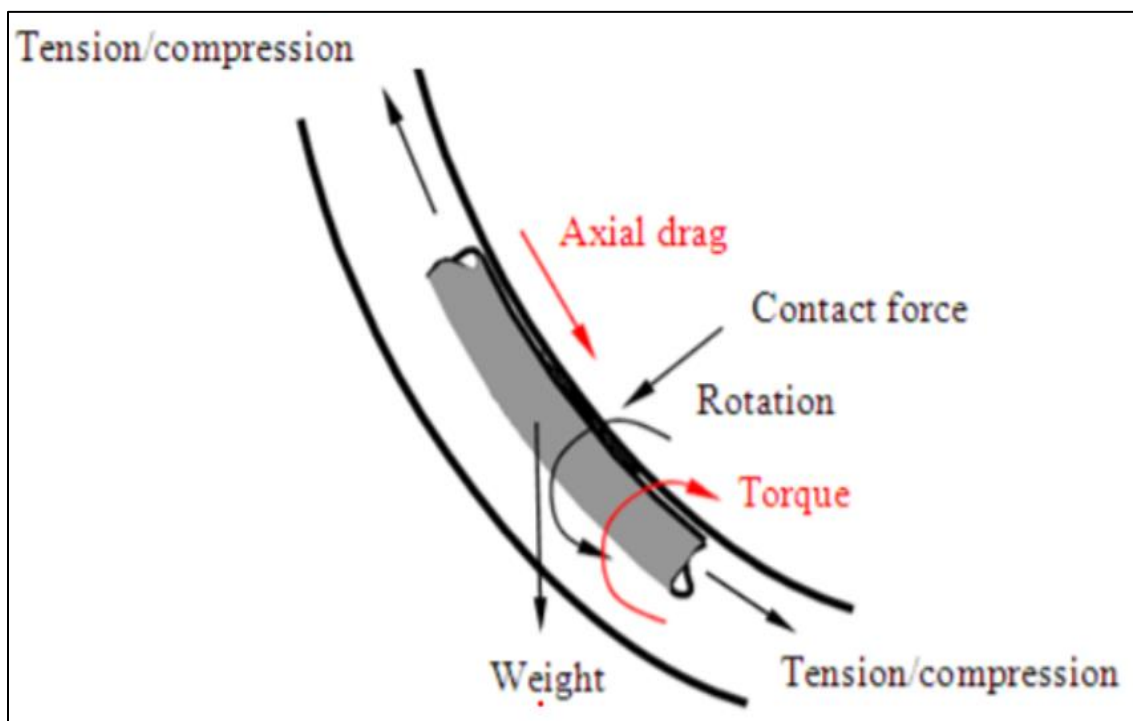- The computed side force and coefficient of friction was used to estimate string tension at each subinterval

Figure 3-4: Forces acting on an element of the drill string including the side force (Andrew, et al., 2011)

3.2.3.1   Details of the model

The model for side force that acts on the drill string in inclined wellbores is adopted from Brechan…et al (2017) as presented in equation 3-5.

Assuming that, the tool joint is within a dogleg, then the side force is much concentrated on the tool joint compared to any other part of the DS. Basing on this assumption, the side force was estimated at the tool joints in the DS. It was therefore computed beginning from the last well section (section 8.5'') provided in the RTDD.

$$S_F = BW \sin (I) \qquad\qquad (3-5)$$

where S_F is the side force (ton), BW is the average buoyed weight of the drill string in the center of the dogleg (kg), and I is the well inclination (^{0}).

3.2.3.1.1   Derivation of side force and evaluation of string tension in a drill string

Decomposition of buoyed weight into two components

Side force is equivalent to normal force acting on the inclined plane. The normal force is a product of the buoyed weight of the drill string *(BW)* and average inclination between the first and last point of the subsection *(I)* as seen in figure 3-4. String tension results from of frictional forces caused by side forces along the wellbore. It is mathematically calculated from side force and coefficient of friction as shown in equation 3-11 to 3-15. The coefficient of friction is the factor for taking the smoothness of contact surface between the drill string and drill hole with unknown cuttings bed packing. This factor has been reported in the range of 0.24 to 0.28 by North Sea operators Softdrill, (2018).
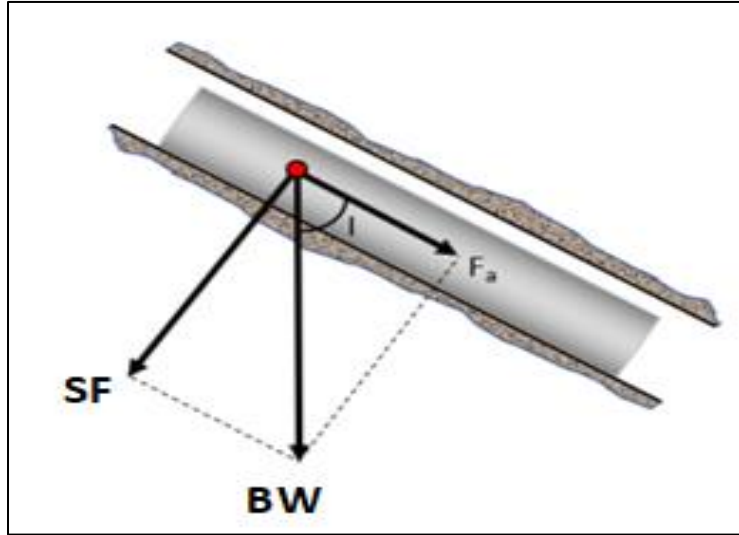
Figure 3-4: Resolution of buoyed weight of the drill string into two components as modified from Softdrill, (2018)

From figure 3-4 above, the two components of the buoyed weight *(BW)* of the drill string were represented by equations 3-6 and 3-7.

$$SF = BW sin(I) \qquad\qquad (3-6)$$

$$F_a = BW cos(I) \qquad\qquad (3-7)$$

Where

$$BW = BF * (Weight\ of\ DS\ at\ a\ particular\ subinterval) \qquad\qquad (3-8)$$

$$I = \frac{I_1 + I_2}{2} \qquad\qquad (3-9)$$

$$BF = 1 - \left(\frac{Mud\ Weight}{Density\ of\ steel}\right) \qquad\qquad (3-10)$$

Formula for computation of SF and string tension at subintervals

The plan behind computation of side force and string tension was to divide the drill string into subintervals (finite elements) of 500 m MD long and cumulative tension was calculated at the top of each subsection as depicted in the figure 3-5 below. The division was done just after the BHA and the formula used to calculate SF at each subinterval was adopted from equation 3-6.
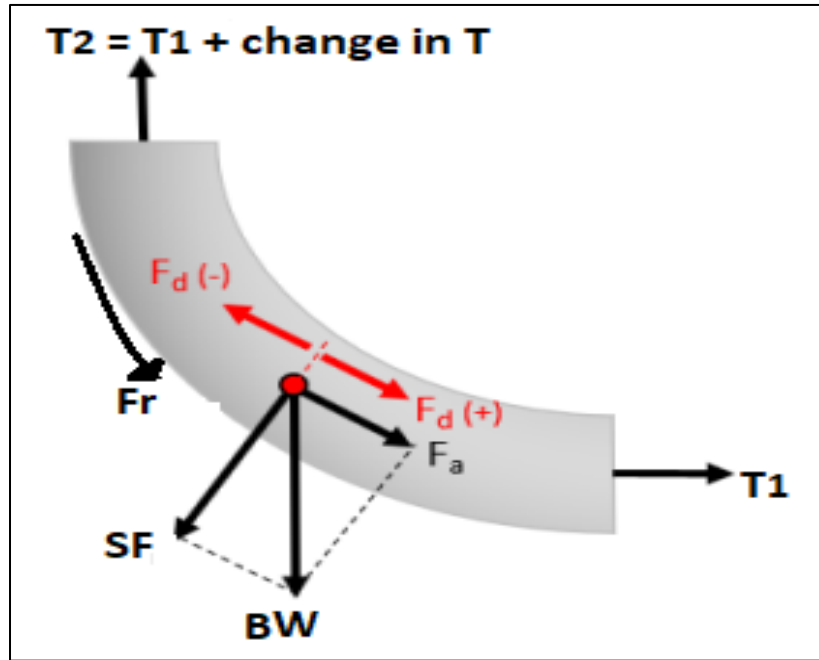
Figure 3-5: String tension and Side force on the subsection of the drill string in inclined wellbores as modified from Softdrill, (2018)

The string tension was calculated from the obtained side force and coefficient of friction as indicated from equation 3-11 to 3-15.

$$Fr = \mu . SF \qquad (3-11)$$

$$\Delta T = Fr + Fa \qquad (3-12)$$

$$\Delta T = \mu . SF + BW cos(I) \qquad (3-13)$$

$$T_2 = T_1 + \Delta T \qquad (3-14)$$

$$T_2 = T_1 \pm \mu . SF + BW cos(I) \qquad (3-15)$$

From equation 3-15, T_2 is string tension at the top of the subinterval, T_1 is string tension at the bottom of the subinterval, μ is the friction coefficient. The sign before μ is + (plus) for tripping out and - (minus) for tripping in of the drill string.

3.2.3.1.2 Input parameters of the model

In order to make relevancy assumptions, most of the input parameters were adopted from the end of well (EoW) reports, the main input parameters of this model were buoyed weight and well inclination. The details of the parameters were expressed below:

Buoyed weight (BW)*:* This is the average buoyed weight of the drill string at BHA and DP in the center of the dogleg. This value was computed at every subinterval starting with BHA followed by the DP at the subintervals.

Well inclination (I): The value of inclination used in this model was obtained from the plot of both azimuth and inclination against depth as shown in figure 3-5 and detailed in appendix C.
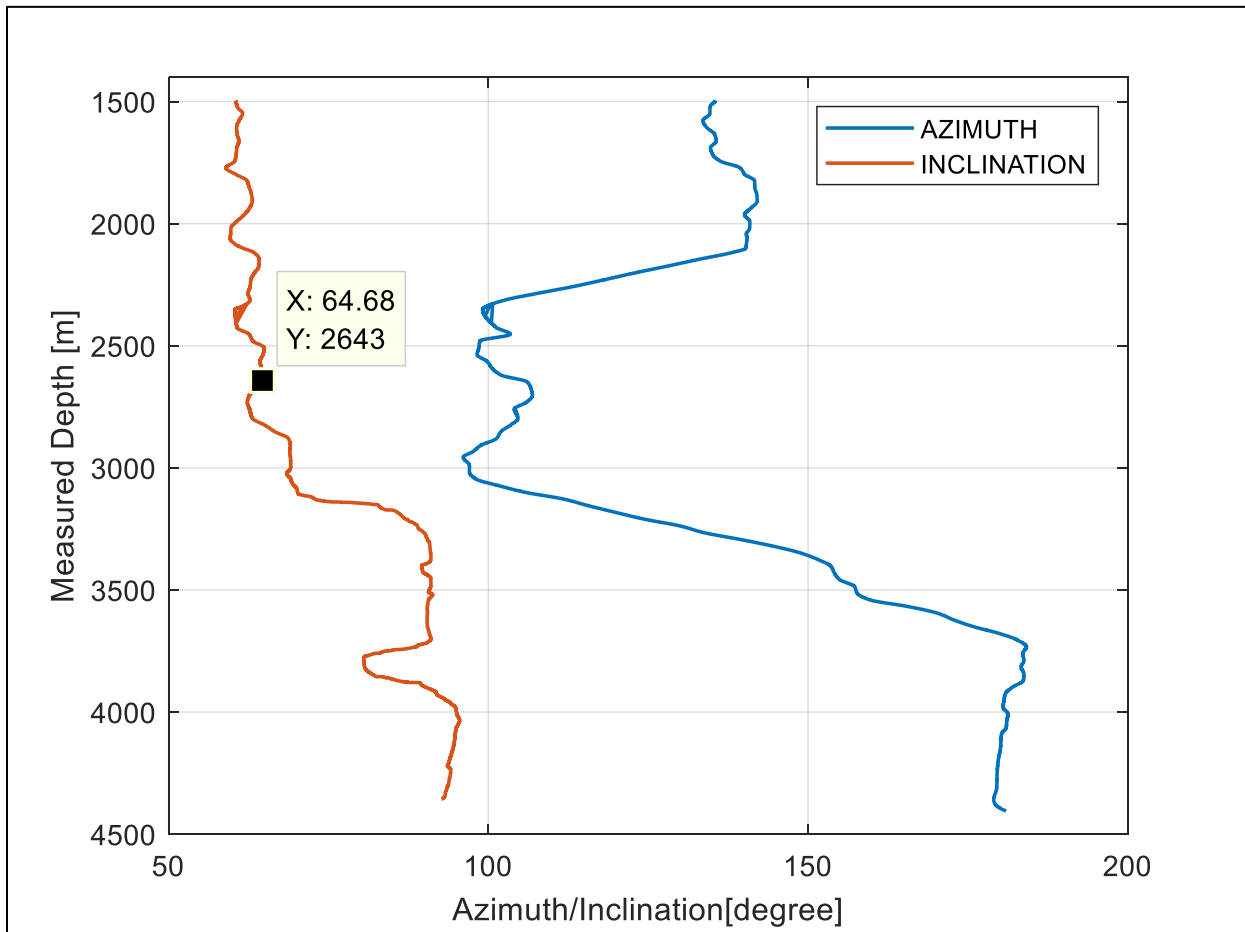

Figure 3-5: Estimated value of inclination as indicated by the yellowish square mark on the plot. The obtained value was used during computation of dogleg and side force

3.2.3.1.3 Evaluation of string tension from side force

The evaluation of string was done at every subinterval by using the computed side force and coefficient of friction as stipulated in equation 3-15. The computation was done by considering the contribution from the weight of DP on the subinterval and the BHA.

3.2.3.1.4 Assumptions used

Upon selection of this model, there are some assumptions that were adopted in order to put the model into physical applicability by focusing on the input parameters of the model. The assumptions adopted are such as;

- The only part of drill string that was under action of side force is tool joint
- The BHA and DP used in all sections of the wellbore were of similar specifications as shown in table 3-2
- The coefficient of friction of 0.24 adopted from Softdrill, (2018) was assumed and treated to be similar at cased and uncased sections of the wellbore
- Similar mud type and weight was used during drilling

3.3 Case Data

The process of implementation of the objective was done by relying on different data types. In this work there was a combination of various data that were used to formulate the base case. Although the number of data available was limited, and their quality was varying, these data were used to portray the overview of the drilling process and validate results from the selected models. Considering the usability and availability, the mostly used data were obtained from:

- RTDD
- Wellbore survey data
- Drill string parameters for side force calculation
- EoW reports
- Others such as NPD

3.3.1 RTDD and survey data

The RTDD and survey data used were obtained from two fields namely Gullfaks and Volve field as presented in detail in appendix E and figure 3-6 and 3-7 give the pictorial location of the fields. Basing on the available time, the data used in this work were from five wells namely 34/10-C-47, 15/9-F-4, 15/9-F-5, 15/9-F-11T2 and 15/9-F-12. Table 3-1 shows each detailed information of these wells.

Table 3-1: Wellbore information from NPD (Norwegian Petroleum Directorate, 2017)

Wellbore name	34/10-C-47	15/9-F-4	15/9-F-5	15/9-F-11T2	15/9-F-12
Type	Development	Development	Development	Development	Development
Purpose	Production	Injection	Injection	Observation	Production
Status	Closed	On	On	On	On
Multilateral	No	No	No	No	No
Main area	North Sea	North Sea	North Sea	North Sea	North Sea
Field	Gullfaks	Volve	Volve	Volve	Volve
Drilled in production licence	050	046 BS	046 BS	046 BS	046 BS
Drilling operator	Statoil ASA (Old)	Statoilhydro ASA	Statoilhydro ASA	Statoil Petroleum AS	Statoil ASA (Old)
Drilling facility	Gullfaks C	Mærsk Inspirer	Mærsk Inspirer	Mærsk Inspirer	Mærsk Inspirer
Production facility	Gullfaks C	Mærsk Inspirer	Mærsk Inspirer	Mærsk Inspirer	Mærsk Inspirer
Drilling days	109	51	22	67	75
Entered date	28.11.2005	13.10.2007	18/12/2007	07/03/2013	14/06/2007
Completed date	16.03.2006	09.03.2008	01.08.2008	05/12/2013	27/08/2007
Content	Oil	Water	Water	Oil	Oil
Discovery wellbore	No	No	No	No	No
Kelly bushing elevation [m]	84.0	54.0	54.0	54.9	54.0
Water depth [m]	217.0	91.0	91.0	91.0	91.0
Total depth (MD) [m RKB]	4399.0	3510.0	3792.0	4562.0	3520.0
NS degrees	61° 12' 54.94" N	58 ° 26 '29.72' N	58 ° 26 '29.66' N	58 ° 26 '29.96' N	58 ° 26 '30.17' N

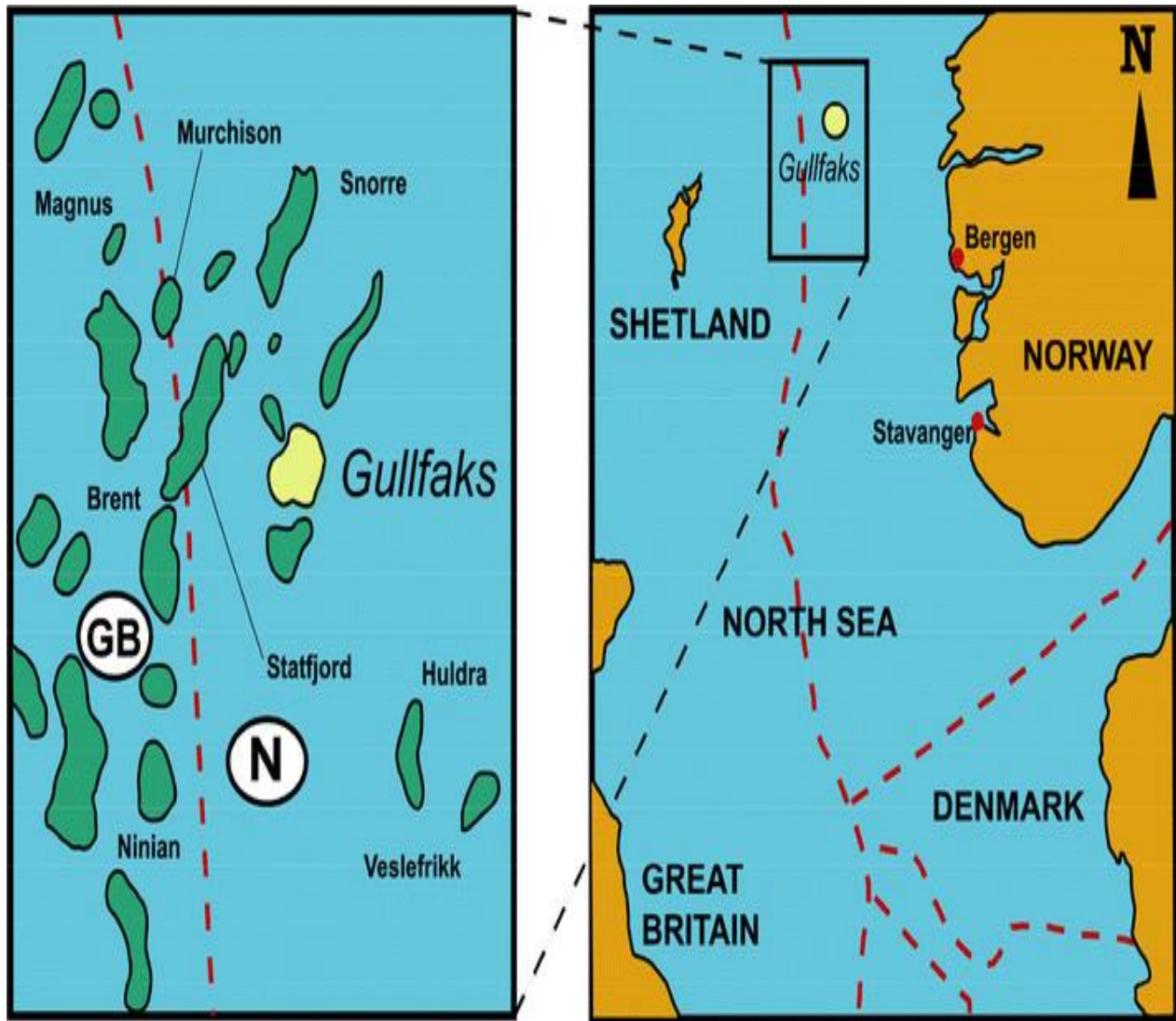| EW degrees	2° 16' 26.39" E	1 ° 53 '14.92' 'E	1 ° 53 '14.99' 'E	1 ° 53 '14.87' 'E	1 ° 53 '14.93' 'E
NS UTM [m]	6787142.43	6,478,560.84	6,478,558.97	6,478,568.28	6,478,574.75
EW UTM [m]	460998.13	435,049.84	435,050.94	435,049.15	435,050.23
UTM zone	31	31	31	31	31

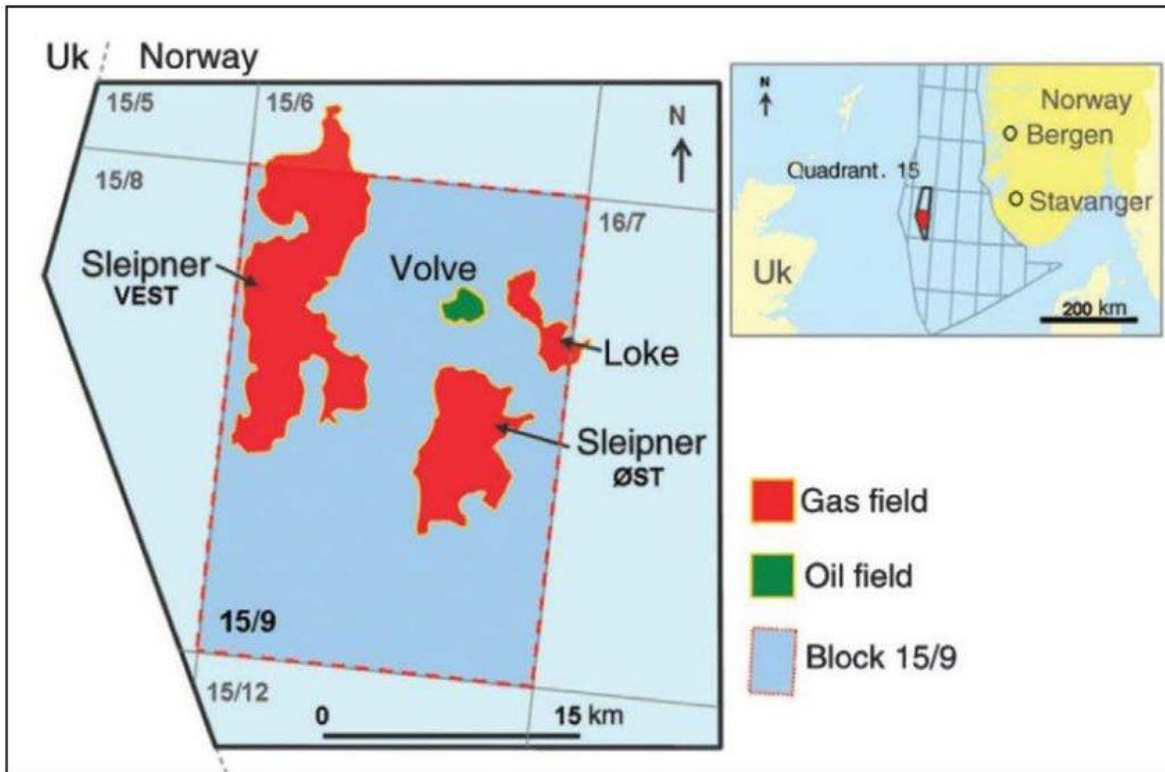**Figure 3-6: Location of Gullfaks field in North Sea (Arild, et al., 2000)**

Figure 3-7: Location of Volve field in North Sea (Ravasi et al., 2015)

3.3.2   Drill string (DS) parameters for side force and string tension calculation

The need of drill string parameters is very important when it comes to estimation of side force acting on the drill string in an inclined wellbore. In this work the most focused part of the drill string was the BHA and the DP, from this part it was assumed that the tool joint was within a dogleg. Therefore, side force was calculated using the components of the DS as presented in section 3.2.3.1. The types and lengths of the DS parameters were adopted by creating a case as adopted from the examination paper by (Tor & Sigbjørn, 2016). In this paper it was assumed that, after starting drilling at 8 1/2" section, a failure in the MWD tool package was developed. The work was to pull the drill string out of the hole to make repairs before continuing drilling. It was therefore required to estimate the associated side force and tension, so that the tension during tripping can be easily determined. These drill string parameters were presented in table 3-2.

Table 3-2: Drill string parameters used to estimate side force and string tension (Tor, et al., 2016)

Type	Length [m]	OD [inches]	ID [inches]	Average dry weight [lb/ft]	Average dry weight [kg/m]
DP S-135	NA	5.5	4.778	21.90	3.02
HWDP	60	5.5	3.25	60.00	8.28
DC	50	6.5	NA	90.60	12.50
PDM	7.5	6.5	NA	81.50	11.25
PDC bit	0.5	8.5	NA	120.00	16.56

3.3.3 EoW reports

The EoW report gives the final well report after drilling in real time. It may be treated as the main source of wellbore information because it consists of all essential details of the wellbore during and after drilling. From the data given, the EoW report included 34/10-C-47, 15/9-F-4, 15/9-F-5, 15/9-F-11T2 and 15/9-F-12 wellbore reports. The summary of the information given in each report is as listed below;

- General well data
- Exemption data
- Health, safety, environmental and quality
- Formation evaluation and activities evaluation

3.4 Results Validation Plan

Validation refers to the process of checking the accuracy of something to the user. In this thesis the validation is done to only two areas which are;

- Validation of selected DLS and side force models
- Validation of the data agent

3.4.1 Validating the models

In validating models, the most important item was to generate test cases to verify the design. This process also helps automate other verification tasks and streamlines the review process by linking test cases and verification objectives to high-level test requirements (Mathworks, 2019)

The validation process of models in this work was adopted from (Mathworks, 2019). It was presented in figure 3-7 and generally involves the following important procedures:

- Creating a model of system requirements for testing, as done in subchapter 3.2

- Generating test data from this requirements-model representation, as done in subchapter 3.3

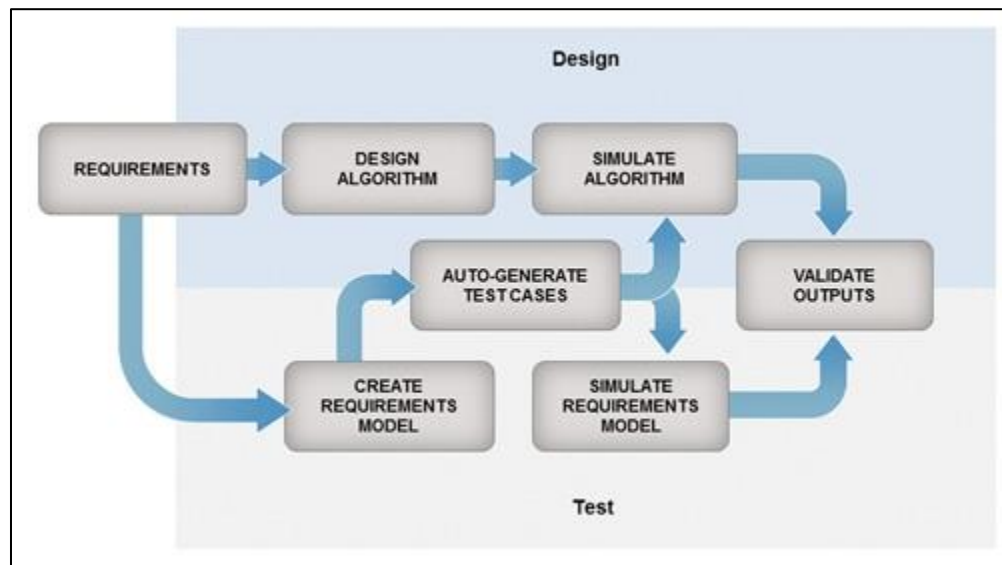- Verifying the models with generated test cases as done assessment of quality of model in chapter 5

Figure 3-8: Model-based testing and validating (Mathworks, 2019)

3.4.1.1   DLS model validation plan

In order to confirm that the selected DLS model meets the requirement needed, the main trick was to check estimated results against given case data. This was done by comparing results obtained from the selected model against results from case data provided. Moreover, results from the EoW reports were used to make verification of results from the selected models.

3.4.1.2   Side force validation plan

There is no any specific means of validating the side force during drilling operation. The possible and acceptable ways suggested could be to monitor the response of inclination, DLS, string tension and hook load (HKL) while pulling out of the wellbore. The side force is the function of DLS and hook load in the sense that, increase of side force results from increase of DLS.

3.5 Data agent testing plan

Data agent testing is defined as a process of executing a program to find errors, it is an important component of software quality assurance. The quality of the data agent/software is measured basing on the effectiveness, productivity, safety and satisfaction of the program (Botella, et al., 2004).

The ISO/IEC 9126 standard introduces and makes a distinction between internal quality and external quality of the software. The quality that can be measured during the development process are referred to as internal. The external quality can be measured during the testing process (Botella, et al., 2004) . The ISO/IEC 9126 standard further groups the external and internal quality of the model basing on their characteristics and sub-characteristics as indicated in table 3-3. This table was used to test the performance of the MATLAB data agents used.

Table 3-3: The ISO/IEC 9126 standard further groups the external and internal quality of the model

CHARACTERISTICS	SUB-CHARACTERISTICS
Functionality	Suitability
	Accuracy
	Interoperability
	Security
	Functionality compliance
Reliability	Maturity
	Fault tolerance
	Recoverability
	Reliability compliance
Usability	Understandability
	Learnability
	Operability
	Attractiveness
	Usability compliance
Efficiency	Time behavior
	Resource utilization

	Efficiency compliance
Maintainability	Analyzability
	Changeability
	Stability
	Testability
	Maintainability compliance
Portability	Adaptability
	Installability
	Co-existence
	Replaceability
	Portability compliance

4 Construction of data agents using MATLAB

The data agent used in this work was constructed using MATLAB software. Before construction of the agents it was important to present the theory behind the agents as explained in the subsections below.

4.1 Theory behind design of the agents

It is a normal practice to build data agents for detection of different threatening errors and failures during drilling operations. Most of the procedures used here were adopted from Best Practice for Constructing Data Agents Manual IGP-NTNU, (Skalle, 2014)
These errors and failures are always deviations from the expected values of any drilling parameter. The most focused parameters in this work are; change in wellbore's expected DLS and associated side force/string tension and agent was prepared for each parameter.

4.2 General data requirements

The data agents required RTDD, survey data and drill string parameters as inputs, which were incorporated in MATLAB software. The RTDD and survey data used in this work were from five different wellbores as presented in chapter 3, whereby the drill string parameters were adopted from EoW reports and the examination paper on Drilling, Completion, Intervention and P&A – design and operations by (Tor & Sigbjørn, 2016).

4.3 Data Agent Development

The data agents were designed by following the steps suggested in Best Practice for Constructing Data Agents Manual (Skalle, 2014) as listed below;

- Manual evaluation of symptoms in the RTDD
- Development of data agent in MATLAB which can perform computations and detect the symptoms in the RTDD
- Implementation of the agent in MATLAB
- Evaluation the performance of the agent

4.3.1 Symptoms in the historical data logs

Before developing data agents, the symptoms in the historical data logs were evaluated manually. The RTDD from the given wellbore sections were displayed in different plots. Two wells were selected to represent others and the main plots used were HKL and BPOS from wells 15/9-F-11 and 15/9-F-11, as presented in figure 4-1 (a) and 4-1 (b). From the figures it was observed that,

- High HKL was recorded from around 2555 m MD to 2755 m MD for well 15/9-F-11 and from around 2600 m MD to around 3000 m MD for well 15/9-F-12 as indicated in figures 4-1 and 4-2.

- At 2500 m MD to 2600 m MD and 3000 m MD to 3100 m MD of well 15/9-F-12, a serious record of erratic values was experienced as indicated by black circles in figure 4-2 and figure 4-3.

- Some RTDD were not recorded by the MWD/LWD tools as shown in figure 4-3, figure 4-4 and figure 4-5.

These observations gave out an important step upon generation of data agent for further assessment and evaluation of the probable areas where problems and errors could occur during computations.
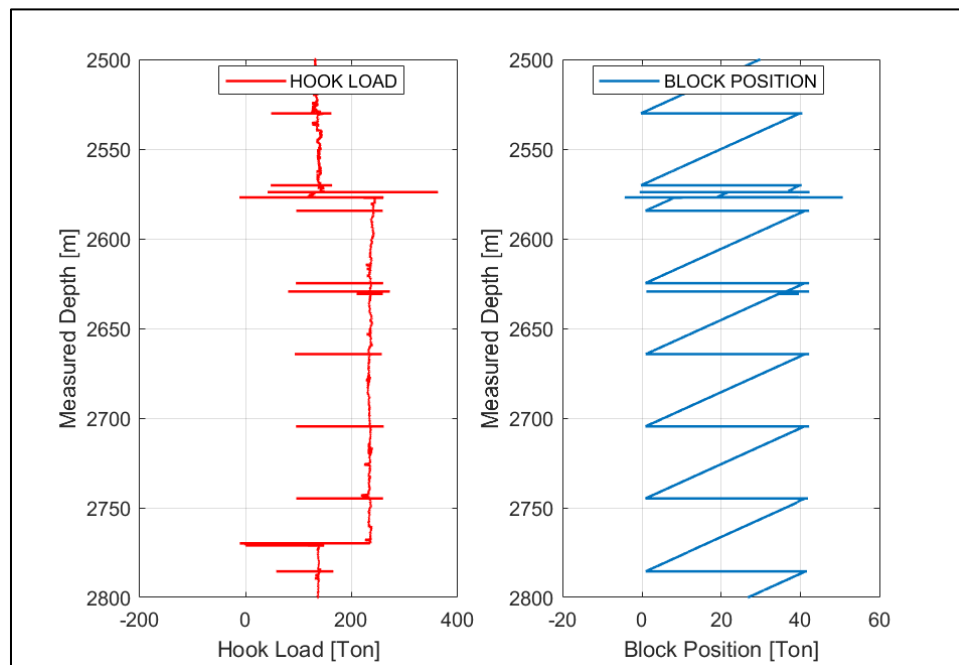
Figure 4-1: High values of Hook Load and block position of well 15/9-F-11
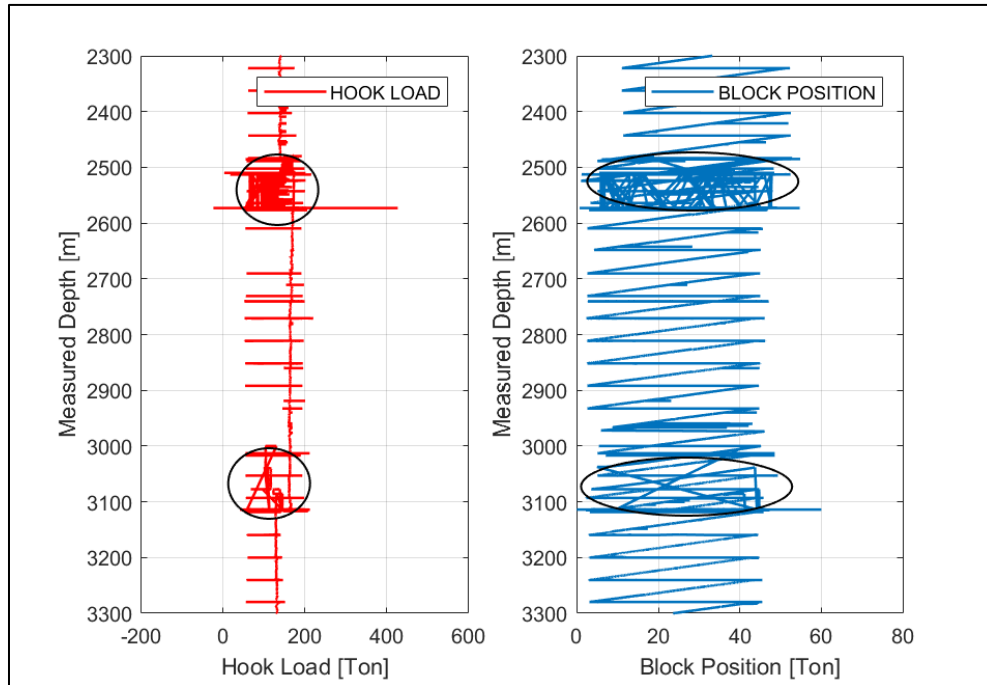
Figure 4-2: High and erratic values of Hook Load and block position of well 15/9-F-12
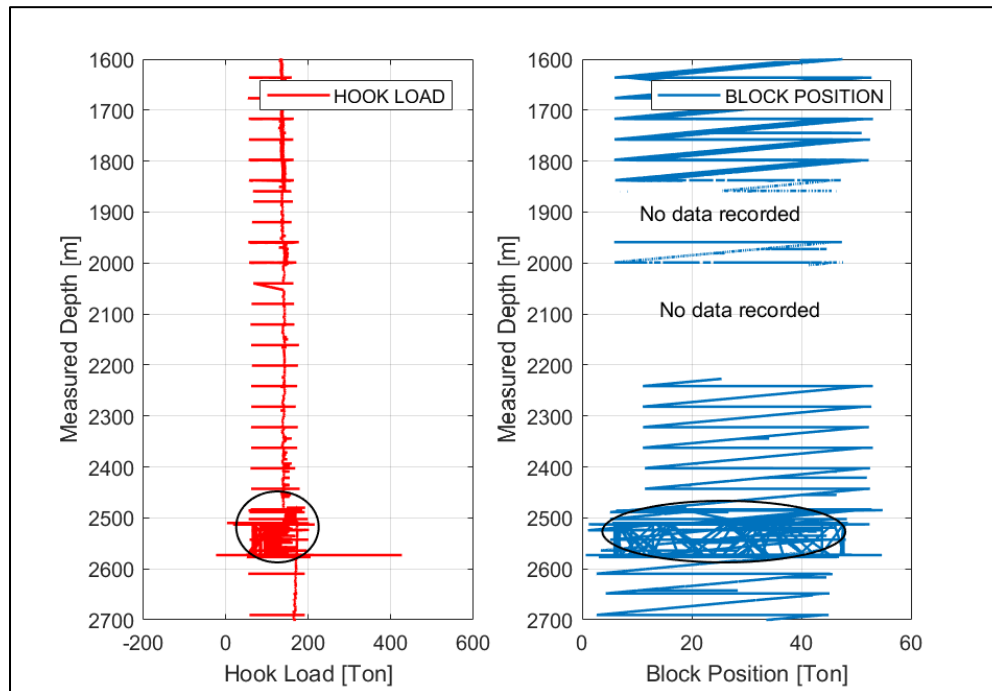
Figure 4-3: Erratic and unrecorded values of Hook Load and block position of well 15/9-F-12
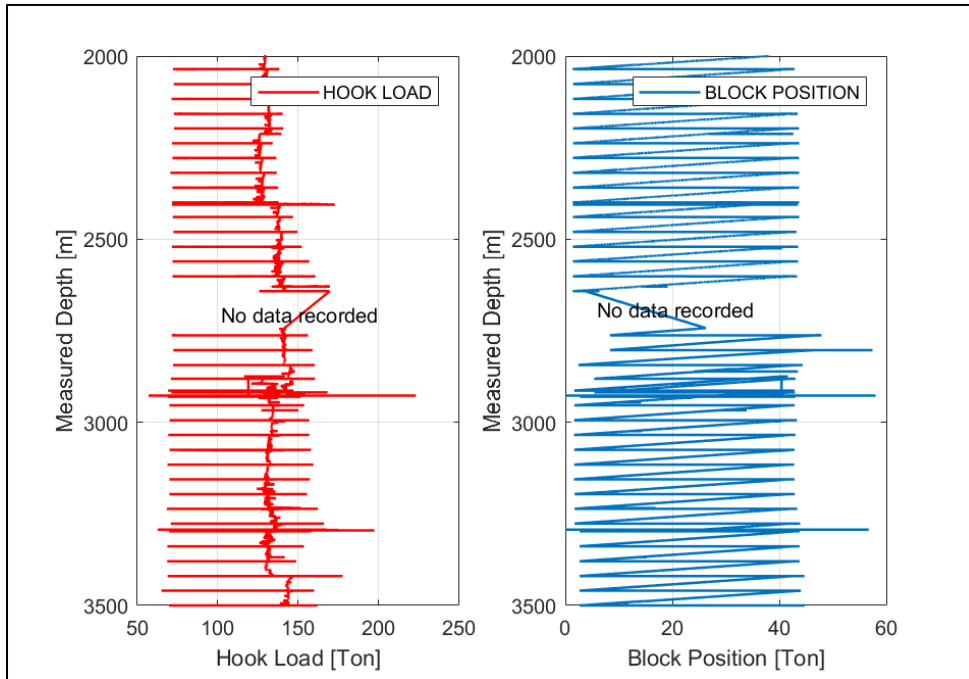
Figure 4-4: Hook Load and block position with unrecorded data of well 15/9-F-5
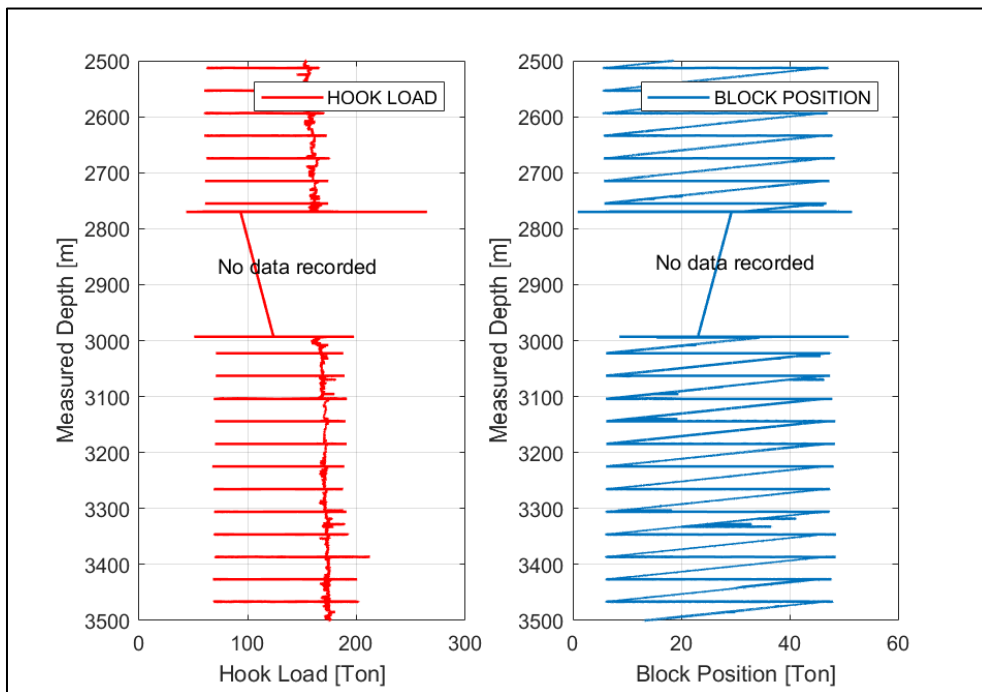
Figure 4-5: Hook Load and block position with unrecorded data of well 15/9-F-4

4.3.2 Agent implementation in MATLAB

Following the availability and selection of the DLS and side force models, as well as availability of base case data as presented in chapter 3, it was possible to implement these models using MATLAB. The overall workflow of implementation required the following items;

- Creating a model of system requirements for testing as presented in chapter 3.
- Generating test data from this requirements-model representation as presented in chapter 3
- Verifying the design algorithm with generated test cases as shown in chapter 3

4.3.2.1 Algorithm of the data agent

Computation of results involved a step by step method of solving a problem using MATLAB. This included processing of some raw data to obtain valid and valuable data set. The processing was done to sort, clean and remove unnecessary data from the raw data, followed by calculation and other related computer and mathematical operations. Two different codes were developed purposefully for computation of DLS, side force and string tension. Summary of coding steps used to compute DLS was presented in a flow chart in figure 4-6, whereby the summary of codes for computation of side force and string tension was presented in figure 4-7.
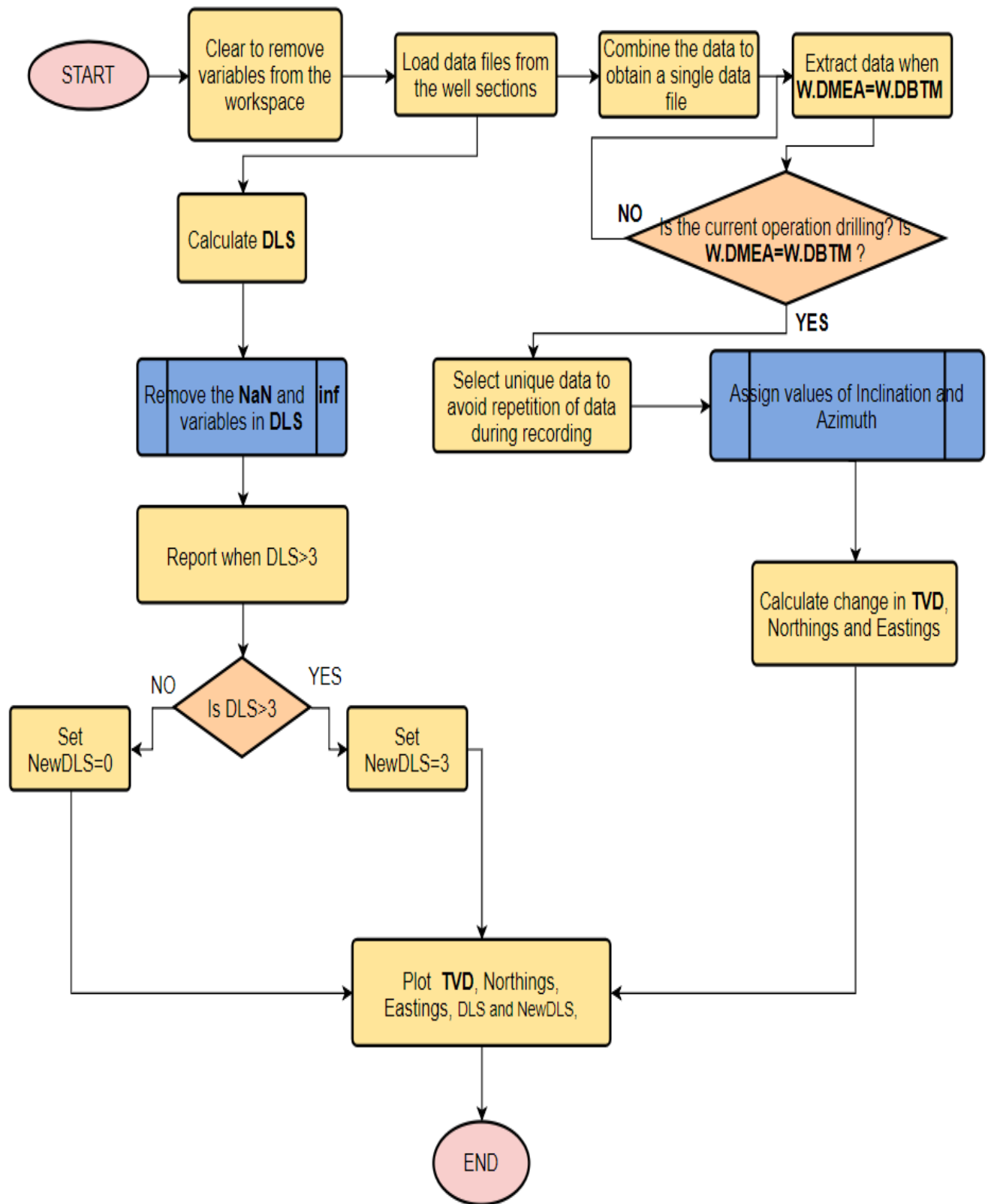
Figure 4-6: Flow chart for computation of wellbore position and DLS using MATLAB created by Visual Paradigm Online Express Edition (Visual_Paradigm, 2019)
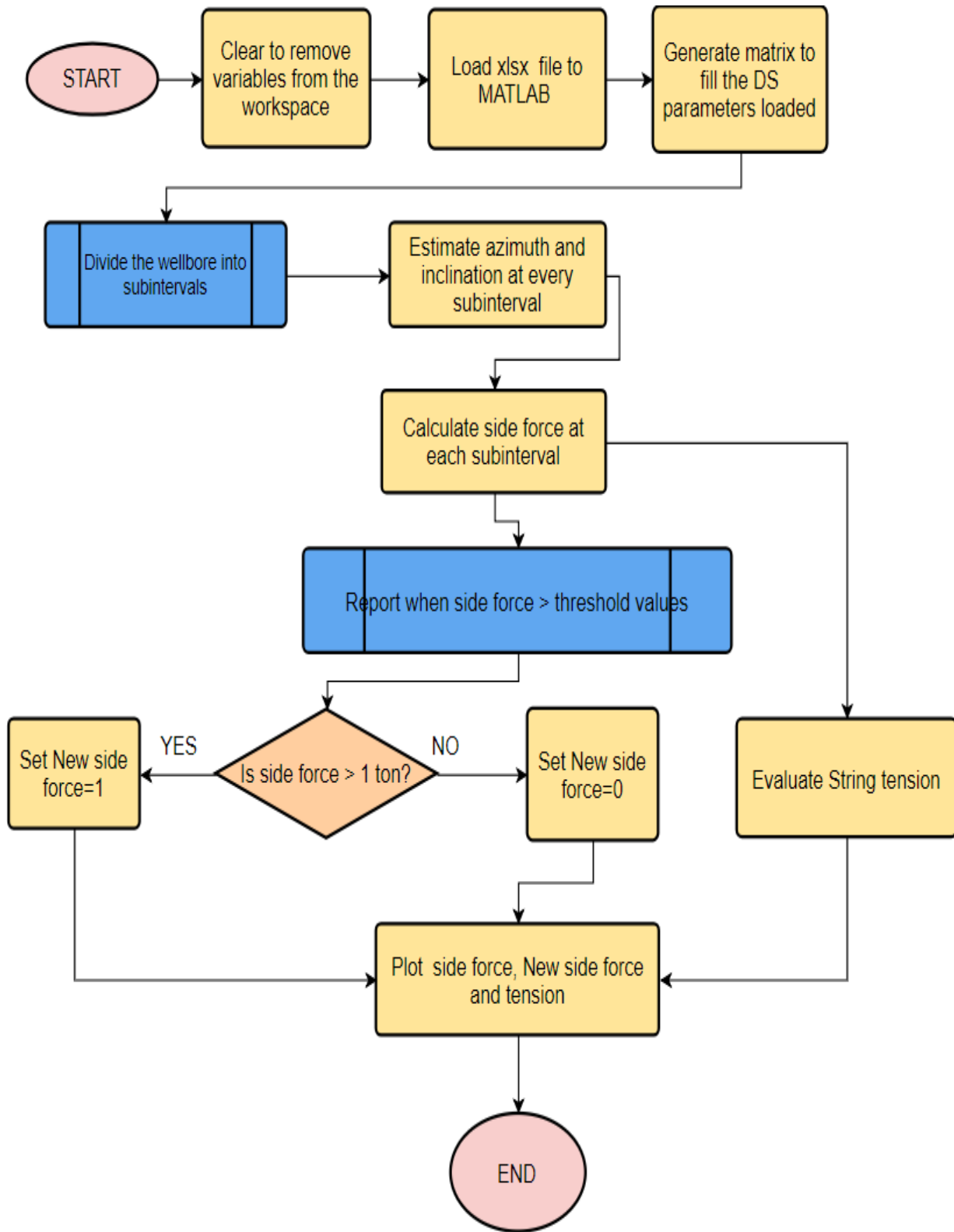
Figure 4-7: Flow chart for computation of Side force and string tension using MATLAB created by Visual Paradigm Online Express Edition (Visual_Paradigm, 2019)

4.3.2.2   Coding of the data agent

The flow charts presented in figures 4-6 and 4-7 were referred for development of the MATLAB codes. The codes were prepared for the wellbore 34/10-C-47, 15/9-F-4, 15/9-F-5, 15/9-F-11T and 15/9-F-12, and they were separately prepared for computation of DLS and side force. In order to save time and space, codes for well 34/10-C-47 were chosen to represent other wellbores and the detail codes are attached in appendix A and appendix B.

As stated earlier, that before coding was done, the files were processed to match the required file format, the number of data file required, and the type of input parameters needed. The file format needed to run the agent generated was. *mat* and *.xlsx* formats. The *.mat* files included the RTDD and survey files while the *.xlsx* files included only the drill string parameters data file.

4.3.2.2.1   DLS code

The DLS code presents three main parts namely; computation of position of well, computation of DLS and plotting of results. The whole code is included in appendix A for further details.

Required inputs

From given drilling data, the agent was able to extract the following data as inputs to the selected models; Measured depth (DMEA), Bit depth (DBTM), Inclination, Azimuth and Dogleg severity from the data file for model validation.

Loading and combining the RTDD

As presented in the flow chart in figure 4-6, the coding began with clearing to remove other and unnecessary variable from the workspace. Then the given RTDD files from 8.5'', 12.25'' and 17.5'' wellbore sections were loaded, these files were combined to obtain a single set of data representing a wellbore with all sections given. The syntax for loading and combination is shown in the code below.

```
%%%%%%%%%%%%%%%%%%%%%%%%%%%%%%%%%%%%%%%%%%%%%%%%%%%%%%%%%%%%%%%%%%%%%%%%%%%%
load C47IncAzDLS-8_5
Z=X;
load C47IncAzDLS-12_25
Y=X;
load C47IncAzDLS-17_5
%%%%%%%%%%%%%%%%%%%%%%%%%%%%%%%%%%%%%%%%%%%%%%%%%%%%%%%%%%%%%%%%%%%%%%%%%%%%
% 3. COMBINING THE DATA FILES TO OBTAIN A SINGLE DATA FILE
%%%%%%%%%%%%%%%%%%%%%%%%%%%%%%%%%%%%%%%%%%%%%%%%%%%%%%%%%%%%%%%%%%%%%%%%%%%%
f=fieldnames(X);
for i=1:length(f)
    W.(f{i})=[X.(f{i});Y.(f{i});Z.(f{i})];
end
%%%%%%%%%%%%%%%%%%%%%%%%%%%%%%%%%%%%%%%%%%%%%%%%%%%%%%%%%%%%%%%%%%%%%%%%%%%%
```

Extracting and selecting unique data

The given RTDD were recorded by MWD/LWD tools, therefore some of the data were not as correct as expected. Sometimes the tools recorded data at point at which drilling was not taking place and in other cases the tools recorded multiple data or repeated data at the same point. For computation of position of the well purposes, only unique RTDD at which drilling was being conducted could be used by the data agent. This condition was met by performing the following command in MATLAB;

- Sorting all RTDD at which DMEA was equal to DBTM to obtain data at which drilling was conducted
- Selecting data without repetitions using the unique command as seen in the code below

```
%%%%%%%%%%%%%%%%%%%%%%%%%%%%%%%%%%%%%%%%%%%%%%%%%%%%%%%%%%%%%%%%%%%%%%%%%%%%
md=unique(DMEA, 'stable');
incazicoord = unique(DMEA, 'stable');%DMEA for survey points.
azis = unique(AZI,'stable');% Azimuth for survey points
incl=unique(INC,'stable');
% %%%%%%%%%%%%%%%%%%%%%%%%%%%%%%%%%%%%%%%%%%%%%%%%%%%%%%%%%%%%%%%%%%%%%%%%%%
```

Assignment of the values of azimuth and inclination

The models selected in chapter 3 requires assignment of azimuth and inclination for computations. Two values of azimuth and inclination are used as inputs to the selected models; therefore, these values were assigned from RTDD to comply to the selected models as indicated in the main code in appendix A.

Computations

The first computation was to determine the well position by obtain different views of the well. The focused views of the well were vertical view, plan view as well 3D view. This was important to

give a simple outlook of the profile of the well for evaluation of different errors problems or failures during drilling. The views were also important to indicate the way drilling was conducted in terms of directions. These views were obtained by calculating the change in easting, northing and TVD using the minimum of curvature survey method presented in chapter 3

The other computation was to obtain DLS of the wellbore. This computation was the main focused as it carried the whole theme of the thesis. The computation was done after making a close look of the wellbore profile using the projections done in the first part of computations. In order to enable making comparison of the model selected, DLS was calculated using raw and unprocessed RTDD and survey data given. The computation was done using the model displayed in equation 3-4 presented in chapter 3.

Reporting the allowable limit of DLS

The limit of allowable and acceptable DLS was obtained with reference to the literatures. The acceptable limit that is harmless and could not cause any problem when drilling or tripping is $0\ °/30$ m to $3\ °/30$ m. The allowable DLS limit was obtained by setting new DLS with two values in a sense that, when DLS $< 3\ °/30$ m, new DLS $= 0\ °/30$ m, and when DLS $> 3\ °/30$ m, new DLS $= 3\ °/30$ m as indicated in the code below

```
%%%%%%%%%%%%%%%%%%%%%%%%%%%%%%%%%%%%%%%%%%%%%%%%%%%%%%%%%%%%%%%%%%%%%%%%%%%%%%%%%%%
%Apply the limits of allowable DLS
DLSNew(1:length(DLS))=0;
DLSNew(DLS>3)=3;
%%%%%%%%%%%%%%%%%%%%%%%%%%%%%%%%%%%%%%%%%%%%%%%%%%%%%%%%%%%%%%%%%%%%%%%%%%%%%%%%%%%
```

4.3.2.2.2 Side force and string tension code

This code was prepared to compute side force and evaluate string tension as presented in chapter 3. The code was prepared basing on the flow sheet presented in figure 4-4 and the details are presented in appendix B.

Required input parameters

The code for computation of side force required different parameters as presented in chapter 3. The most important parameters are; BHA parameters, WOB, mud properties such as MW, inclination and azimuth. Coefficient of friction was also included during calculation of string tension.

Loading the parameters

The BHA parameters were prepared in xlsx file using Microsoft excel, this file was loaded and incorporated in MATLAB to enable various computations using the data agent as indicated in codes below.

```
%%%%%%%%%%%%%%%%%%%%%%%%%%%%%%%%%%%%%%%%%%%%%%%%%%%%%%%%%%%%%%%%%%%%%%%%%%
T = xlsread('para');%read the xlsx file contaning the DS parameters
%%%%%%%%%%%%%%%%%%%%%%%%%%%%%%%%%%%%%%%%%%%%%%%%%%%%%%%%%%%%%%%%%%%%%%%%%%
```

Preparation of matrix for the DS parameters

The loaded parameters were prepared and filled into special matrix to make easy computations as shown in the code below.

```
%DS parameters
a=T(1,5);%average dry weight of DP (kg/m)
b=T(2,1);%length of HWDP
c=T(2,5);%average dry weight of HWDP (kg/m)
d=T(3,1);%length of DC
e=T(3,5);%average dry weight of DC (kg/m)
f=T(4,1);%length of PDM
g=T(4,5);%average dry weight of PDM (kg/m)
h=T(5,1);%length of PDC
i=T(5,5);%average dry weight of PDC (kg/m)
```

Computations

The computation was done basing on the procedures proposed in the methodology. To make it short, the idea was to compute side force from doglegs and evaluate string tension from side force and friction coefficient by diving the wellbore into different subinterval. The first subinterval was the BHA, other subintervals were spaced 500 m MD between each and a total of six subintervals were obtained on every well. The main duty was to estimate azimuth, inclination and dogleg at every interval. From the estimated values, side force was also computed before string tension was estimated from side force and coefficient of friction.

Reporting the allowable limit of side force

From the literature reviewed, the international accepted threshold value of side force is around 2000 lbs equivalent to 1 ton (Brechan, et al., 2017). This value is harmless to the drill string during

tripping. Basing on the assumptions of parameters used to estimate side force, the allowable threshold values were obtained by setting new side force with two values in a sense that, when side force < 1 ton, new side force = 0 ton, and when side force > 1 ton, new side force = 1 ton as shown in the code below.

```
%%%%%%%%%%%%%%%%%%%%%%%%%%%%%%%%%%%%%%%%%%%%
%. REPORTING WHENEVER SF > threshold values
%%%%%%%%%%%%%%%%%%%%%%%%%%%%%%%%%%%%%%%%%%%%
SFNew=zeros(length(J),1);
for j=1:length(J)
if J(j)>1
    SFNew(j)=1;
else
    SFNew(j)=0;
end
end
```

4.3.2.3 Outputs from the data agent

Although the details of findings are presented in the results and discussion chapter, this section gives a summary of what was given out from the data agent developed. The data agent designed produced the results from both DLS computation and side force and string tension evaluation with all results being presented by plotting.

4.3.2.3.1 Output from DLS computation

- Projection of the wellbore
- Computed DLS
- Report when DLS > 3 º/ 30 m is achieved

Projection of the wellbore: This was done to simply and make a clear understanding of the profile and direction of the wellbore. The projection was done by first limit the view of the wellbore in 2-D (plan and vertical view) and finally presenting its 3-D view. These views were obtained by calculating the change in TVD, Eastings and Northings using the minimum of curvature survey method. The plan view was obtained by plotting northing against easting. The vertical views were obtained by projecting the well on both S-N and W-E planes then plotting northing against TVD and easting against TVD respectively.

Computed DLS

The DLS was computed using the selected mathematical model from chapter 3. Some of the results from the computation were not valid as they included infinity values of the computed DLS. It was therefore very important to make the results obtained valid by making some modifications as presented in section 4.3.3. The final modified DLS was compared to the DLS from the survey file by making a single plot against measured depth. Furthermore, the difference between them was also computed in order to measure their degree of deviation.

Report when DLS > 3 º/ 30 m

The allowable DLS limit was obtained by setting new DLS with two values in a sense that, when DLS < 3 º / 30 m, new DLS = 0 º / 30 m, and when DLS > 3 º / 30 m, new DLS = 3 º / 30 m Then, new DLS was plotted together with the computed DLS against measured depth. From the plot, it was clear to establish a point at which computed DLS was higher than the recommended threshold value. All new DLS with value of zero represented allowable DLS, while all new DLS with values of 3 represented unaccepted DLS

4.3.2.3.2   Output from side force and string tension computation

- Computed side force and string tension
- Report when side force > threshold values is obtained

Side force and string tension

Side force was one of the values that was very difficult to obtain, because it consisted of input parameters which were assumed thus reducing the clarity of the work. The computation was done using the model accepted from chapter 3, whereas most of the input parameters were adopted from different sources such as EoW reports. This computation was done as per assumptions in chapter 3, one of the assumptions was that; the computation was done at assuming that drilling was being conducted at 8.5'' of the wellbore and the BHA was the same in all five wells used.

Since it is difficult to validate side force model, it was necessary to relate the response of side force, string tension and HKL by making plots of side force and HKL against measured depth.

Report when side force > threshold values

The acceptable value of SF is around 2000 lbs equivalent to 1 ton (Brechan, et al., 2017). This value is harmless to the drill string during tripping. Basing on the assumptions of parameters used to estimate side force, the allowable threshold values were obtained by setting new side force with two values in a sense that, when side force < 1 ton, new side force = 0 ton, and when side force > 1 ton, new side force = 1 ton. Then, new side force was plotted together with the computed side force against measured depth. From the plot, it was clear to establish a point at which computed side force was higher than the recommended threshold value. All new side force with value of zero represented allowable side force, while all new side force with values of 1 represented unaccepted side force.

4.3.2.4 Testing of the codes

The code generated was tested to find programming mistakes using a MATLAB built-in testing framework. The testing was included in the main code during development of the agent program to automatically make sure that the agents give the expected output for various "normal" conditions and for typical corner cases. The `runtests` MATLAB testing built-in commands was used in one of the files given and it revealed excellent programming results as indicated in table 4-1.

Table 4-1: Test Result from MATLAB with properties

File Name	ThesisC47
Passed	1
Failed	0
Incomplete	0
Duration/testing time	2.5909 seconds

4.3.3 Evaluating the performance of the data agents

In most cases, the data agent did what it was intended to be done. Some of the logical problem observed were;

- False negative DLS; one point of the file C47, indicated false negative value of the calculated DLS at around 1567 m MD as shown in figure 4-9. This problem was solved by applying the absolute sign to eradicate negativity.

- NaN and Inf values of computed DLS; in cases where the dogleg angle and course length was zero, the value of computed DLS from the agent was either NaN or Inf as shown in figure 4-8

Figure 4-8: NaN values of calculated DLS

The problem above, was settled by performing linear interpolation by nearest values of DLS using the MATLAB built-in commands such as $fillmissing$ command. The syntax of the command is as shown in the codes below

```
%%%%%%%%%%%%%%%%%%%%%%%%%%%%%%%%%%%%%%%%%%%%%%%%%%%%%%%%%%%%%%%%%%%%%%%%%%
% 7. CALCULATE  DLS
%%%%%%%%%%%%%%%%%%%%%%%%%%%%%%%%%%%%%%%%%%%%%%%%%%%%%%%%%%%%%%%%%%%%%%%%%%
DLS1=abs(acosd(cosd(W.INC(1:(end-1)))...
    .*cosd(W.INC(2:(end)))+sind(W.INC(1:(end-1))).*sind(W.INC(2:(end)))...
    .*(cosd(W.AZI(2:(end))-W.AZI(1:(end-1))))))./abs(diff(W.DMEA))*30;
%Convert obtained inf entries to NaN entries
DLS1(isinf(DLS1)) = NaN;
% Fill leading and trailing NaN entries with their nearest neighbors using
% linear interpolation
DLS=fillmissing(DLS1,'linear','EndValues','nearest');
%%%%%%%%%%%%%%%%%%%%%%%%%%%%%%%%%%%%%%%%%%%%%%%%%%%%%%%%%%%%%%%%%%%%%%%%%%
```
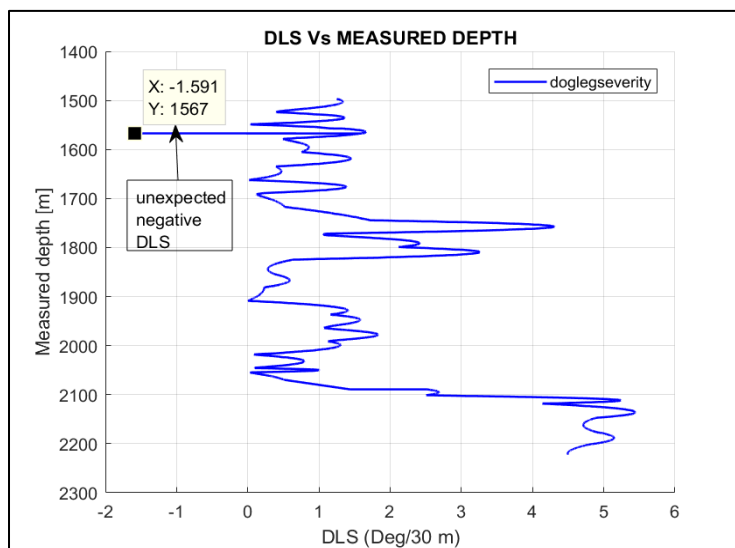

Figure 4-9: False negative DLS

5 Results and Discussion

Following the computations performed using the selected models, the results obtained were portrayed in plots to give an easy means to discuss them. These results were mainly the outputs from the data agent generated in chapter 4, and they included; the views (projections) of the wellbore, estimated DLS together with the DLS from survey data and side force together with string tension. The output from evaluation of maximum allowable DLS and side force limits were also presented.

5.1 Results of views of the well bore

Indication of the views of the wellbore was necessary for portraying the wellbore profile and directions to make a clear understanding of the way the wellbore was drilled. The focused views were vertical, plan view and 3D projection.

5.1.1 Vertical and plan views

The vertical view consisted of two components, namely;

- o A view from south on TVD projected on a vertical W-E plane. This was the plot of computed easting against computed TVD
- o A view from east on TVD projected on a vertical S-N plane. This was the plot of computed northing against computed TVD

The plan view was obtained by projecting the wellbore on the horizontal plane of the wellbore. Both views (vertical and plan) of the wellbores were presented for all five well selected as seen from figure 5-1 to 5-5.

5.1.2 3-D view

This view was obtained by plotting the computed northing, easting and TVD on the same graph. The resulting plots were presented in figure 5-6 to 5-10.
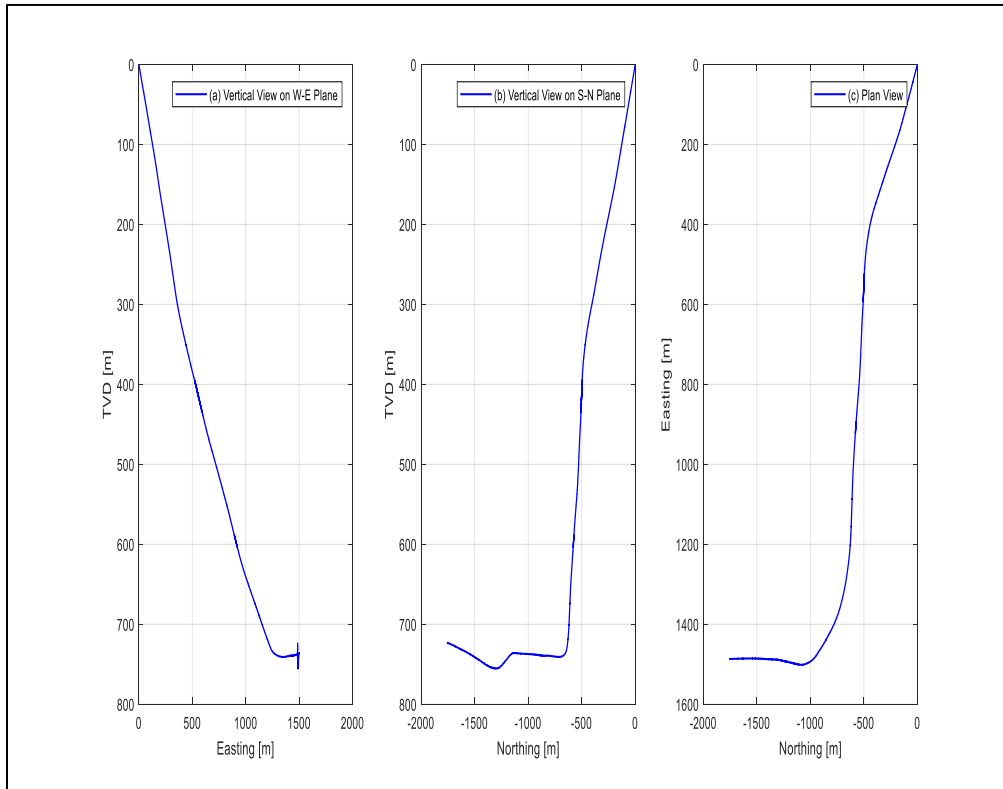
Figure 5-1: 34/10-C-47 Wellbore plan and vertical projection, (a) Vertical projection on W-E plane, (b) Vertical projection on S-N plane, (c) Plan projection on horizontal plane.
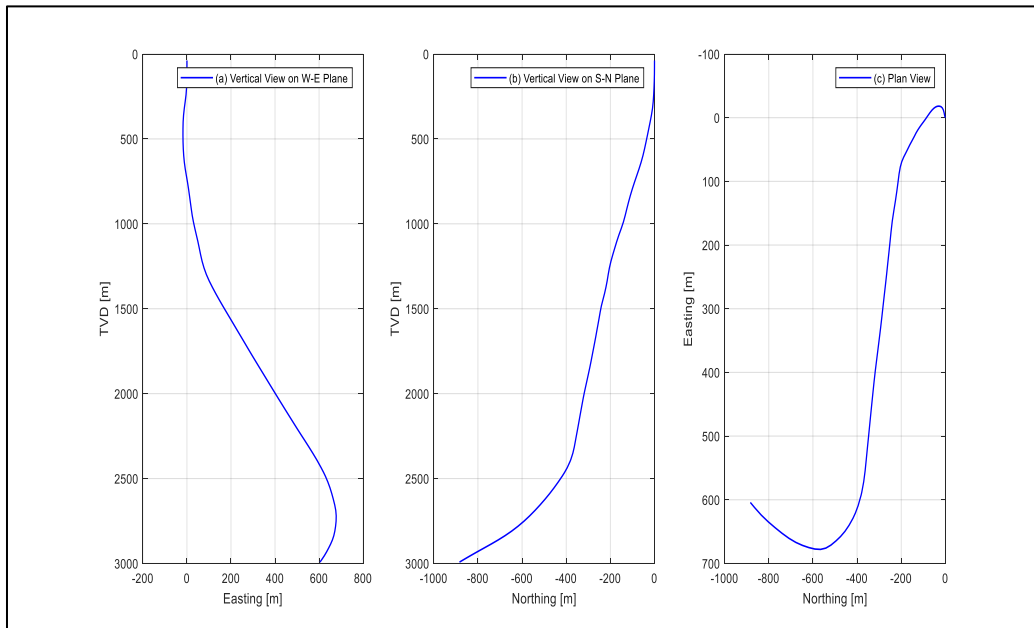
Figure 5-2: 15/9-F-4 Wellbore plan and vertical projection, (a) Vertical projection on W-E plane, (b) Vertical projection on S-N plane, (c) Plan projection on horizontal plane.
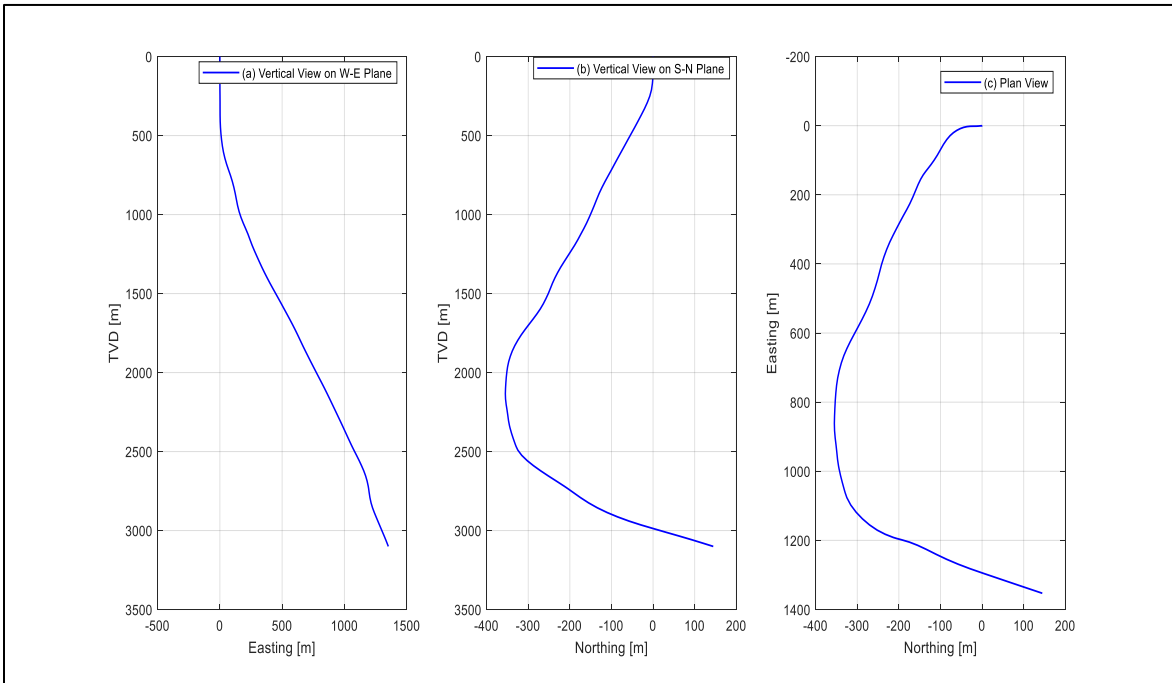
Figure 5-3: 15/9-F-5 Wellbore plan and vertical projection, (a) Vertical projection on W-E plane, (b) Vertical projection on S-N plane, (c) Plan projection on horizontal plane.
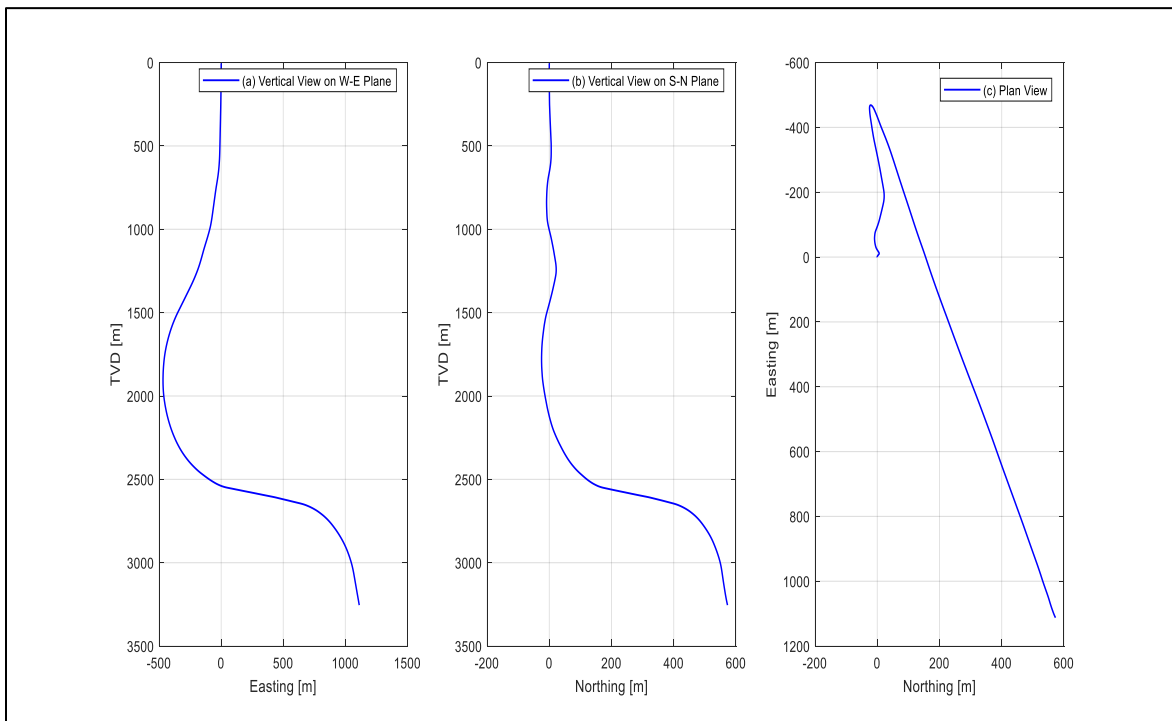
Figure 5-4: 15/9-F-11T2 Wellbore plan and vertical projection, (a) Vertical projection on W-E plane, (b) Vertical projection on S-N plane, (c) Plan projection on horizontal plane.
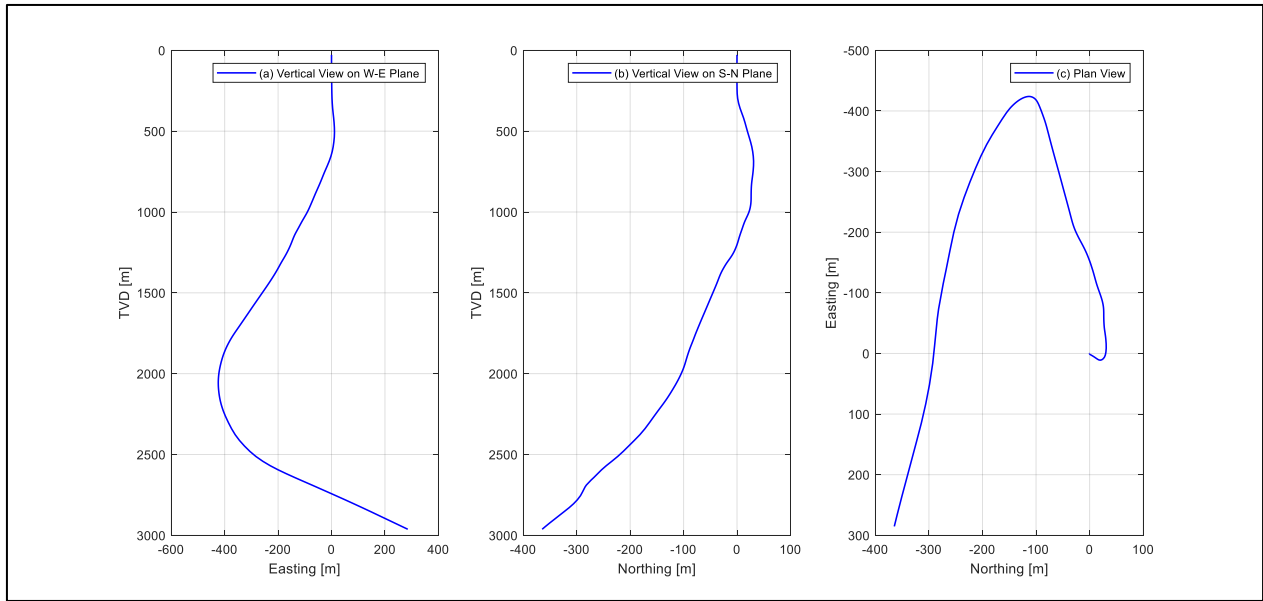
Figure 5-5: 15/9-F-12 Wellbore plan and vertical projection, (a) Vertical projection on W-E plane, (b) Vertical projection on S-N plane, (c) Plan projection on horizontal plane.
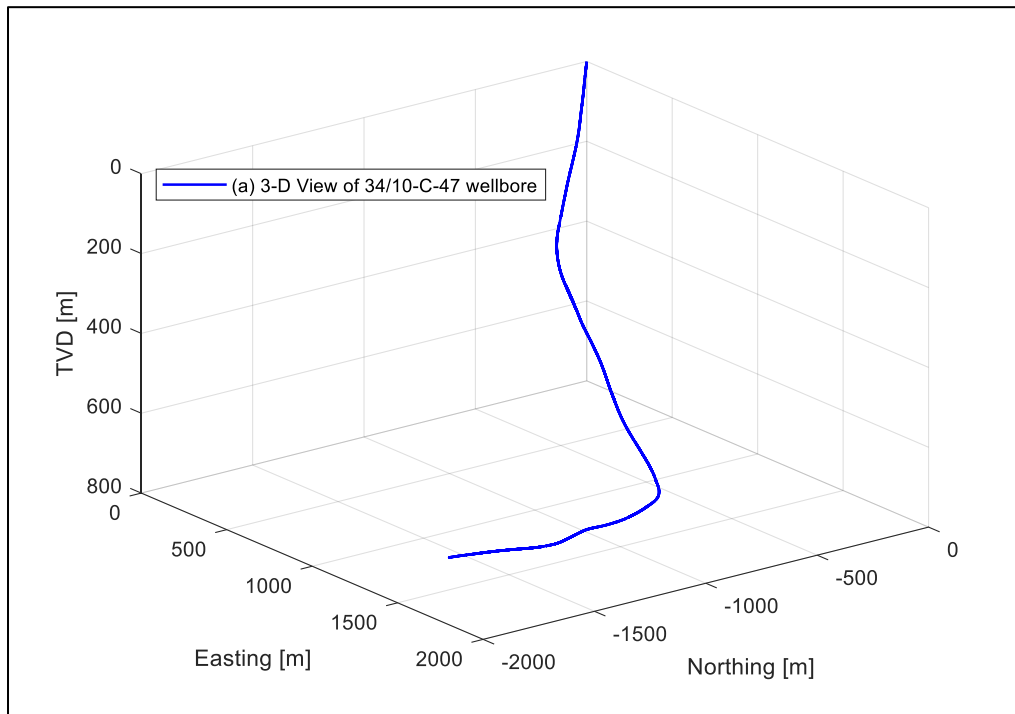
Figure 5-6: Three-dimension view of the 34/10-C-47 well.
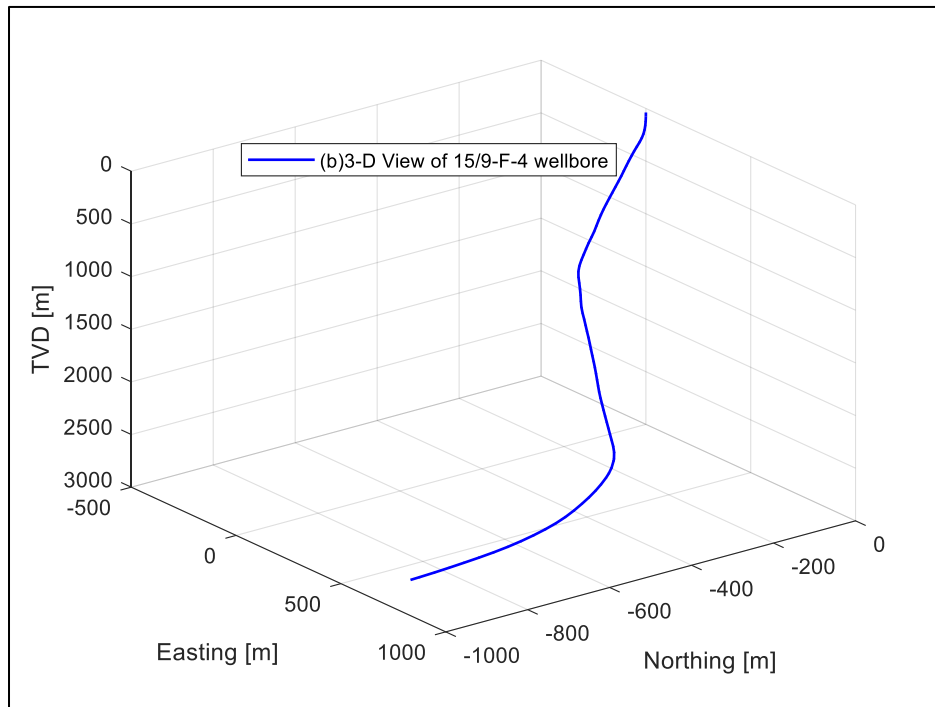
Figure 5-7: Three-dimension view of the 15/9-F-4 well.
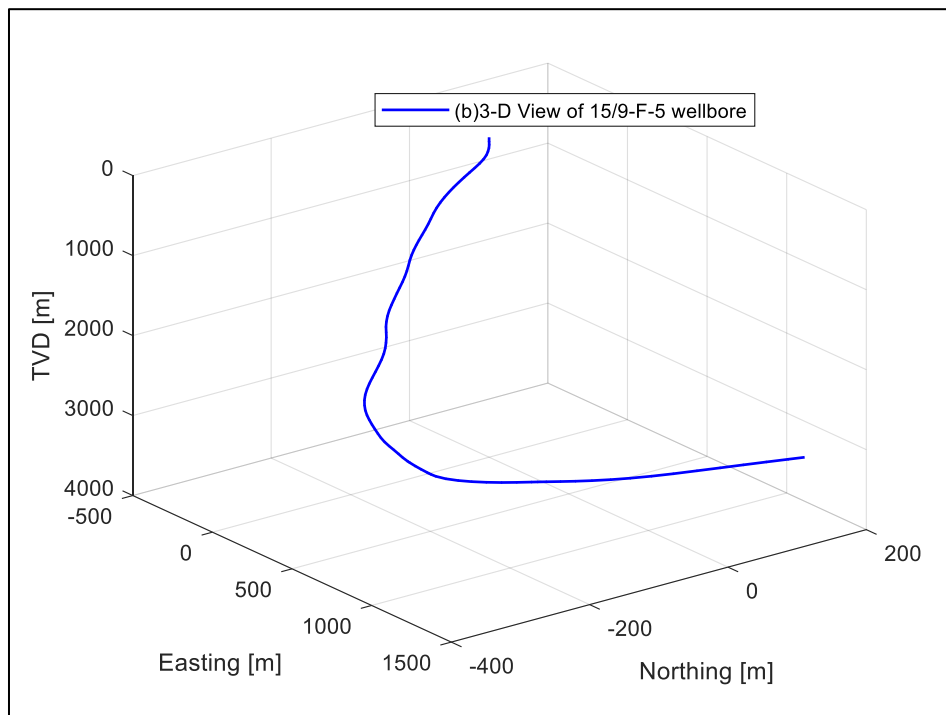
Figure 5-8: Three-dimension view of the 15/9-F-5 well.
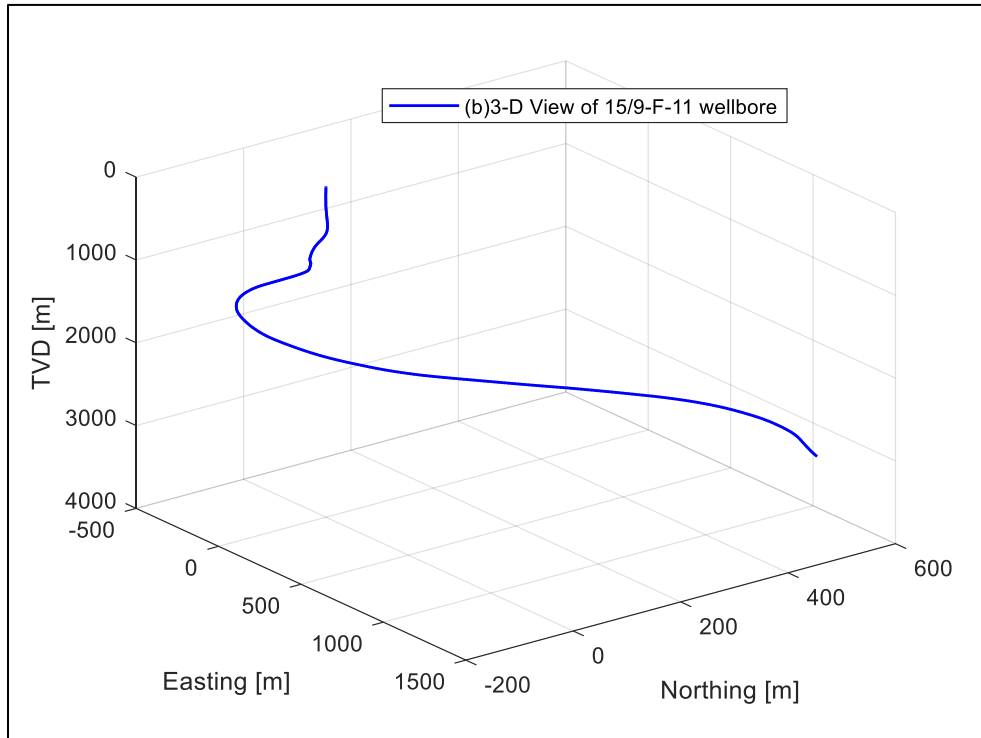
Figure 5-9: Three-dimension view of the 15/9-F-11 well.
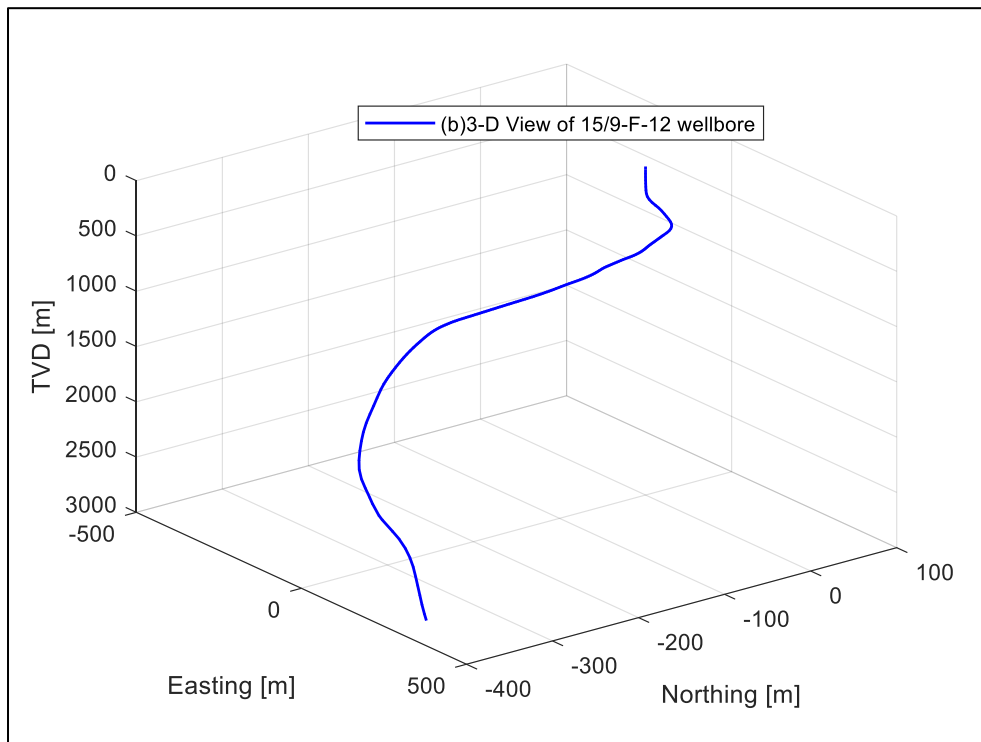
Figure 5-10: Three-dimension view of the 15/9-F-12 well

5.2   Discussion of results of wellbore views

The projection and presentation of wellbore in different views was very important during determination and detection of DLS and side force in the respective wells. However, the views and projections were all seen to be not realistic in some of the wells such as well 34/10-C-47. This was because the TVD seemed to have limited expected range as presented on figures 5-1 and 5-6. This was caused by;

- Processing and sorting of the RTDD to obtain data that were easily computed
- Use of data from only three wellbore sections as representative data.

Despite the fact the views were not realistic, well 34/10-C-47 was seen to be drilled starting from the junction of E-W plane and N-S plane towards east, then back to west, then towards north and finally towards east heading to N-S plane. Well 15/9-F-4 was drilled from west to east of the N-S plane, then downwards towards the horizontal plane and finally towards S-N plane as shown in figure 5-7.Well 15/9-F-5 was seen to be drilled from west to east of the S-E plane, then back to the same plane from east to west as shown in figure 5-8. Well 15/9-F-11 was drilled from south to north of E-W plane then back to N-S from east to west as depicted in figure 5-9. Well 15/9-F-12 was drilled from west to east of the N-S plane as depicted in figure 5-10.

The most interesting and abnormal view was observed in figure 5-4 and 5-9 of 15/9-F-11 well. The well contains a serious curve at around 1390 mTVD to around 2270 mTVD. This happened since 12.25''section of that well was not included in the survey data given as it was used for sidetracking as presented in the EoW report by Linn, et al., (2013). Moreover, the abnormality could probably result from failure of MWD tools to record appropriate values of required data such as azimuth and inclination. This is supported by the plot of azimuth and inclination of this well as stipulated in appendix C (c), from that appendix the azimuth does not behave as expected at 2156 mMD.

5.3   Results from computed of DLS

The computed DLS using the selected model in chapter 3 and data agent in chapter 4 was plotted against depth. To make a simple evaluation of the functionality, efficiency and usefulness of the model selected, a plot of DLS form the survey file was also added. Moreover, the difference

between the computed DLS and DLS from the survey file was also computed. The details of the outputs were presented from figure 5-11 to 5-15.
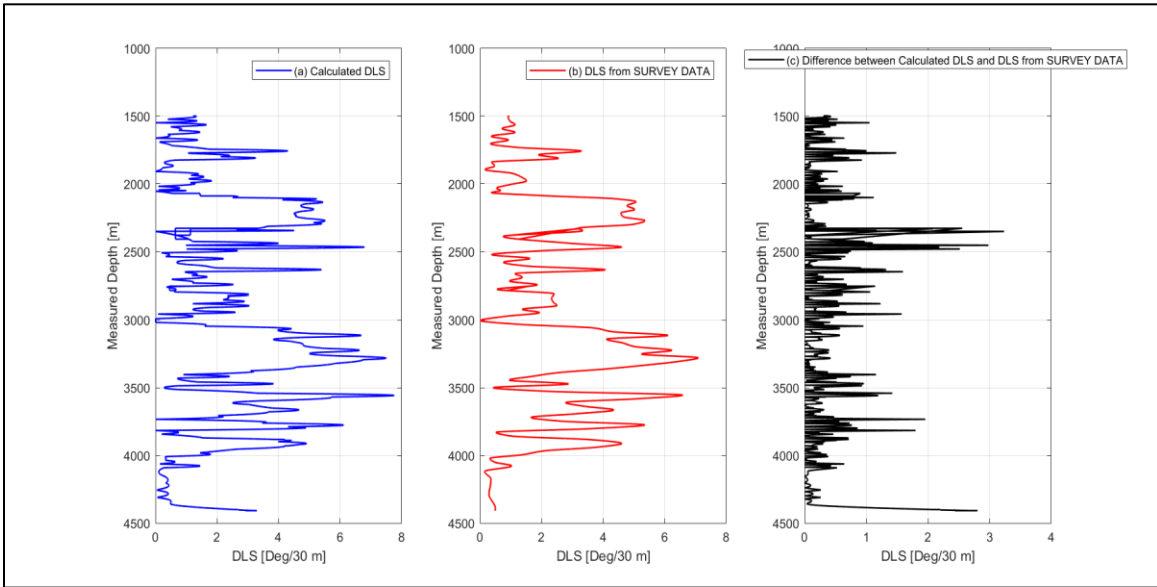
Figure 5-11: DLS for 34/10-C-47 wellbore: (a) Computed DLS from the selected model, (b) DLS from the base case survey file, (c) Difference between computed DLS and DLS from the survey file
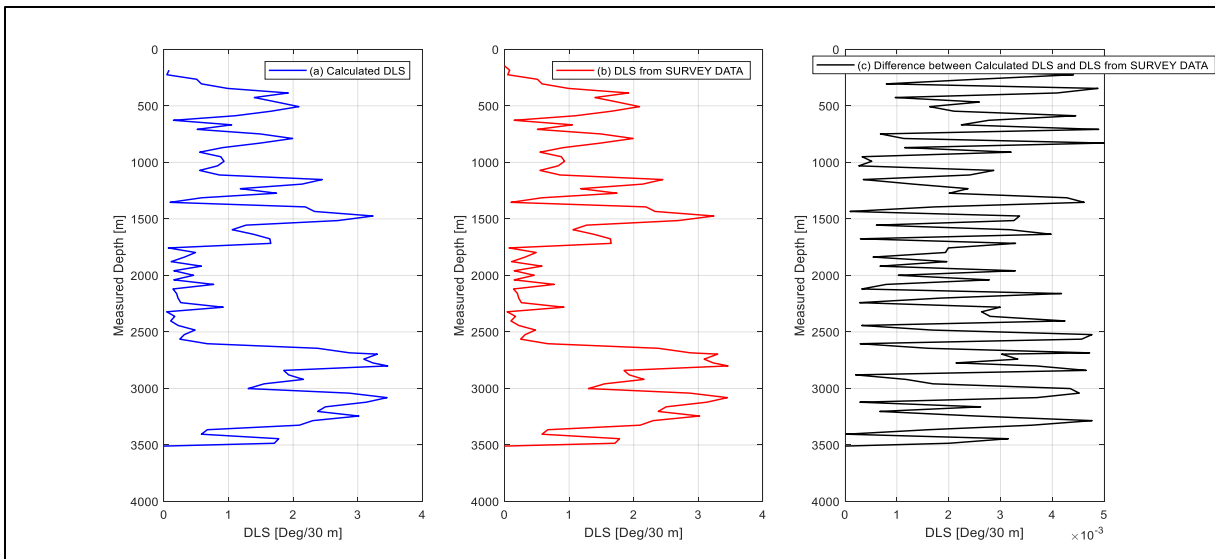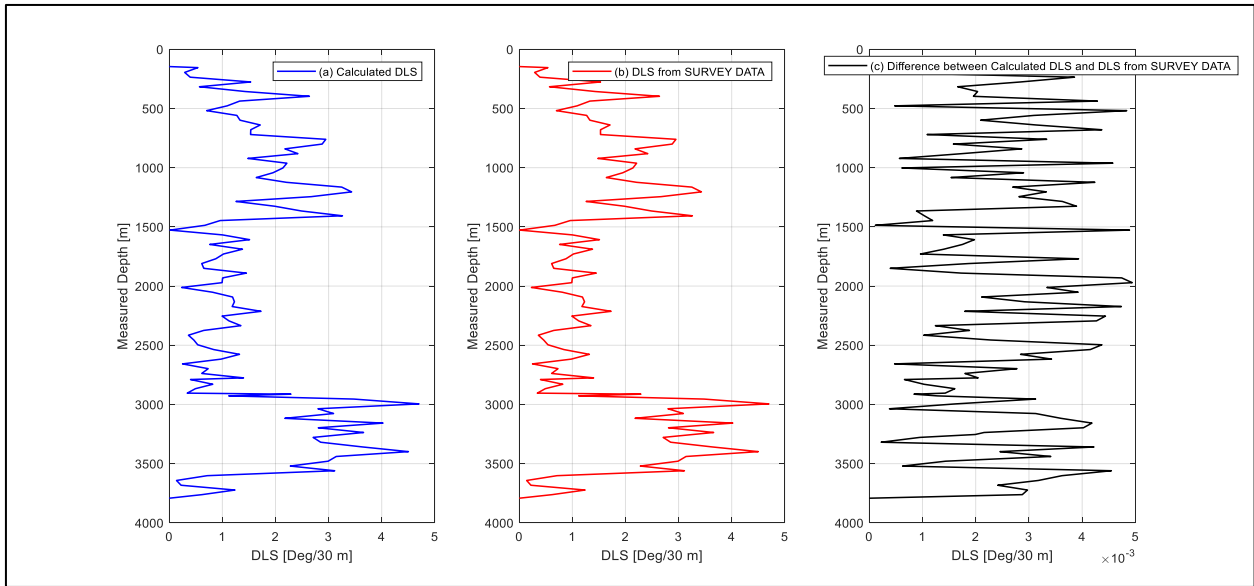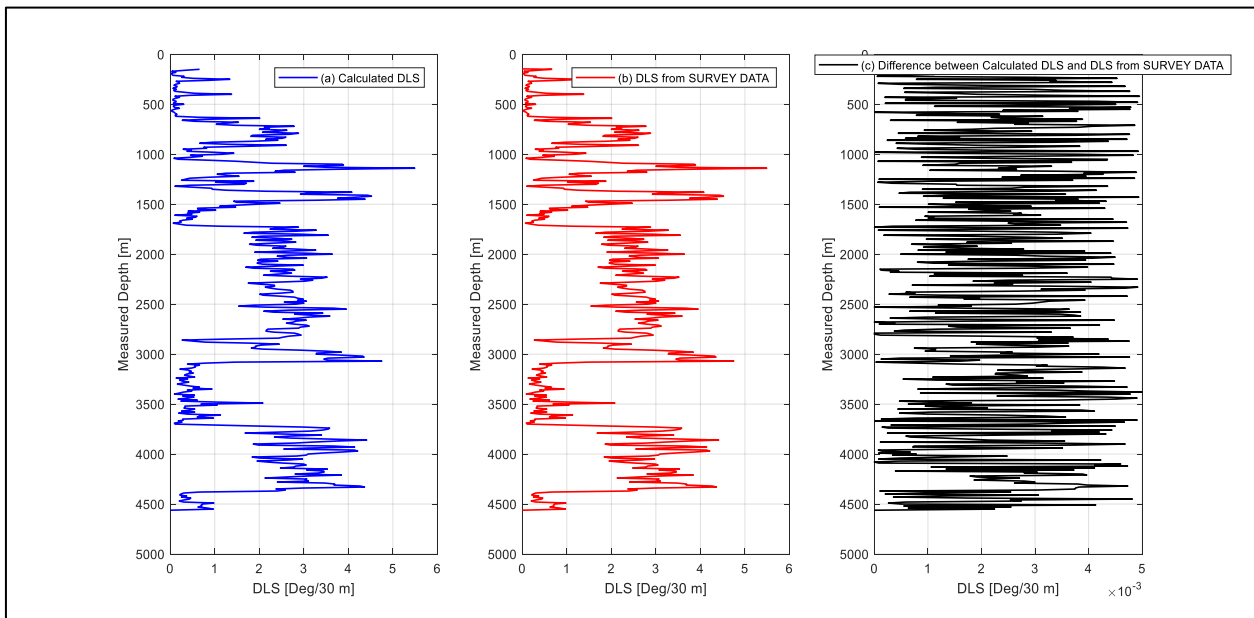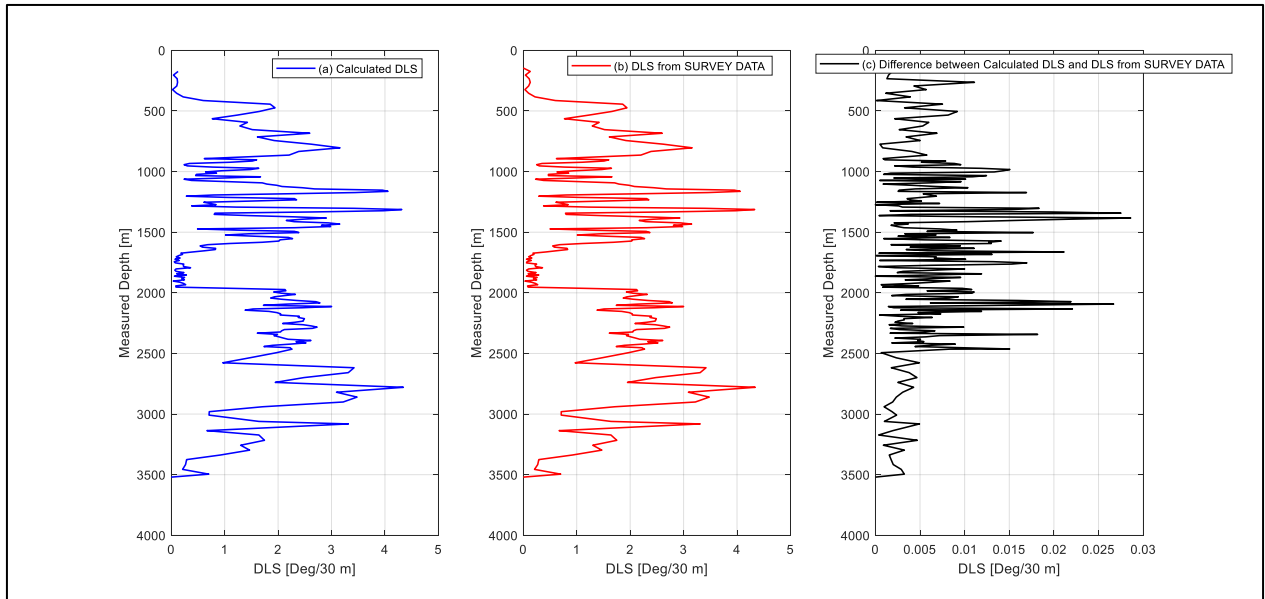

Figure 5-12: DLS for 15/9-F-4 wellbore: (a) Computed DLS from the selected model, (b) DLS from the base case survey file, (c) Difference between computed DLS and DLS from the survey file

Figure 5-13: DLS for 15/9-F-5 wellbore: (a) Computed DLS from the selected model, (b) DLS from the base case survey file, (c) Difference between computed DLS and DLS from the survey file

Figure 5-14: DLS for 15/9-F-11T2 wellbore: (a) Computed DLS from the selected model, (b) DLS from the base case survey file, (c) Difference between computed DLS and DLS from the survey file

Figure 5-15: DLS for 15/9-F-12 wellbore: (a) Computed DLS from the selected model, (b) DLS from the base case survey file, (c) Difference between computed DLS and DLS from the survey file

5.4 Discussion of computed DLS

The idea here was to make comparison between the model used to compute DLS and the model given in the survey file given. The computation was done to quantify the amount of curviness of the well and its possibility towards causing stuck pipe during tripping operation. As indicated by the plots from figure 5-12 to 5-15, the model selected produced almost similar results as the ones from the survey file. This can be proved by the minimum difference between the results from the compared models as shown from figure 5-12 to 5-15.

In real sense this difference was supposed to be zero, but it was realized that well 34/10-C-47 was seen to have huge difference. From figure 5-11, the maximum observed difference was at 2351 mMD with the value of 3.2 (^{o}/30 m) of difference. This incidence could be due to improper recording of data by MWD/LWD tools; as it can also be seen from the appendix C (a) that the tools recorded multiple values of azimuth and inclination at this depth thus improper computation of DLS. Moreover, this effect could result from sorting and processing of the RTDD and survey data for computation.

5.5 Results from computed side force and estimated string tension

The obtained values of computed side force from the selected model in chapter 3 and data agent in chapter 4 was plotted against depth. To make a simple validation of the model used, string tension evaluation was done from side force, and the results were plotted together against measured depth. The details of the outputs were presented in figure 5-16 to 5-20.
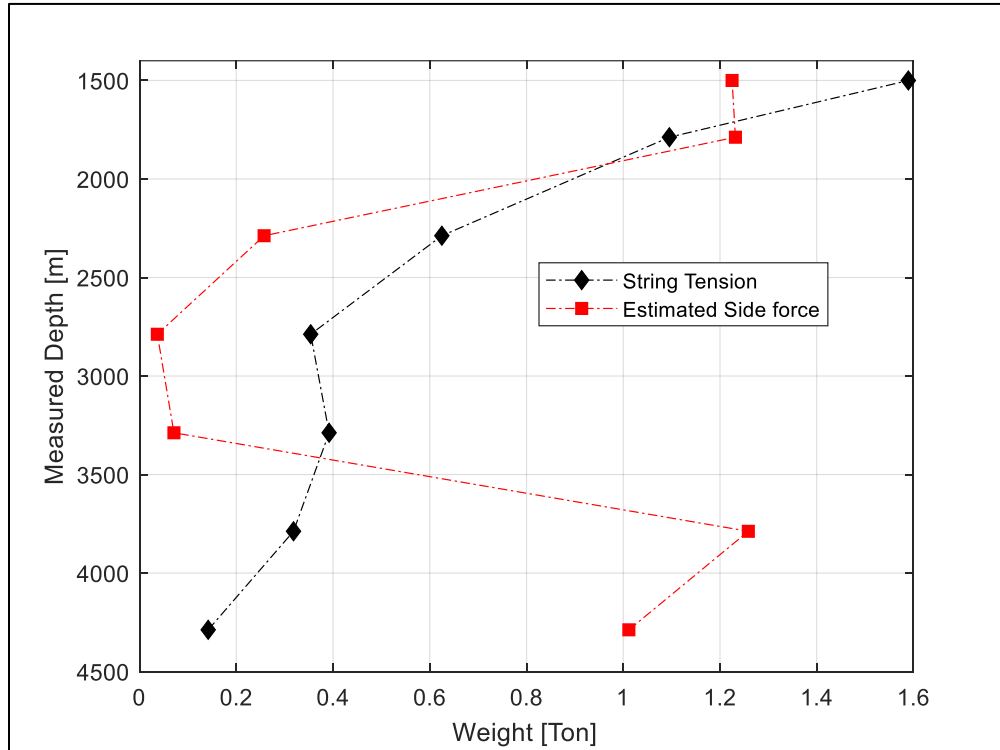
Figure 5-16: Computed side force and string tension for the 34/10-C-47 wellbore
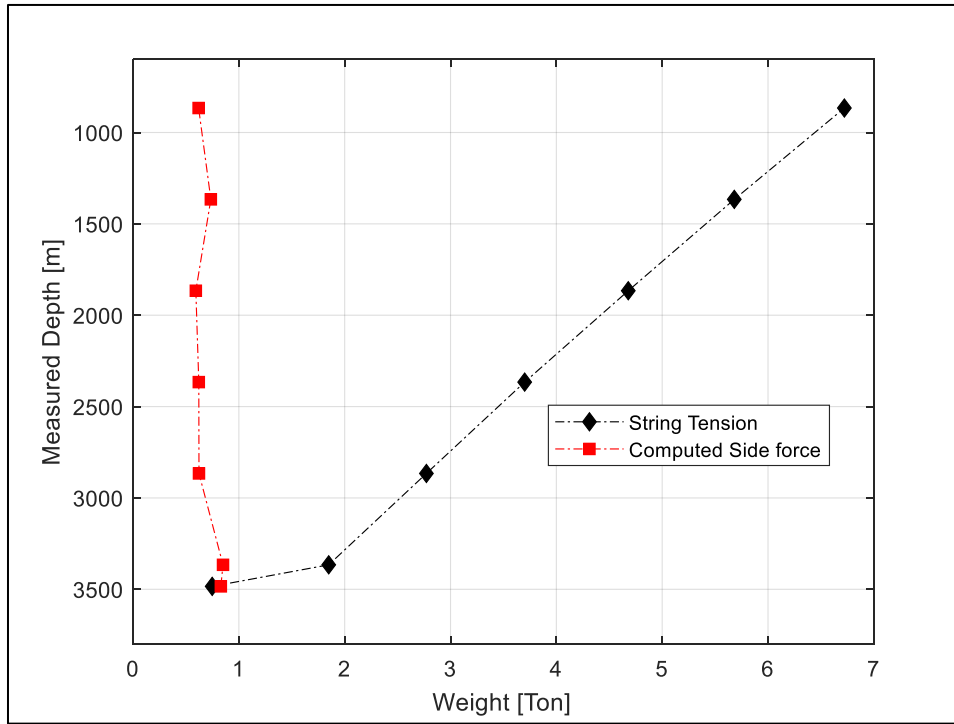
Figure 5-17: Computed side force and string tension for the 15/9-F-4 wellbore
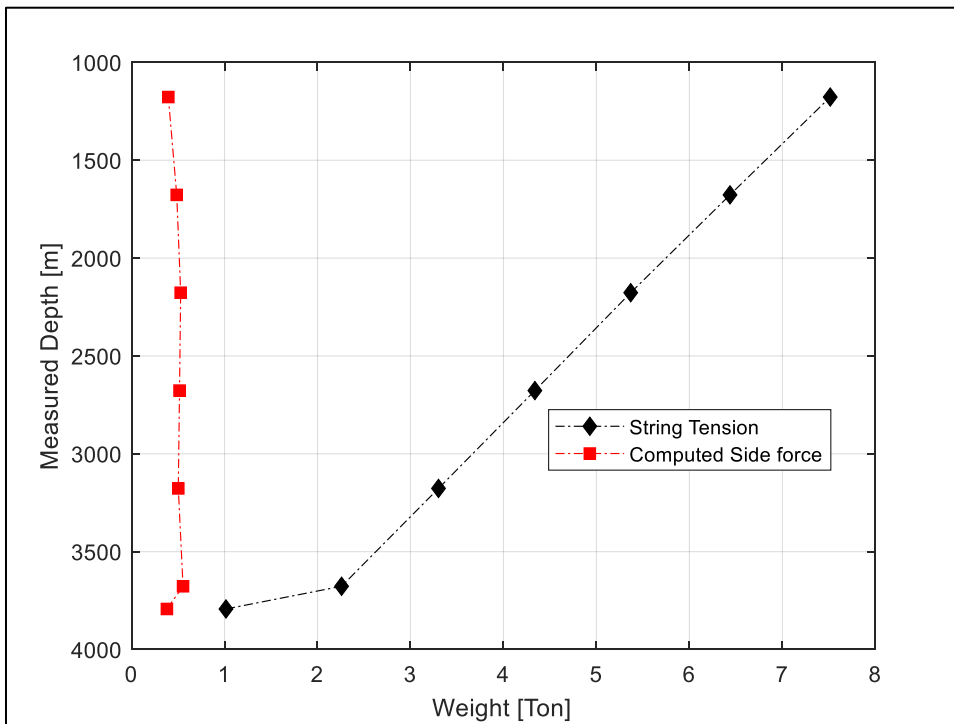
Figure 5-18: Computed side force and string tension for the 15/9-F-5 wellbore
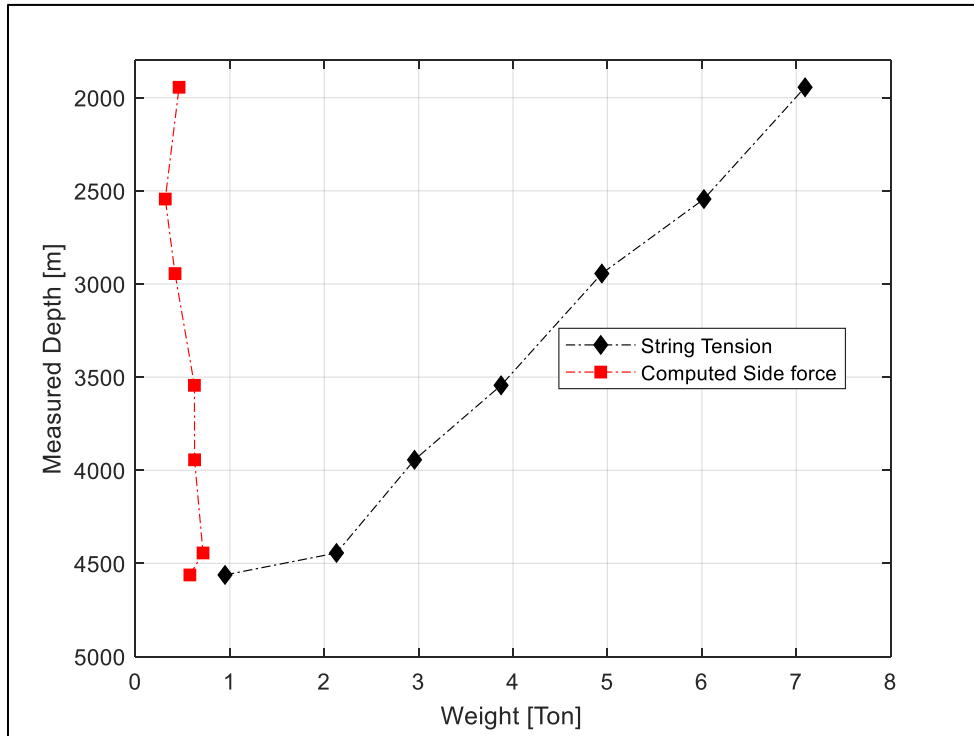
Figure 5-19: Computed side force and string tension for the 15/9-F-11T2 wellbore
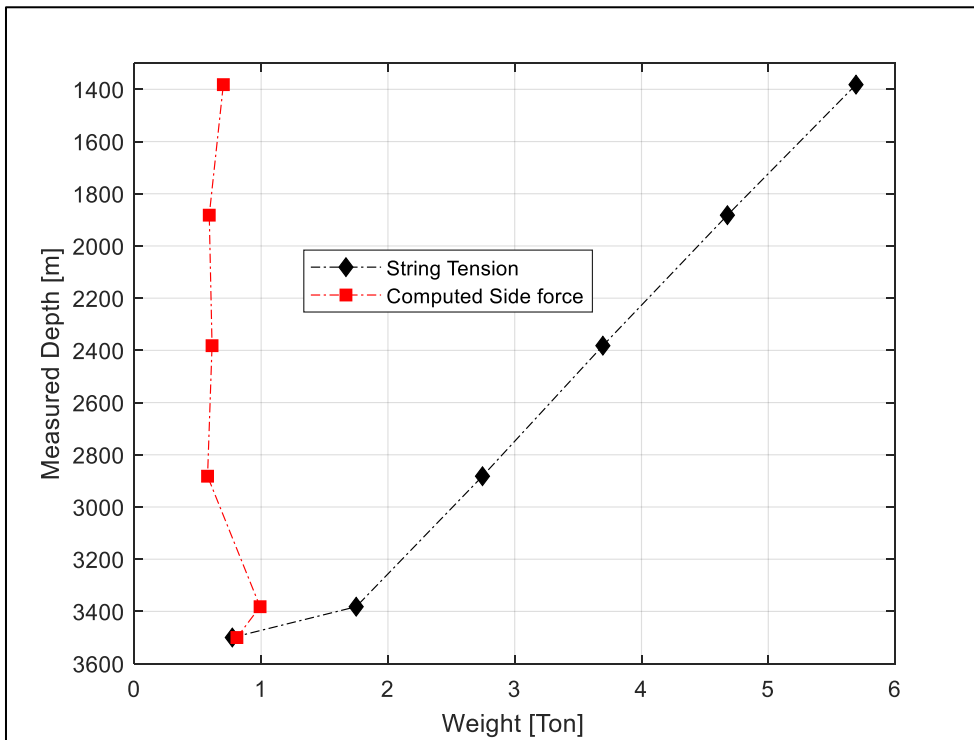
Figure 5-20: Computed side force and string tension for the 15/9-F-12 wellbore

5.6   Discussion of computed side force and string tension

As indicated by the plots from figure 5-16 to 5-20, the side force and string tension obtained were discussed basing on the response of other parameters such as DLS and inclination angle. This was due to the absence of reference case data for validation. The details of discussion are presented below:

- From well 34/10-C-47 the side force was observed to increase at the beginning and then decreased from 1788 mMD towards 3288 mMD, it increased again towards 3788 m MD before it finally decreased towards 4288 mMD as seen in figure 5-16. This behavior of the side force was supported by the nature of the curve of computed DLS in figure 5-9 at which it increased and decreased in the similar manner as the SF. The string tension computed was observed to decrease with depth from 1500 mMD to 2788 mMD, it increased towards 3288 mMD then decreased towards 4288 mMD.

- The 15/9-F-4 wellbore indicated that the side force increased from 866 mMD towards 1366 mMD. It then started to decrease towards 2866 mMD and increasd again towards 3366 mMD and finally decresed to 3484 mMD as observed in figure 5-17. This behavior can be caused by the effect of incraease and decrease of comuted DLS as shown on figure 5-10. The string tension computed was observed to decrease with depth from the begginng to to the end of the selected depth interval.

- As observed from the plot of 15/9-F-5 wellbore in figure 5-18, the side force started to increase from 1177 mMD towards 3677 mMD before it derceased towards 3793 mMD. The string tension computed was seen to decrease with depth from 1177 mMD towards 3793 m MD. The decrease and incraese of side force results from the increase/decrease trend of computed DLS as seen in figure 5-11.

- The side force computed for 15/9-F-11 wellbore was seen to decrease from 1944 mMD towards 2944 mMD, then increased towards 3544 mMD and finally decreased toward 4562 mMD as supported by the plot in figure 5-19. The string tension computed was observed to decrease with depth from the begginng to to the end of the selected depth interval.

- From 15/9-F-12 wellbore the side force began to decrease from 1382 mMD towards 2882 mMD, it increased towards 3382 mMD and finally decreased toward 3500 mMD. The string tension computed was observed to decrease with depth from 1382 mMD towards 3500 mMD.

5.7   Results of allowable DLS and side force limits

5.7.1   Allowable DLS limits results

The allowable DLS was obtained by setting new DLS with two values in a sense that, when DLS < 3, new DLS = 0, and when DLS > 3, new DLS = 3. Then, new DLS was plotted together with the computed DLS from the selected models as indicated from figures 5-21 to 5-25.
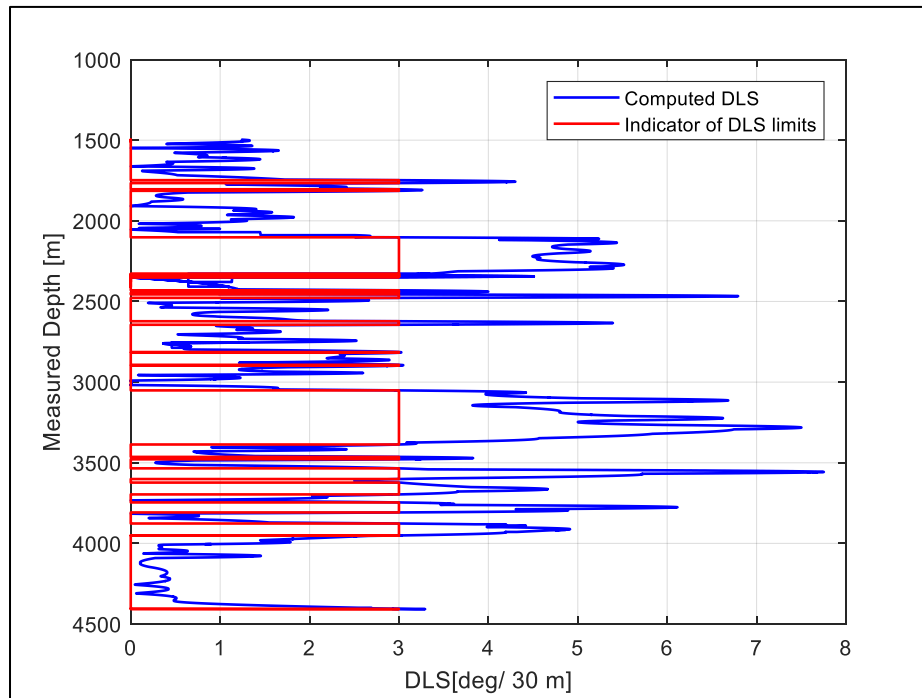

Figure 5-21: Indication of the exceedance of allowable DLS for 34/10-C-47 wellbore. When the red line reads zero, DLS is allowable and when it reads 3, DLS is not allowable
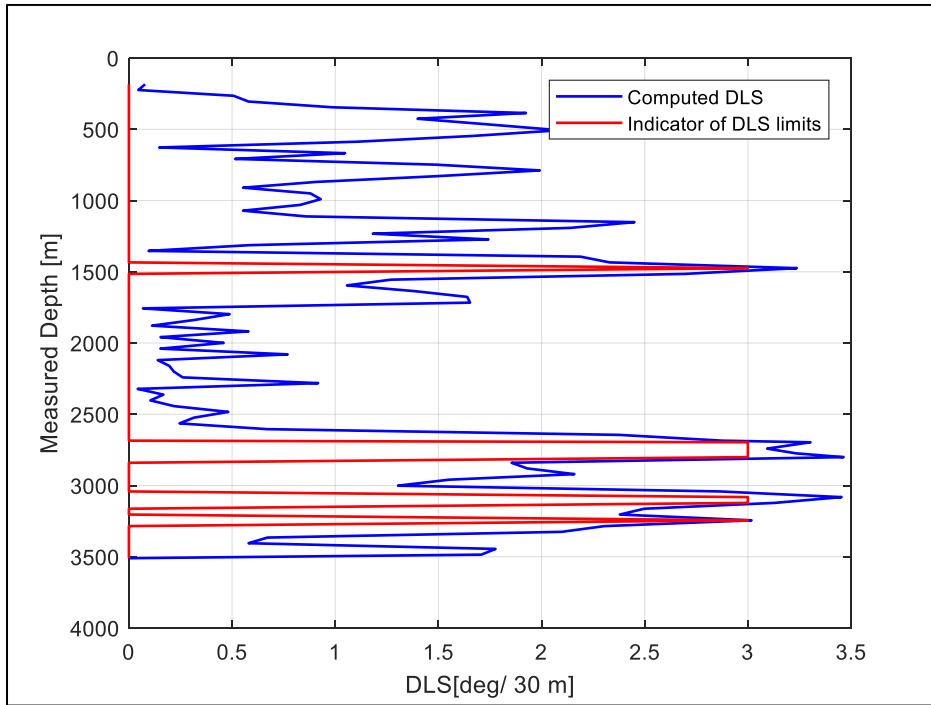
Figure 5-22: Indication of the exceedance of allowable DLS for 15/9-F-4 wellbore. When the red line reads zero, DLS is allowable and when it reads 3, DLS is not allowable
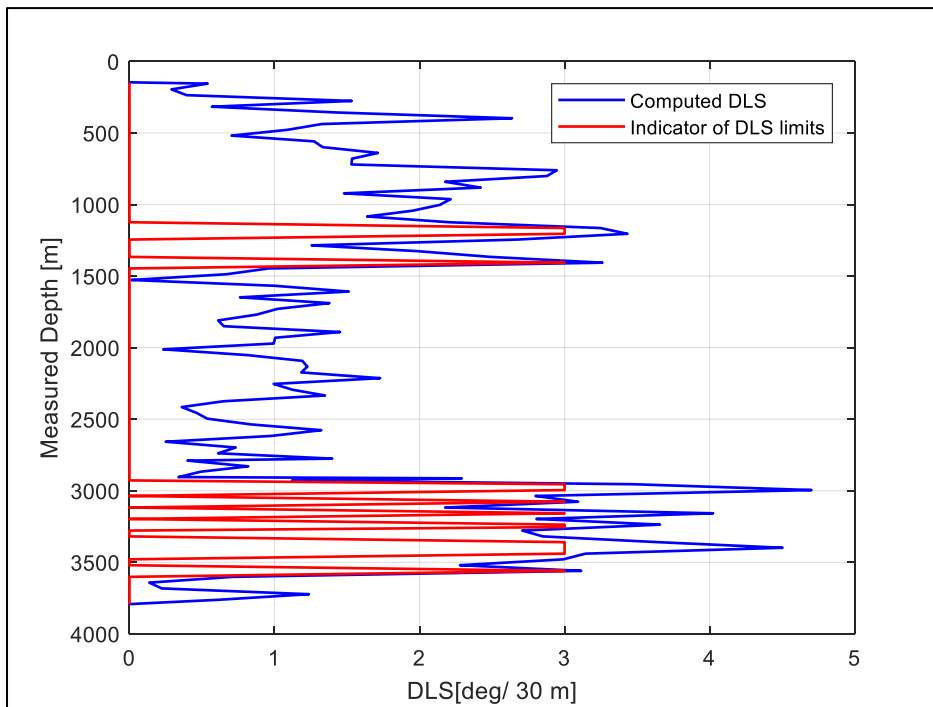
Figure 5-23: Indication of the exceedance of allowable DLS for 15/9-F-5 wellbore. When the red line reads zero, DLS is allowable and when it reads 3, DLS is not allowable
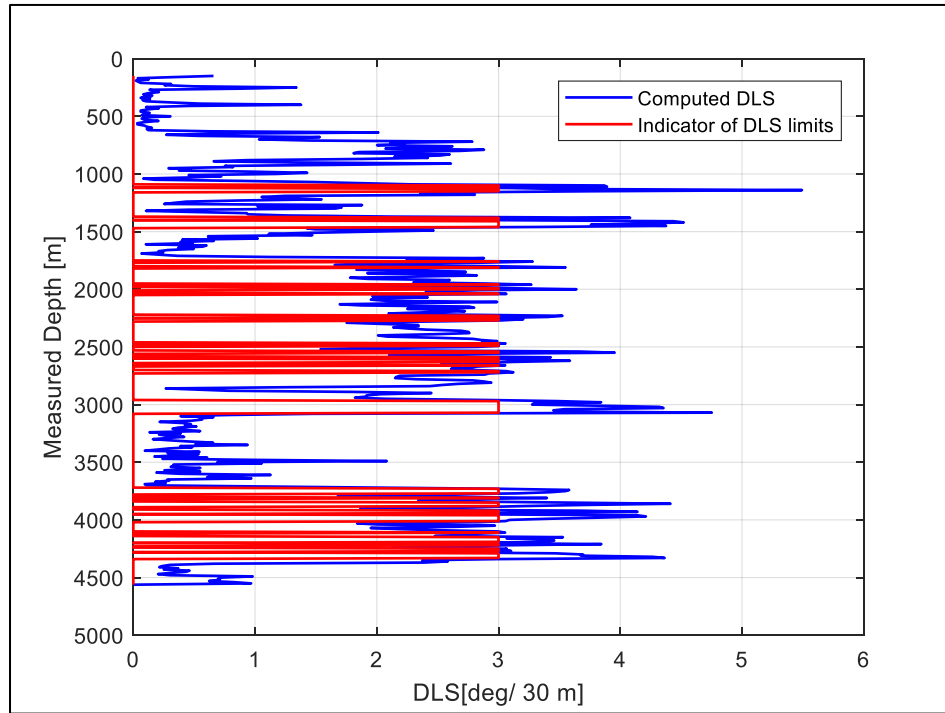
Figure 5-24: Indication of the exceedance of allowable DLS for 15/9-F-11 wellbore. When the red line reads zero, DLS is allowable and when it reads 3, DLS is not allowable
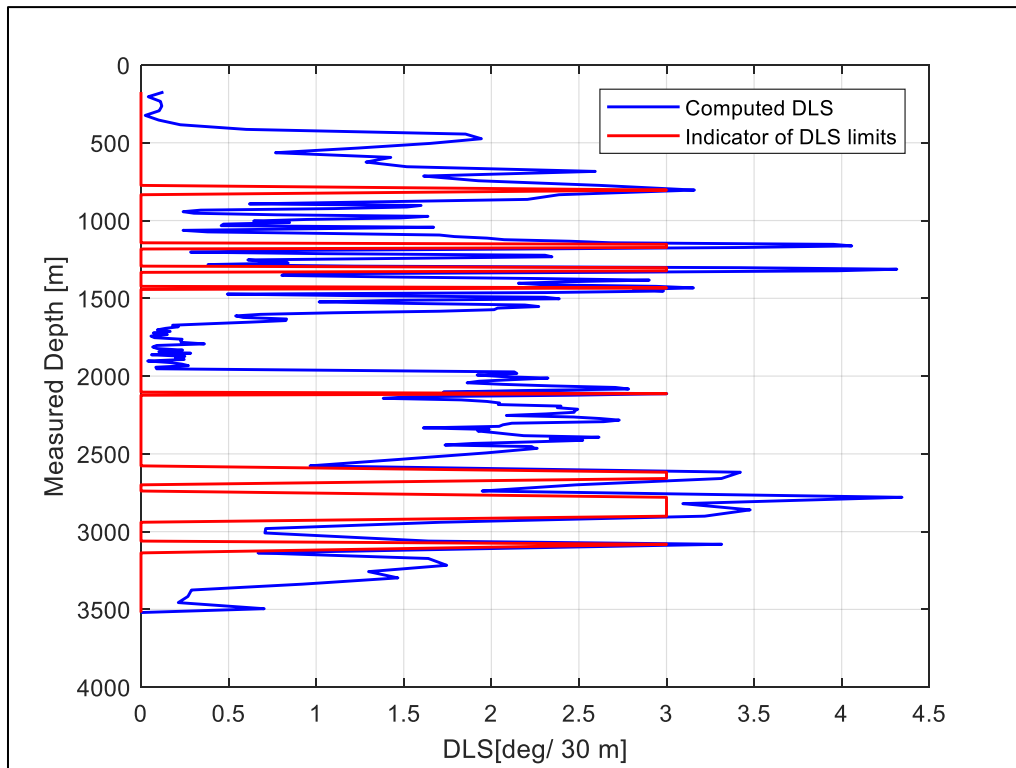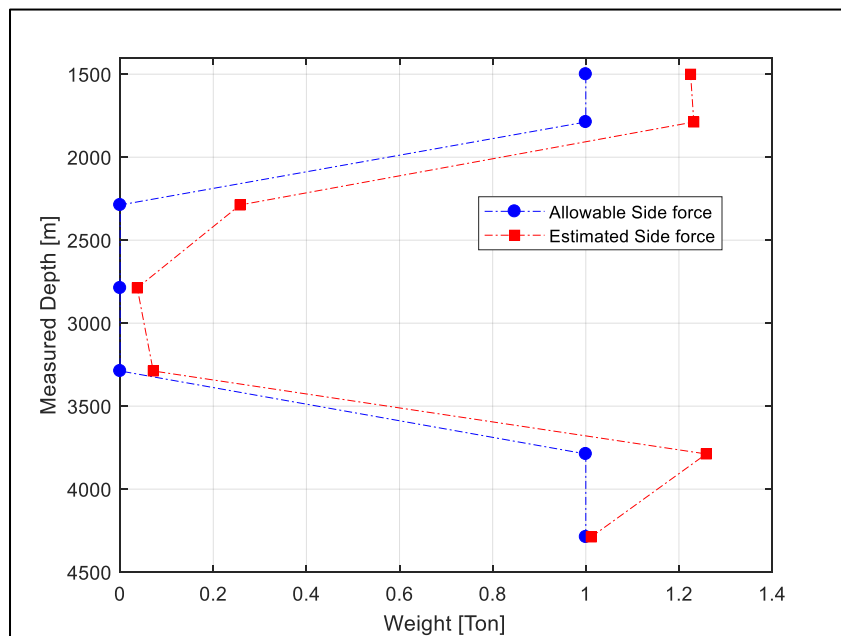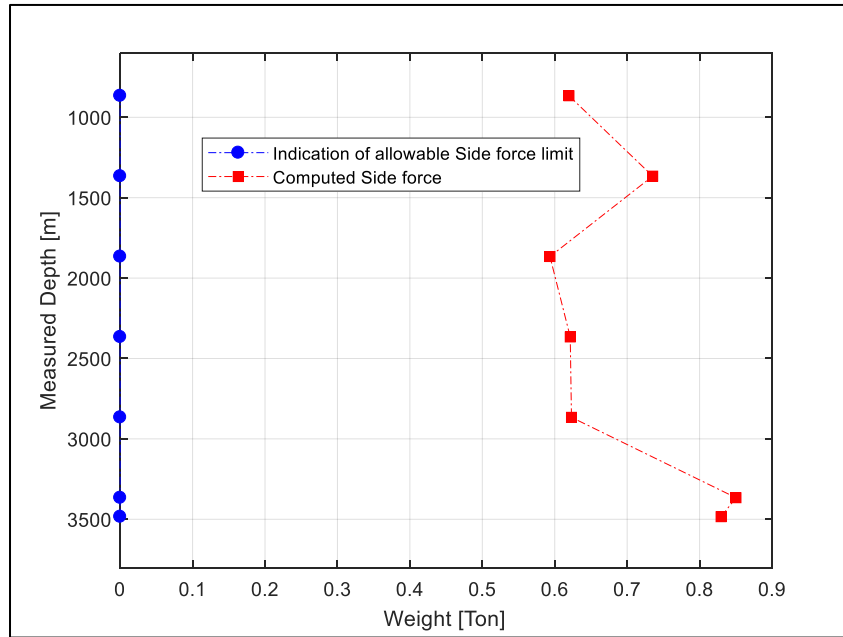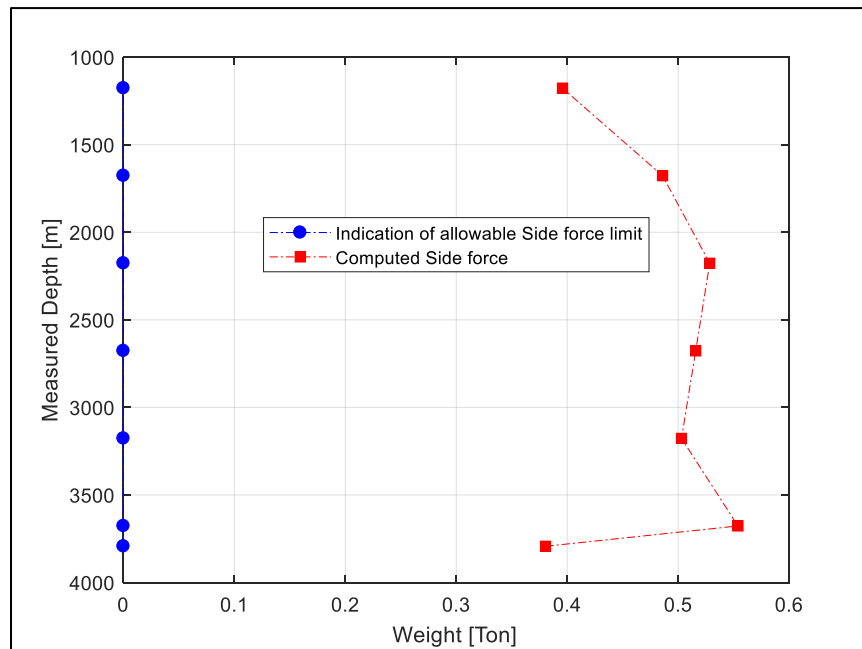

Figures 5-25: Indication of the exceedance of allowable DLS for 15/9-F-12 wellbore. When the red line reads zero, DLS is allowable and when it reads 3, DLS is not allowable.

5.7.2 Discussion from allowable limits of DLS

From the literature reviewed particularly on the work by Eastman Oil Well Survey Co presented by Arthur, (1961), the hole curvature of less than 3 º / 30 m does not cause any problem during tripping operation. This limit is acceptable and allowable to avoid failures such as stuck pipe.

From the plot, it was clear to establish a point at which computed DLS was higher than the recommended threshold value. All new DLS with value of zero represented allowable DLS, while all new DLS with values of 3 º / 30 m represented unaccepted DLS. The point was to establish DLS greater than 3º / 30 m in order to make analysis of potential areas prone stuck pipe during tripping as shown from figure 5-21 to 5-25. From these plots there were many areas that were indicated to have DLS greater than 3 º/30 m as listed below.

- From Figure 5-21, high values were seen at different measured depth. The mostly focused parts were at 2466 mMD, 3115 mMD, 3280 mMD, 3556 mMD and 3775 mMD and the highest of all was 7.7 º / 30 m at 3556 m MD. These high values could possibly result from several faults drilled in the well 34/10-C-47 from 3120 mMD to 4350 mMD. Furthermore, these faults had layers whose eastern dip angle was about 5-10 degrees as presented in the EoW report by Lise, et al., (2007)

- Based on figure 5-22, the DLS computed was slightly higher than the recommended, these values were observed at 1449 mMD, 2693 mMD, 2763 mMD, 3057 mMD and 3226 mMD with the highest of all being 3.5 º / 30 m which was observed at 2801 mMD. This value was high possibly due to dynamic behavior of the drill string especially the BHA because it had been stated in the EoW report that; the BHA at this point was not capable of achieving the planned DLS and the walk tendencies whilst drilling were not consistent (Birkeland, et al., 2008).

- From figure 5-23, unaccepted values of computed DLS were seen at 1385 mMD, 2970 mMD, 3135 mMD, 3384 mMD and 3532 mMD. The highest value of all was 4.7 º/30 m at 2995 mMD. One of the reasons for these values could be that the well trajectory at this depth was off because of the inability to control the survey tool and there was a trip for a new BHA as it has been indicated in the EoW report by John, et al., (2009).

- Figure 5-24 indicated that the unaccepted values of computed DLS were seen at 1140 mMD, 1420 mMD, 1810 mMD, 3070 mMD and 3860 mMD with the highest value of 5.5⁰/30 m at 1140 mMD. The EoW by Linn, et al., (2013) shows that, this high value could probably be due to pick up of the 8 ½" BHA and reduction of ROP due to problems with building angle.
- From Figure 5-25, the noticeable high and unaccepted values of computed DLS were observed at 1163 mMD, 1313 mMD, 2779 mMD, 2839 mMD and 3070 m MD whose highest value was 4.3 ⁰/30 m. This could be due to bad signal quality of signals presented at the same depth in the EoW especially at the start of the 12.25'' section (Colin, 2007).

5.7.3   Allowable side force limit results

As it was done when reporting the allowable DLS limit, the allowable values were obtained by setting new side force with two values in a sense that, when side force < 1 ton, new side force = 0 ton, and when side force > 1 ton, new side force = 1 ton. Then, new side force was plotted together with the computed side force against measured depth as shown from figure 5-26 to 5-30. All new side force with values of zero represented allowable side force, while all new side force with values of 1 represented unaccepted side force.

Figure 5-26: Indication of the exceedance of allowable side force for 34/10-C-47 wellbore. When the red line reads zero, side force is allowable and when it reads 3, SF is not allowable

Figure 5-27: Indication of the exceedance of allowable side force for 15/9-F-4 wellbore. When the red line reads zero, side force is allowable and when it reads 3, side force is not allowable.
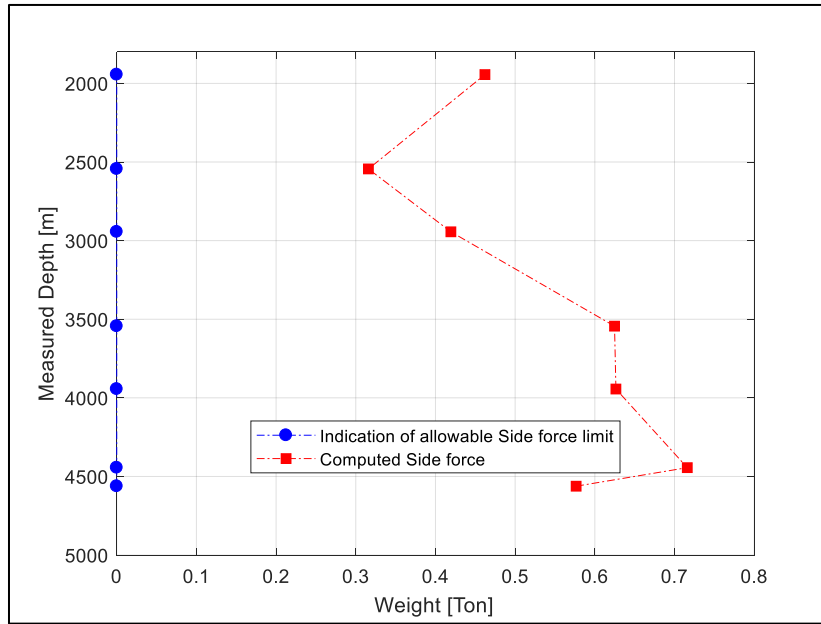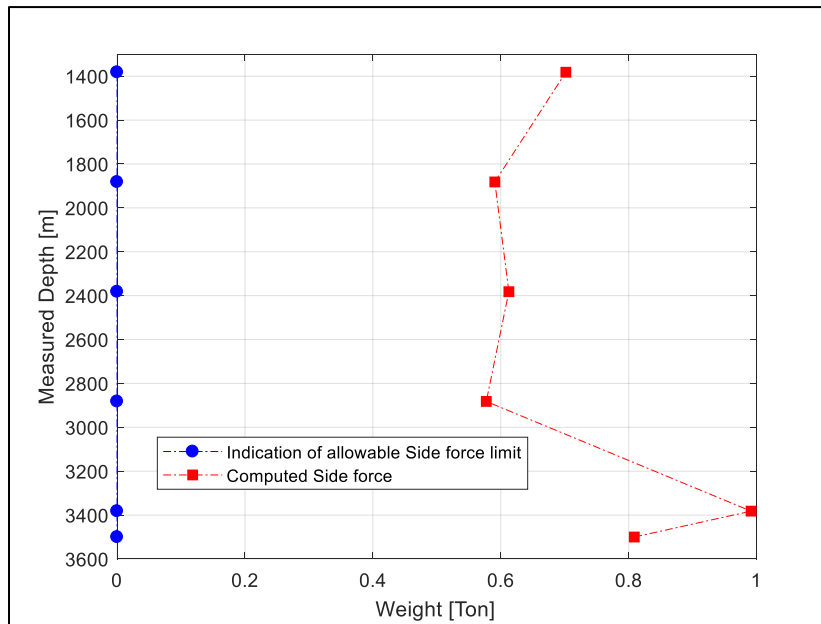

Figure 5-28: Indication of the exceedance of allowable side force for 15/9-F-5 wellbore. When the red line reads zero, side force is allowable and when it reads 3, side force is not allowable.

Figure 5-29: Indication of the exceedance of allowable side force for 15/9-F-11 wellbore. When the red line reads zero, side force is allowable and when it reads 3, side force is not allowable.

Figure 5-30: Indication of the exceedance of allowable side force for 15/9-F-12 wellbore. When the red line reads zero, side force is allowable and when it reads 3, side force is not allowable.

5.7.4 Discussion from Allowable limits of side force

Based the literature reviewed, the side force whose value is not greater than 2000 lbs (equivalent to 1 ton) does not cause any problem during tripping operation. This limit is believed to be allowable to avoid failures such as stuck pipe.

From the plot from figure 5-26 to 5-30 presented, it was easy and clear to establish a point at which computed SF was higher than the recommended threshold value as expressed below.

- Referring to figure 5-26, unacceptable values were observed at 1500 m MD, 1788 m MD, 3788 m MD and 4288 m MD with the maximum value of 1.3 ton. Other values computed at specific depths were acceptable.
- From figure 5-27 to 5-30 it was interesting to see that all computed side forces at the subintervals were allowable. This implied that the side force imposed on these wellbores could not produce a serious problem such as suck pipe when tripping.

5.8 Self-assessment

This was done to show the reflection of this work in terms of challenges, weakness and limitations met when fulfilling the objectives set. The self-assessment was important for future improvement of this work. The areas that were mostly focused were: quality of data, quality of method and potential improvements

5.8.1 Assessment of the quality of data

The quality analysis of data given was important to give out the weakness of data basing on the missing data or poor data. The data used included RTDD, survey data as well as DS parameters, and their uncertainty is as explained below:

5.8.1.1 Quality of RTDD

These data were enough for computation, but the most disturbing challenge was the way they were recorded. Most of tools used for recording data did not perform as expected because some data were repeatedly recorded, and other data were not recorded as stipulated on figure 4-4 and 4-5 in chapter 4.

The data were therefore processed to make them valid for computations but resulted into non-realistic results as indicated in projections of well 34/10-C-47 from figures 5-1 to 5-10. Some of the data were not processed in order to produce compatibility with base case data for making comparison. For example, DLS was computed using raw RTDD in order to make it easy to compare with the DLS given in the survey file.

5.8.1.2 Survey data

There only serious problem observed with this data was that, sometimes the MWD/LWD tools could not give realistic values of azimuth and inclination for well for example, well 15/9-F-11 at 2156 m MD as stipulated in appendix C (d). This resulted in wrong computations of values such as DLS, easting, northing and TVD and thus making validation harder.

5.8.1.3 DS parameters

It was very difficult to assess the quality of DS parameters as all data used were assumed. This is because there was no given data file for computation and validation of side force. The data used were assumed from other.

5.8.2 Quality of method

This part points to the weakness, problems or challenges of models selected and data agent used for computation. The selected models and the data agents were assessed separately.

5.8.2.1 Quality of DLS model

In most cases the model selected to estimate DLS performed well as depicted from figure 5-11 to 5-15. The only problem with this model was that, it did not produce the intended DLS value when the survey interval was very small. Figure 4-8 shows some NaN values that were obtained when both dogleg angle and survey interval were zero. The model produced extremely large (close to infinite) values when the survey interval was almost zero.

5.8.2.2 Quality of side force and string tension models

It was not easy to assess the quality of the model used to calculate side force and evaluate string tension. This is because of use of a lot assumptions to obtain the drill string parameters and neglection of some important factors during computation. Lack of reference data source for side

force validation was also the hindering problem towards assessment of the model. The only way used to evaluate the findings from computation was to relate the doglegs and inclinations.

5.8.2.3 Quality of data agent

The quality of data agent used in this work was tested to check the programming mistakes as presented in chapter 4 subsection 4.3.2.4. From that test it was observed that the data agents used provided excellent programming results as the test was performed just in 2.5909 seconds without any failure and incomplete execution.

Another factor used to check the quality of data agents developed was to assess the efficiency basing on the time behavior of the codes as presented on Table 3-3 in chapter 3. This was done by using the run and time functionality of MATLAB to measure execution time as presented in figure 5-21. The functionality provides the time spent by the data agent to execute the RTDD given using profile time. Based on the figure 5-21, the main function was called just once while utilizing a total time of only 5 seconds. The time behavior of other agents was as indicated on Table 5-1. From that table it indicated that all data agents used in the present work did not exceed 5 seconds of execution. Based on the normal drilling operation, this execution time provided fast outputs and thus its efficiency is high and acceptable (Donne, 2017)

Table 5-1: Execution time of five wells tested basing on time behavior using run and time MATLAB command

Function name	Calls	Total time (s)	Self-time (s)
ThesisC_47	1	4.366	1.742
ThesisF_4	1	2.269	0.253
ThesisF_5	1	2.290	0.260
ThesisF_11T2	1	2.261	0.236
ThesisF_12	1	2.015	0.196
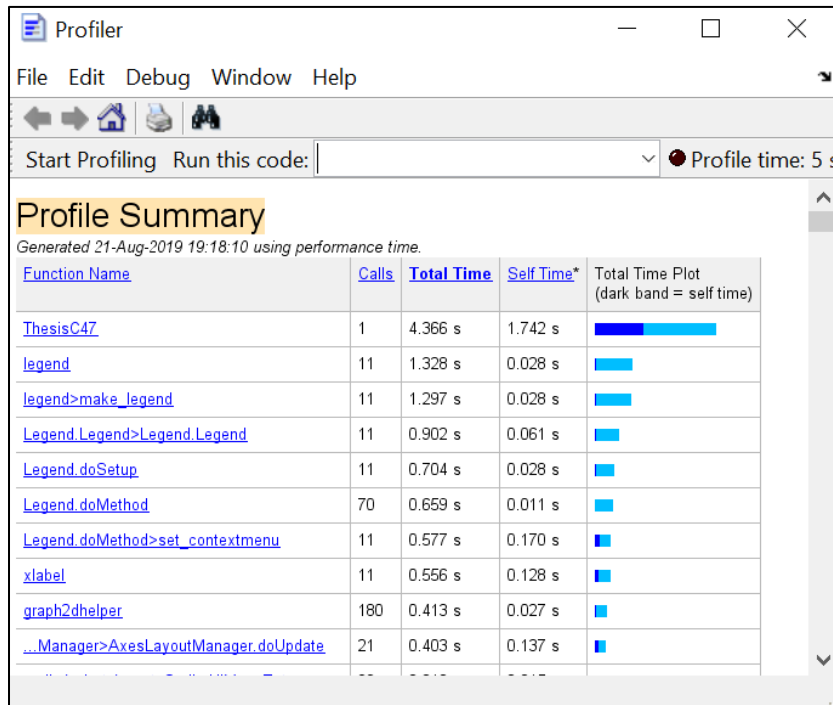
Figure 5-31: The time behavior of the data agent for 34/10-C-47 wellbore using run and time MATLAB command

Based on the assessment conducted on the quality of various inputs used to accomplish this work, the following limitations are presented as general challenges faced.

- The mathematical model selected to compute DLS did not produce the intended results when the course length was very small. The model produced some big and infinite values especially when the survey interval between two points was almost equal to zero
- The outputs from the computation of side force and evaluation of string tension were not realistic because a lot of assumptions were used during computation. It was difficult to assess the validity of side force due to lack of base case for reference
- Some of the well projections obtained were not realistic due to RTDD processing and use of only three wellbore sections data set
- The MWD/LWD tools could not produce the desired readings since they were observed to not give correct data in some areas of wellbores

5.8.3 Potential improvements

Based on the above-stated limitations, the logical improvements were to attack all the limitations for future development. This can be done by solving the limitations one by one by relying on:

- Improvement of DLS model by taking into account the effect of survey interval by including a scale factor for rectifying the effect
- Involvement of case data such as drill string parameters in order to make a proper validation of side force. Moreover, a reference base case for computation of side force should be provided
- Making a close checkup of MWD/LWD tools in order to record correct and appropriate data
- All data set from wellbore sections should be included to give out a proper and realistic wellbore view and projection
- The RTTD and survey data should be clean enough for computation in order to avoid unrealistic results from data processing

6 Conclusions

The present work was very significant because it produced data agent using MATLAB that was used to compute DLS and side force, this agent was also used to locate the areas in the well with acceptable and non-acceptable DLS and side force. However, the model selected for calculation of side force was not realistically validated due to lack of effective and efficient side force base case data. From results and discussion done it can be concluded that:

- The highest value of computed DLS from the model was 7. 7 ^{o}/ 30 m seen from 34/10-C-47 wellbore at 3556 mMD. This value deviated for more than 156% from the recommended and allowable value of DLS
- The computed side force was observed to be maximum at 3788 mMD from the 34/10-C-47 wellbore. This force was seen to increase by 30% of the recommended and acceptable value
- The MATLAB data agent is very useful when identifying different parts of the well at which such problems as stuck pipe could occur by producing some plots. The data agent developed and used in this work performed perfectly as planned
- Processing of RTDD and survey data may lead in production of unrealistic outputs

The main recommendation on this work was to make an improvement of the model used to compute DLS by considering the effect of survey interval between two points. This can be done by including a specific scale factor for taking into account such an effect.

7 Nomenclature

7.1 List of Symbols

7.1.1 Roman symbols

a	Rate of change of direction
b	Rate of change of inclination
A_1	Azimuth 1
A_2	Azimuth 2
F	Ratio factor
F_a	Axial force
F_d	Drag force
ft	Feet
I_1	Inclination 1
I_2	Inclination 2
kg	Kilogram
L_1	Length 1
L_2	Length 2
lbs	Pounds
m	Meter
ppf	Pound per feet
T	Tension
T_1	String tension at the bottom of the subinterval
T_2	String tension at the top of the subinterval
ton	Ton
ΔE	Change in Easting
ΔMD	Change in measured depth
N	Newton
ΔN	Change in Northing
ΔT	Change in tension
ΔTVD	Change in Total Vertical Depth
2D	Two dimension
3D	Three dimension

7.1.2 Greek symbols

β	Azimuth
α	Inclination
ϕ	Dogleg angle
μ	Coefficient of friction

7.2 List of abbreviations

ANTHEI	Angolan Norwegian Tanzanian Higher Education Initiative
BF	Buoyance Factor
BPOS	Block Position
BW	Buoyed Weight
CL	Course Length
CME	Chemical and Mining Department
CoET	College of Engineering and Technology
DC	Drill Collar
DLS	Dogleg severity
DBTM	Bit Depth (MD)
DMEA	Hole depth (MD)
DP	Drill Pipe
DS	Drill String
E	East
EnPe	Energy and Petroleum
ERB	Engineers Registration Board
EoW	End of well
FWR	Final Well Report
GPA	Grade Point Average
HKL	Hook-Load
IGP	Institutt for geovitenskap og petroleum
ID	Inner Diameter
Inf	Infinity
MATLAB	Matrix Laboratory
MD	Measured Depth
MW	Mud Weight
MWD/LWD	Measurement While Drilling/Logging While Drilling
N	North
NA	Not Applicable

NaN	Not a Number
NPD	Norwegian Petroleum Directory
NPT	Non-Productive Time
NORAD	Norwegian Program for Capacity Development in Higher Education and Research for Development
NTNU	Norwegian University of Science and Technology
OD	Outer Diameter
PA	Path Angle
PDC	Polycrystalline Diamond Compact
PDM	Positive Displacement Motor
P&A	Plug and abandon
RTDD	Real Time Drilling Data
S	South
SF	Side force
S-N	South North plane
TVD	True Vertica Depth
T & D	Torque and Drag
UDSM	University of Dar es Salaam
W	West
$W_{DP-String}$	Buoyed Weight of the drill string
W-E	West East plane
WOB	Weight On Bit

8 References

A.Asadi, N.Parhizgar, & E.Momeni. (2011). Prediction of Collapse in a Casing and Tubing: With Case Study of Iran. A paper, 5(11): 831-840, 2011 ISSN 1991-8178 presented at Australian Journal of Basic and Applied Sciences, Fars, (pp. 10)

Aadnoy, B. S., Larsen, K., & Berg, P. C. (1999). Analysis of Stuck Pipe in Deviated Boreholes. SPE-56628-MS paper presented at the 1999 SPE Annual Technical Conference and Exhibition, Houston, 3-6 October, 1999 (pp. 16).

Abbas Roohi, G. T. (2016). ISSN 2229-5518 Paper on An Investigation of Stuck Pipe Occurrences in Iran, Volume 7, Issue 3, Tehran, March-2016, (pp. 6).

Ahmed A. Elgibaly, M. S. (2016). A study of friction factor model for directional wells. Egyptian Petroleum Research Institute, Suez.

Andrew, W., Geir, H., & Mohammad, F. (2011). Torque & Drag Analysis Using Finite Element Method, Calgary, (pp. 1-16).

Ansari, S. A. (2018). SlideShare. Retrieved from www.slideshare.net:

https://www.slideshare.net/sarwaralamsarwaralam12/stuck-pipe-78634606

Arild, H., & Petter, E. (2000). Introduction to the Gullfaks area. Statoil. Stavanger.

Arthur, L. (1961). Maximum Permissible Dog-Legs in Rotary Boreholes. SPE 1543-G, Tulsa, (pp. 175-363).

Attaway, S. (2009). MATLAB: A Practical Introduction to Programming and Problem Solving, Boston, (pp. 41-267).

Azar, J., & Robello Samuel, G. (2007). Drilling Problem and Solutions. In Drilling Engineering, Tusla, (pp. 433-454).

Bailey, L., Jones, T., Belaskie, J., Orban, J., sheppard, M., Houwen, O., . . . McCann, D. (1991). Stuck Pipe: Causes, Detection and Prevention, Cambridge, October 1991, (pp.13-p.26).

Bang, J., Jegbefume, O., Ledroz, A., & Thompson, J. (2015). Wellbore Tortuosity Analysed by a Novel Method May Help to Improve Drilling, Completion, and Production Operations. A paper SPE/IADC-173103-MS presented at the SPE/IADC Drilling Conference and Exhibition, London, 17-19 March, 2015 (pp. 16).

Birkeland, Colin, C., & Colin, C. (2008). End of Well Report for StatoilHydro Well Number 15/9-F-4, Stavanger.

Bjørn, B., Sigve, H., & Pål, S. (2016). Compendium on Introduction to Drilling Engineering, Trondheim, (pp. 1-18 & 317-327).

Botella, X, B., J.P, C., X, F., Grau, Marco, & C, Q. (2004). ISO/IEC 9126 in practice: What do we need to know?, Paper presented at the Software Measurement.

Brechan, B. A., Corina, A. N., Gjersvik, T. B., Sangesland, S., & Skalle, P. (2017). Compendium; TPG4215 Drilling Engineering, Drilling, Completion, Intervention and P&A –design and operations; Autumn 2017, Revision 1:, Trondheim, (pp1-23).

Brechan, B., Hovda, S., & Skalle, P. (2016). Compendium; Introduction to Drilling Engineering: Subsection 5.7.4, Trondheim, (pp 136-148).

Cairncross. (1969). Long-Range Forecasting From Crystal Ball to Computer. Not Indicated.

Choudhany, D. (2011, July 8). Directional Drilling Technology (Directional, Horizontal and Multilateral Drilling). Retrieved from directionaldrilling.blogspot.com/2011/07/dog-leg-severity-dls: http://directionaldrilling.blogspot.com/2011/07/dog-leg-severity-dls.html

Colin, C. (2007). End of Well Report for Statoil Well Number 15/9-F-12. Stavanger.

Donne, C. P. (2017). Masters Thesis on Parameters Detection in Real Time Drilling Data, NTNU. Trodheim.

Drilling Templates. (2015, December 25). Retrieved from drillingtemplates.wordpress.com: https://drillingtemplates.wordpress.com/category/dogleg-severity/

Gaynor, T. M., Chen, D. C.-K., Stuart, D., & Comeaux, B. (2001). Tortuosity versus Micro-Tortuosity - Why Little Things Mean a Lot. Paper SPE/IADC-67818-MS Presented At SPE/IADC Drilling Conference, Amsterdam, 27 Feb.-1 March, 2001, (p. 12).

Gaynor, T., Hamer, D., Chen, D. C.-K., & Stuart, D. (2002). Quantifying Tortuosities by Friction Factors in Torque and Drag Model. Paper SPE-77617-MS presented at SPE Annual Conference and Exhibition, San Antonio, 29 Sept- 2 October 2002 (p. 8).

Gharib, H., & Kirkhope, K. (2017). A Modified Three-Point Contact Approach for Dogleg Severity Modeling. SPE-183870-MS paper presented at the SPE Middle East Oil & Show and Conference, Manama, 6-9 March, 2017, (pp. 16).

Hess, J. (2016). Pipe Sticking Prediction Using LWD Real-Time Measurements. SPE-178828-MS presented at IADEC/SPE Drilling Conference and Exhibition, Fort Worth, 1-3 March, 2016 (pp. 15).

Holt, C. C. (2004). Forecasting seasonal and trends by exponentially weighted moving averages. International Journal of Forecasting 20 (2004), Austin, (pp. 5-10).

Houcque, D. (2005). Introduction to MATLAB for Engineering Students (Version 1.2), Northwestern, (pp. 1-74).

Hughes, B. (1995). Drilling engineering workbook.

John, W., Espen, T., Eivind, K., & Tore, E. (2009). Final Well Report, Well NO 15/9-F-5, Stavanger.

Linn, B., Per, H., Trond, K., & Per, F. (2013). Final Well Report for Wells: NO 15/9-F-11 & T2, NO 15/9-F-11 A, NO 15/9-F-11 B, Stavanger.

Lise, C., Jørn, G., & Sigurd, V. (2007). Final Well Report, Drilling and Completion, 34/10-C-47, Gullfaks C, Stavanger.

Lubinski, A. (1960). Maximum Permissible Doglegs in Rotary Boreholes. SPE 1543-G paper presented at Annual Fall Meeting of SPE, Denver, Oct. 2-5, 1960, (pp. 175-194).

Lyomov, S. (2017, January 11). Directional Diamond Drilling – Definitions, terms and simple calculations. Retrieved from Coringmagazine.com/article/directional-diamond-drilling-definitions-terms-simple-calculations: https://coringmagazine.com/article/directional-diamond-drilling-definitions-terms-simple-calculations/

Mathworks. (2019, May 12). mathworks.com. Retrieved from www.mathworks.com/discovery/model-based-testing.html: https://www.mathworks.com/discovery/model-based-testing.html

Menand, S., Mills, K. A., & Suarez, R. (2016). Micro Dogleg Detection with Continuous Inclination Measurements and Advanced BHA Modeling. SPE-183299-MS paper presented at SPE Abu Dhabi International Petroleum Conference and exhibition, Abu Dhabi, 7-10 Novemeber, 2016 (pp. 15).

Mitchell, R. F. (2006). Drilling Engineering. In Petroleum Engineering Handbook, Richardson TX (pp. 442-463).

Muqeem, A., M., Weekse, E., A., Al-Hajji, & A., A. (2012). Stuck Pipe Best Practices - A Challenging Approach to Reducing Stuck Pipe Costs. SPE-160845-MS paper presented at SPE Saudi Arabia section Technical Symposium and Exhibition, Al-Khobar, 8-11 April 2012 (pp. 10).

Norwegian Petroleum Directorate. (2017). Fact Pages of drillled and completed wells. Retrieved
September 23, 2018, from factpages.npd.no:
http://factpages.npd.no/FactPages/default.aspx?nav1=field&nav2=PageView%7cAll&nav
3=4444332

Oketch, B. A. (2014). A report No. 27 on Analysis of Stuck Pipe Incidents in Menengai, Nakuru,
2014, (pp.567-594)

Salminen, K., Cheatham, C., Smith, M., & Valiulin, K. (2016). Stuck Pipe Prediction Using
Automated Real-Time Modeling and Data Analysis. SPE-178888-MS paper presesnted at
IADC/SPE Drilling Conference and Exhibition, Fort Worth, 1-3 March, 2016 (p. 20).

Schlumberger. (2019, June 11). glossary.oilfield.slb.com. Retrieved from
www.glossary.oilfield.slb.com/en/Terms/d/dog_leg.aspx:
https://www.glossary.oilfield.slb.com/en/Terms/d/dog_leg.aspx

Skalle, P. (2014). Best Practice For Construction of Data Agents. Trondheim.

Softdrill. (2018, June 12). www.softdrill.nl. Retrieved from A Softdrill Web site:
https://www.softdrill.nl/help/tdrag/index.htm?context=150

Techopedia. (2019, July 14). Techopedia. Retrieved from www.techopedia.com:
https://www.techopedia.com/definition/1292/agent

The MathWorks, I. (2005). MATLAB: The Language of Technical Computing (Programming,
Version 7), Natick, (pp. 179-296).

Tony, W. (1999). Arpwhite Lecture notice on 'Software Agents'.

Tor, B., & Sigbjørn, S. (2016). Drilling Engineering Advanced Course 1, High Deviation Drilling
(TPG 4215). An examination paper on Drilling Engineering Advanced Course 1, High
Deviation Drilling , (pp. 1-6).

Visual_Paradigm. (2019, May 01). visual-paradigm. Retrieved from www.visual-paradigm.com:
https://online.visual-paradigm.com/

9 Appendices

9.1 Appendix A: Main code for compuation of DLS

```matlab
%%%%%%%%%%%%%%%%%%%%%%%%%%%%%%%%%%%%%%%%%%%%%%%%%%%%%%%%%%%%%%%%%%%%%%%%%
%%%%%%%%        DLS IN WELLBORES      %%%%%%%%%%%%%%%%%%%%%%%%%%%%%%%%%%%
%%%%%%%%%%%%%%%%%%%%%%%%%%%%%%%%%%%%%%%%%%%%%%%%%%%%%%%%%%%%%%%%%%%%%%%%%
clear % to remove all variables from the workspace
%%%%%%%%%%%%%%%%%%%%%%%%%%%%%%%%%%%%%%%%%%%%%%%%%%%%%%%%%%%%%%%%%%%%%%%%%
% 1. LOADING THE RTDD FROM DIFFERENT SECTIONS OF THE WELL
%%%%%%%%%%%%%%%%%%%%%%%%%%%%%%%%%%%%%%%%%%%%%%%%%%%%%%%%%%%%%%%%%%%%%%%%%
load C47IncAzDLS-8_5
Z=X;
load C47IncAzDLS-12_25
Y=X;
load C47IncAzDLS-17_5
%%%%%%%%%%%%%%%%%%%%%%%%%%%%%%%%%%%%%%%%%%%%%%%%%%%%%%%%%%%%%%%%%%%%%%%%%
% 2. COMBINING THE DATA FILES TO OBTAIN A SINGLE DATA FILE
%%%%%%%%%%%%%%%%%%%%%%%%%%%%%%%%%%%%%%%%%%%%%%%%%%%%%%%%%%%%%%%%%%%%%%%%%
f=fieldnames(X);
for i=1:length(f)
    W.(f{i})=[X.(f{i});Y.(f{i});Z.(f{i})];
end
%%%%%%%%%%%%%%%%%%%%%%%%%%%%%%%%%%%%%%%%%%%%%%%%%%%%%%%%%%%%%%%%%%%%%%%%%
% 3. REMOVING RTTD FROM OPERATIONS OTHER THAN DRILLING
%%%%%%%%%%%%%%%%%%%%%%%%%%%%%%%%%%%%%%%%%%%%%%%%%%%%%%%%%%%%%%%%%%%%%%%%%
DBTM=W.DBTM(W.DBTM==W.DMEA);
DMEA=W.DMEA(W.DBTM==W.DMEA);
INC=W.INC(W.DBTM==W.DMEA);
AZI=W.AZI(W.DBTM==W.DMEA);
DL_S=W.DLS(W.DBTM==W.DMEA);
WOB=W.WOB(W.DBTM==W.DMEA);
HKL=W.HKL(W.DBTM==W.DMEA);
%%%%%%%%%%%%%%%%%%%%%%%%%%%%%%%%%%%%%%%%%%%%%%%%%%%%%%%%%%%%%%%%%%%%%%%%%
% 4. SORTING TO AVOID REPITION OF DATA DURING RECORDING
%%%%%%%%%%%%%%%%%%%%%%%%%%%%%%%%%%%%%%%%%%%%%%%%%%%%%%%%%%%%%%%%%%%%%%%%%
md=unique(DMEA, 'stable');
incazicoord = unique(DMEA, 'stable');%DMEA for survey points.
azis = unique(AZI,'stable');% Azimuth for survey points
incl=unique(INC,'stable');
%%%%%%%%%%%%%%%%%%%%%%%%%%%%%%%%%%%%%%%%%%%%%%%%%%%%%%%%%%%%%%%%%%%%%%%%%
% 5. ASSIGN THE VALUES OF INCLINATION and AZIMUTH FROM 1 TO n-1
%%%%%%%%%%%%%%%%%%%%%%%%%%%%%%%%%%%%%%%%%%%%%%%%%%%%%%%%%%%%%%%%%%%%%%%%%
inc1=incl(1:(end-1));
inc2=inc1(1:(end));
azi1=azis(1:(length(inc1)));
azi2=azis(1:(length(inc2)));
%%%%%%%%%%%%%%%%%%%%%%%%%%%%%%%%%%%%%%%%%%%%%%%%%%%%%%%%%%%%%%%%%%%%%%%%%
% 6. CALCULATE EASTING, NORTHING AND TVD FOR PROJECTION OF WELL
%%%%%%%%%%%%%%%%%%%%%%%%%%%%%%%%%%%%%%%%%%%%%%%%%%%%%%%%%%%%%%%%%%%%%%%%%
%Calculating the ratio 'F' from dogleg
dogleg=acosd(cosd(inc1).*cosd(inc2)+sind(inc1).*sind(inc2)...
    .*(cosd(azi2-azi1)));
F1=(2./dogleg).*(180./pi).*tand(dogleg./2);
```

```matlab
F=fillmissing(F1,'linear','EndValues','nearest');%removing the NaN values
%by interpolation
%Calculating the change in TVD(Z)
dZ=F.*diff(md(1:length(incl)))./2.*(cosd(inc1)+cosd(inc2));
Za=cumsum(dZ);%Cumulative sum of elements in dZ
%Calculating the change in Northings(X)
dX=F.*diff(md(1:length(incl)))./2.*(sind(inc1).*cosd(azi1)+sind(inc2)...
    .*cosd(azi2));
Xa=cumsum(dX);%Cumulative sum of elements in dX
%Calculating the change in Eastings(Y)
dY=F.*diff(md(1:length(incl)))./2.*(sind(inc1).*sind(azi1)+sind(inc2)...
    .*sind(azi2));
Ya=cumsum(dY);%Cumulative sum of elements in dY
%%%%%%%%%%%%%%%%%%%%%%%%%%%%%%%%%%%%%%%%%%%%%%%%%%%%%%%%%%%%%%%%%%%%%%%%%%%
% 7. CALCULATE  DLS
%%%%%%%%%%%%%%%%%%%%%%%%%%%%%%%%%%%%%%%%%%%%%%%%%%%%%%%%%%%%%%%%%%%%%%%%%%%
DLS1=abs(acosd(cosd(W.INC(1:(end-1)))...
    .*cosd(W.INC(2:(end)))+sind(W.INC(1:(end-1))).*sind(W.INC(2:(end)))...
    .*(cosd(W.AZI(2:(end))-W.AZI(1:(end-1))))))./abs(diff(W.DMEA))*30;
%Convert obtained inf entries to NaN entries
DLS1(isinf(DLS1)) = NaN;
% Fill leading and trailing NaN entries with their nearest neighbors using
% linear interpolation
DLS=fillmissing(DLS1,'linear','EndValues','nearest');
%%%%%%%%%%%%%%%%%%%%%%%%%%%%%%%%%%%%%%%%%%%%%%%%%%%%%%%%%%%%%%%%%%%%%%%%%%%
% 8. REPORT THE ALLOWABLE LIMITS OF CALCULATED DLS
%%%%%%%%%%%%%%%%%%%%%%%%%%%%%%%%%%%%%%%%%%%%%%%%%%%%%%%%%%%%%%%%%%%%%%%%%%%
DLSNew(1:length(DLS))=0;
DLSNew(DLS>3)=3;
%%%%%%%%%%%%%%%%%%%%%%%%%%%%%%%%%%%%%%%%%%%%%%%%%%%%%%%%%%%%%%%%%%%%%%%%%%%
% 9. PLOTTING
%%%%%%%%%%%%%%%%%%%%%%%%%%%%%%%%%%%%%%%%%%%%%%%%%%%%%%%%%%%%%%%%%%%%%%%%%%%
figure(1)
subplot(1,3,1)%VERTICAL PROJECTION ON W-E PLANE
plot(Ya,Za,'b','linewidth', 1.2);
grid on
legend('(a) Vertical View on W-E Plane')
xlabel('Easting [m]')
ylabel('TVD [m]')
set(gca,'ydir','reverse')
subplot(1,3,2)%VERTICAL PROJECTION ON S-N PLANE
plot(Xa,Za,'b','linewidth', 1.2);
grid on
legend('(b) Vertical View on S-N Plane')
xlabel('Northing [m]')
ylabel('TVD [m]')
set(gca,'ydir','reverse')
subplot(1,3,3)%PLAN PROJECTION
plot(Xa,Ya,'b','linewidth', 1.2)
grid on
legend('(c) Plan View')
xlabel('Northing [m]')
ylabel('Easting [m]')
set(gca,'ydir','reverse')
figure(2)% 3D PRESENTETION OF THE WELL
plot3(Xa,Ya,Za,'b','linewidth',1.2)
grid on
```

```matlab
legend('(a) 3-D View of 34/10-C-47 wellbore')
xlabel('Northing [m]')
ylabel('Easting [m]')
zlabel('TVD [m]')
set(gca,'zdir','reverse')
set(gca,'ydir','reverse')
figure(3)% COMPUTED DLS AND DLS FROM THE SURVEY FILE
subplot(1,3,1)
plot(DLS,W.DMEA(2:end),'b','linewidth',1.2);%Calculated DLS from the model
grid on
hold on
legend('(a) Calculated DLS')
xlabel('DLS [Deg/30 m]')
ylabel('Measured Depth [m]')
set(gca,'ydir','reverse')
subplot(1,3,2)
plot(W.DLS,W.DMEA,'r','linewidth',1.2) % DLS from the file
legend('(b) DLS from SURVEY DATA')
grid on
xlabel('DLS [Deg/30 m]')
ylabel('Measured Depth [m]')
set(gca,'ydir','reverse')
subplot(1,3,3)
plot(abs(W.DLS(2:end)-DLS),W.DMEA(2:end),'k','linewidth',1.2)%difference...
%between calculated DLS and DLS from the file
legend('(c) Difference between Calculated DLS and DLS from SURVEY DATA')
grid on
xlabel('DLS [Deg/30 m]')
ylabel('Measured Depth [m]')
set(gca,'ydir','reverse')
figure(4)%REPORTING THE ALLOWABLE DLS
plot(DLS,W.DMEA(2:end),'b','linewidth',1.2) % Dogleg from file.
%title('REPORTING THE ALLOWABLE DLS LIMIT FOR 34/10-C-47 WELL')
hold on
plot(DLSNew,W.DMEA(2:end),'r-','linewidth',1.2)% rEPORTING WHEN dls > 3deg/30 m
grid on
xlabel('DLS[deg/ 30 m]')
ylabel('Measured Depth [m]')
legend('Computed DLS','Indicator of DLS limits')
set(gca,'ydir','reverse')
figure(5)%HKL AND BLOCK POSITION
subplot(1,2,1)
plot(W.HKL,W.DMEA,'r','linewidth',1.2)
set(gca,'ydir','reverse')
legend('HOOK LOAD')
xlabel('Hook Load [Ton]')
ylabel('Measured Depth [m]')
grid on
subplot(1,2,2)
plot(W.BPOS,W.DMEA,'linewidth',1.2)
set(gca,'ydir','reverse')
legend('BLOCK POSITION')
grid on
xlabel('Block Position [Ton]')
ylabel('Measured Depth [m]')
figure(6)% AZIMUTH AND INCLINATION
plot(azis,md,'linewidth', 1.2)
```

```
hold on
plot(incl,md(1:length(incl)),'linewidth', 1.2)
%title('Azimuth and Inclination for 34/10-C-47');
set(gca,'ydir','reverse')
grid on
legend('AZIMUTH','INCLINATION')
set(gca,'yLim',[1400 4500])
xlabel('Azimuth/Inclination[degree]')
ylabel('Measured Depth [m]')
%%%%%%%%%%%%%%%%%%%%%%%%%%%%%%%%%%%%%%%%%%%%%%%%%%%%%%%%%%%%%%%%%%%%%%%%%%%%
% 10. TESTING THE CODE TO EVALUATE ERRORS
%%%%%%%%%%%%%%%%%%%%%%%%%%%%%%%%%%%%%%%%%%%%%%%%%%%%%%%%%%%%%%%%%%%%%%%%%%%%
result=runtests('ThesisC47');
```

9.2   Appendix B: Main code for computaion of side force and evaluation of string tension

```
%%%%%%%%%%%%%%%%%%%%%%%%%%%%%%%%%%%%%%%%%%%%%%%%%%%%%%%%%%%%%%%%%%%%
% .CALCULATING THE SIDE FORCE AT EVERY LAST DRILLING RUN IN A WELL
% SECTION
%%%%%%%%%%%%%%%%%%%%%%%%%%%%%%%%%%%%%%%%%%%%%%%%%%%%%%%%%%%%%%%%%%%%
%clear all
T = xlsread('para');%read the xlsx file containing the sideforce parameters
%DS parameters
a=T(1,5);%average dry weight of DP (kg/m)
b=T(2,1);%length of HWDP
c=T(2,5);%average dry weight of HWDP (kg/m)
d=T(3,1);%length of DC
e=T(3,5);%average dry weight of DC (kg/m)
f=T(4,1);%length of PDM
g=T(4,5);%average dry weight of PDM (kg/m)
h=T(5,1);%length of PDC
i=T(5,5);%average dry weight of PDC (kg/m)
MW=1.3; % assumed mud weight
Dsteel=7.85;%density of steel
WOB=10;%assumed WOB (tons)
fr=0.2;%friction factor
%1. Estimation of SF and tensions at the BHA
wtd=b*c+d*e+f*g+h*i;%Average dry weight of the BHA
BF=1-(MW./Dsteel);%bouyance factor
wtt=BF*wtd./1000;%wet weight of the BHA
wdp=BF*500*a./1000; %weight of DP at every subinterval
%inclination and azimuth are estimated fom the plot of INC and AZI against
%measured depth at every 500 m from the BHA (starting 4281 m to 4399 m  )
inc1=93.01;
inc2=93.83;
azi1=179.1;
azi2=180;
%side force at the BHA
SF1=wtt*sind((inc1+inc2)/2);
%Tension below BHA
T1=0;%assuming that tension below the BHA=WOB
T2=T1+wtt*cosd((inc1+inc2)/2)+fr*SF1;%tension at the top of BHA
%2. Estimation of SF and tensions at the first subinterval
%inclination and azimuth are estimated from 3781 m to 4281 m
inc_1=93.01;
inc_2=93.84;
```

```
azi_1=179.1;
azi_2=179.5;
SF2=wdp*sind((inc_1+inc_2)/2);%side force above the BHA
T3=T2+fr*SF2+wdp*cosd((inc_1+inc_2)/2); % tension above the first subinterval
%3. Estimation of SF and tensions at the second subinterval
%inclination and azimuth are estimated from 3281 m to 3781 m
Inc_1=93.01;
Inc_2=80.52;
Azi_1=179.1;
Azi_2=183.8;
SF3=wdp*(sind(Inc_1+Inc_2)/2);%side force at the BHA
T4=T3+fr*SF3+BF*wdp*cosd((Inc_1+Inc_2)/2);%tension above  the second
subinterval
%4. Estimation of SF and tensions at the third subinterval
%inclination and azimuth are estimated from 2781 m to 3281 m
Inc1=93.01;
Inc2=90.33;
Azi1=179.1;
Azi2=138.2;
SF4=wdp*(sind(Inc1+Inc2)./2);
T5=T4+fr*SF4+BF*wdp*cosd((Inc1+Inc2)./2);%tension above  the third
subinterval
%5. Estimation of SF and tensions at the forth subinterval
%inclination and azimuth are estimated from 2281 m to 2781 m
In1=93.01;
In2=62.89;
Az1=179.1;
Az2=104.5;
SF5=wdp*(sind(In1+In2)/2);
T6=T5+fr*SF5+BF*wdp*cosd((In1+In2)/2);%tension above  the forth  subinterval
%6. Estimation of SF and tensions at the fifth subinterval
%inclination and azimuth are estimated from 1788 m to 2288 m
In_1=93.01;
In_2=62.4;
Az_1=179.1;
Az_2=107.3;
SF6=wdp*sind((In_1+In_2)/2);
T7=T6+fr*SF6+BF*wdp*cosd((In_1+In_2)/2);%tension above  the fifth subinterval
%7. Estimation of SF and tensions at the sixth subinterval
%inclination and azimuth are estimated from 1500 m to 1781 m
in_1=93.01;
in_2=59.6;
az_1=179.1;
az_2=139.8;
SF7=wdp*sind((in_1+in_2)/2);
T8=T7+fr*SF7+BF*wdp*cosd((in_1+in_2)/2);%tension above  the sixth subinterval
%COMBINING THE OBTAINED RESULTS
J=abs([SF1,SF2,SF3,SF4,SF5,SF6,SF7])';%Combining the estimated SF
N=[T2, T3,T4,T5,T6,T7,T8]'; %Combining the estimated tensions
D=[4288,3788,3288,2788,2288,1788,1500]';%Depth of subintervals
%%%%%%%%%%%%%%%%%%%%%%%%%%%%%%%%%%%%%%%%%%%%%%%%%%%%%%%%%%%%%%%%%%%%%%%%%%%
%. REPORTING WHENEVER SF > threshold values
%%%%%%%%%%%%%%%%%%%%%%%%%%%%%%%%%%%%%%%%%%%%%%%%%%%%%%%%%%%%%%%%%%%%%%%%%%%
SFNew=zeros(length(J),1);
for j=1:length(J)
if J(j)>1
    SFNew(j)=1;
```

```
else
    SFNew(j)=0;
end
end
%%%%%%%%%%%%%%%%%%%%%%%%%%%%%%%%%%%%%%%%%%%%%%%%%%%%%%%%%%%%%%%%%%%%%%%%%%%%%
% : PLOTTING
%%%%%%%%%%%%%%%%%%%%%%%%%%%%%%%%%%%%%%%%%%%%%%%%%%%%%%%%%%%%%%%%%%%%%%%%%%%%%
figure(1)
plot(N,D,'-.dk','MarkerEdgeColor','k','MarkerFaceColor','k');
%title('Computed side force and string tension for 34/10-C-47 wellbore');
grid on
hold on
plot(J,D,'-.sr','MarkerEdgeColor','r','MarkerFaceColor','r');
legend('String Tension','Estimated Side force','location','best');
ylabel('Measured Depth [m]')
xlabel('Weight [Ton]')
set(gca,'ydir','reverse')
set(gca,'yLim',[1400 4500])
figure(2)
plot(SFNew,D,'-.ob','MarkerEdgeColor','b','MarkerFaceColor','b');
%title('Computed and allowable side force for 34/10-C-47 wellbore');
hold on
plot(J,D,'-.sr','MarkerEdgeColor','r','MarkerFaceColor','r');
legend('Allowable Side force','Estimated Side force','location','best');
ylabel('Measured Depth [m]')
xlabel('Weight [Ton]')
grid on
set(gca,'ydir','reverse')
set(gca,'yLim',[1400 4500])
```

9.3   Appendix C: Plots of azimuth and inclination against depth
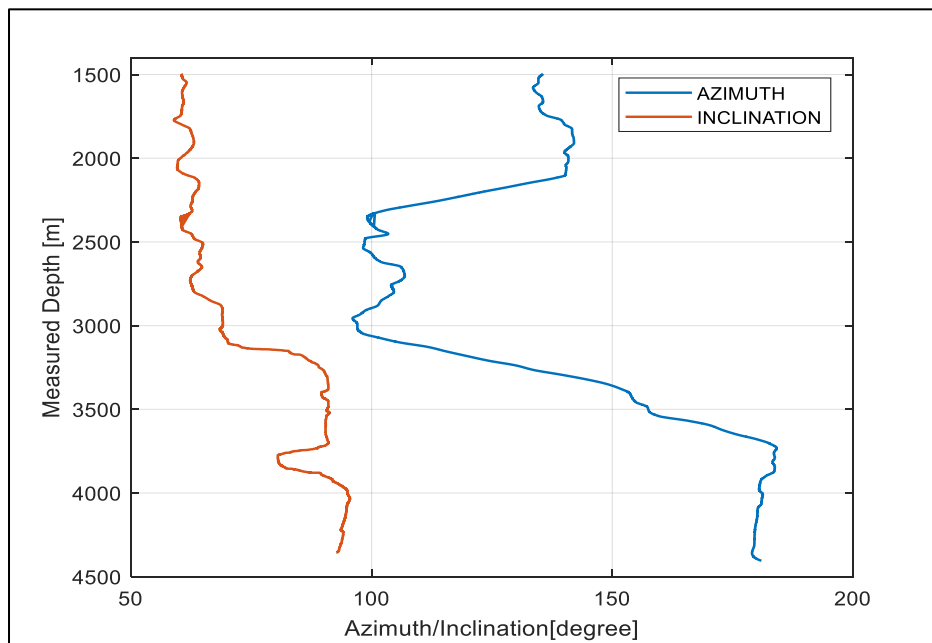
(a) Well 34/10-C-47
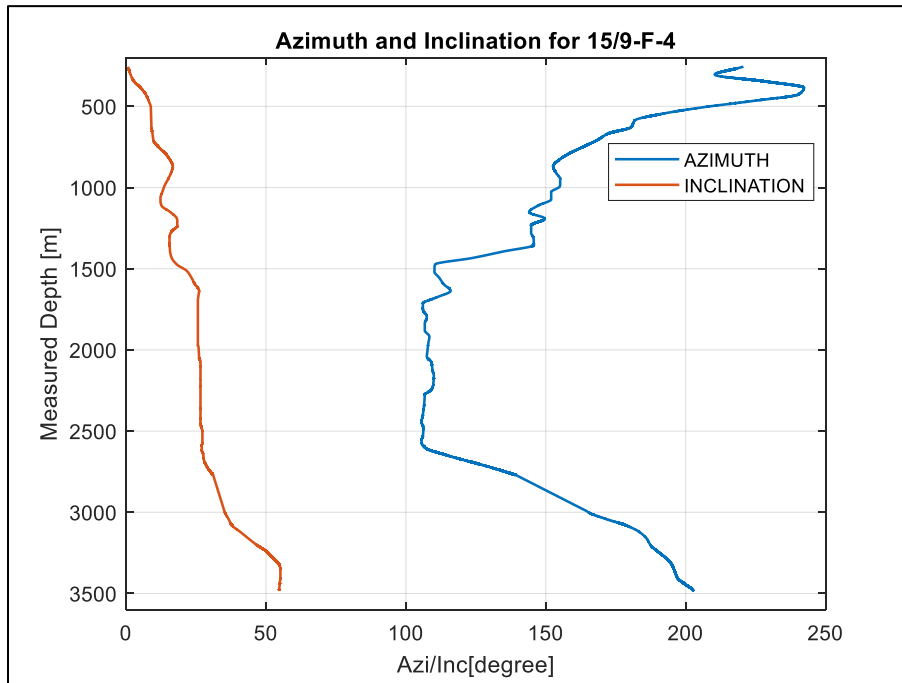
(b) Well 15/9-F-4
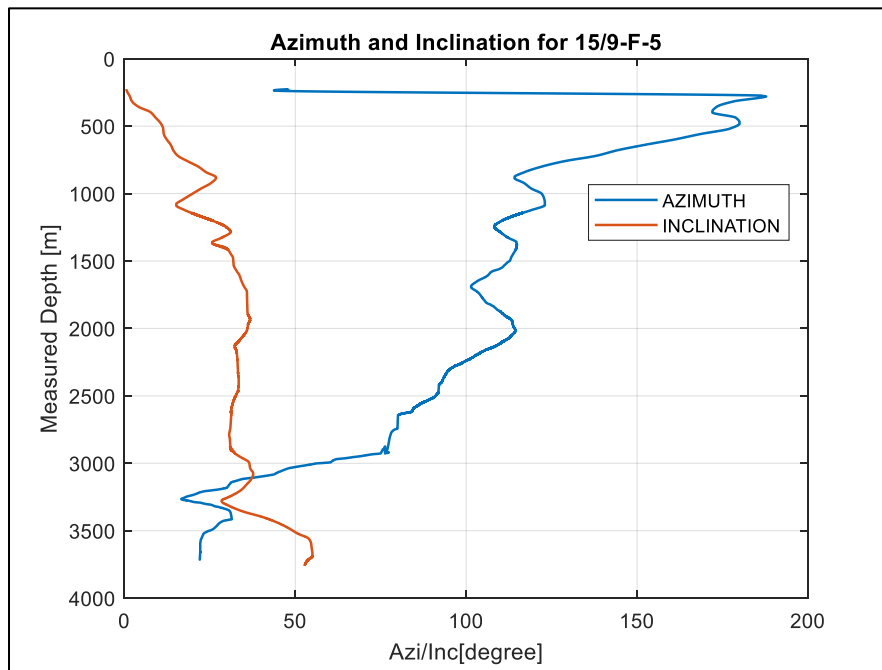
(c) Well 15/9-F-5
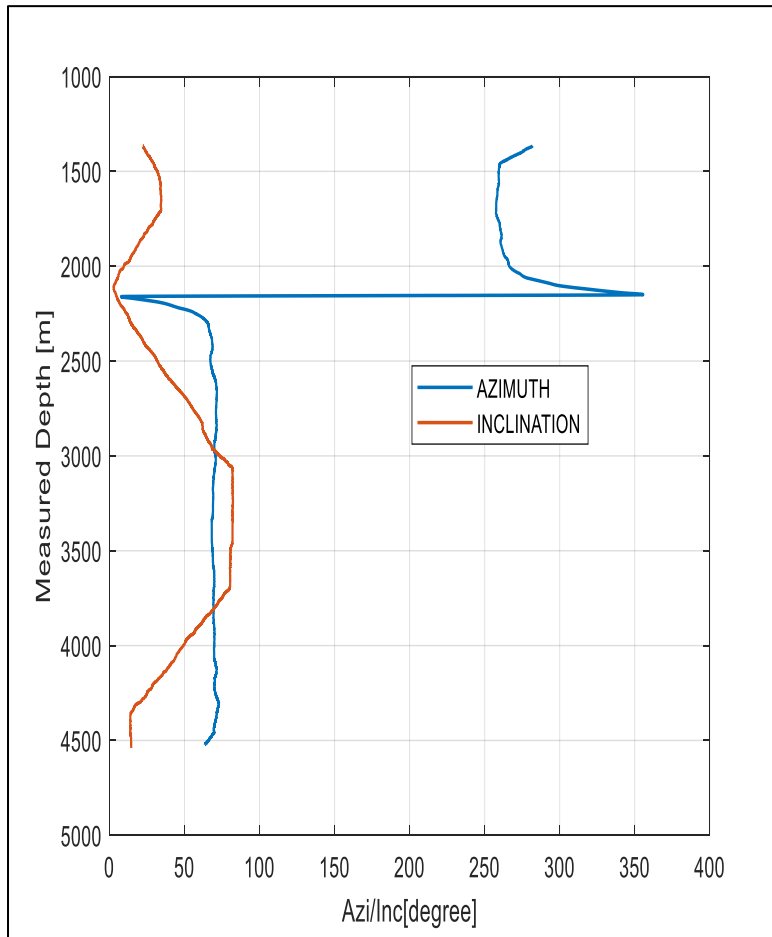
(d) Well 15/9-F-11
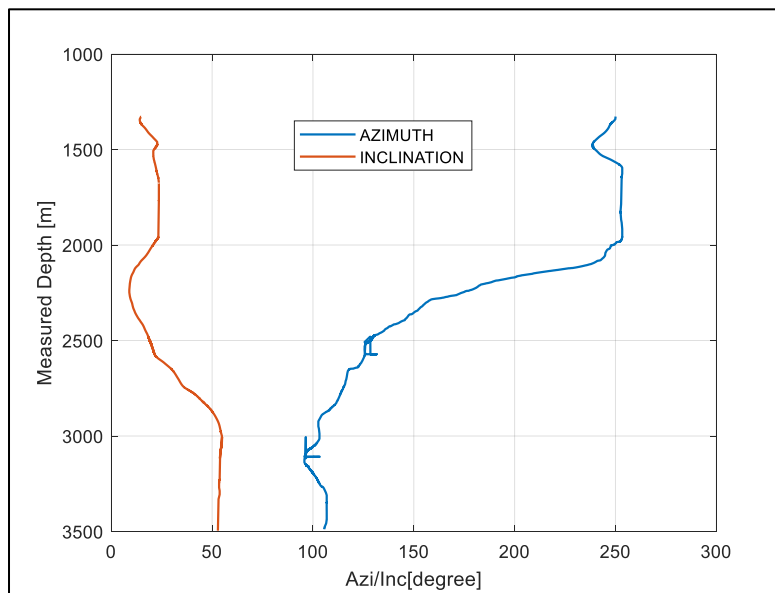
(e) Well 15/9-F-4

9.4 Appendix D: Plots of Hook Load and Block Position against measured depth
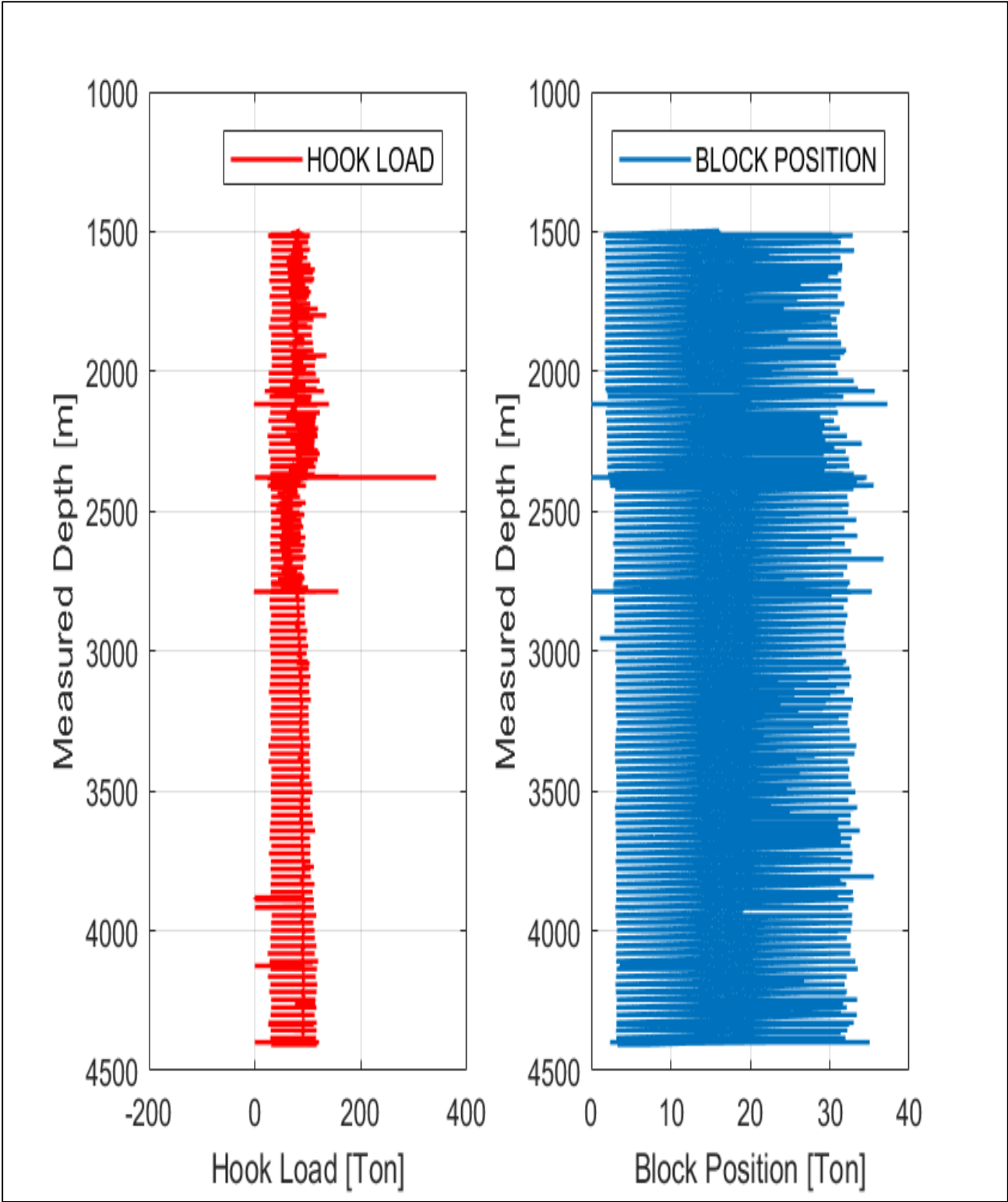
(a) HKL and BPOS for well 34/10-C-47
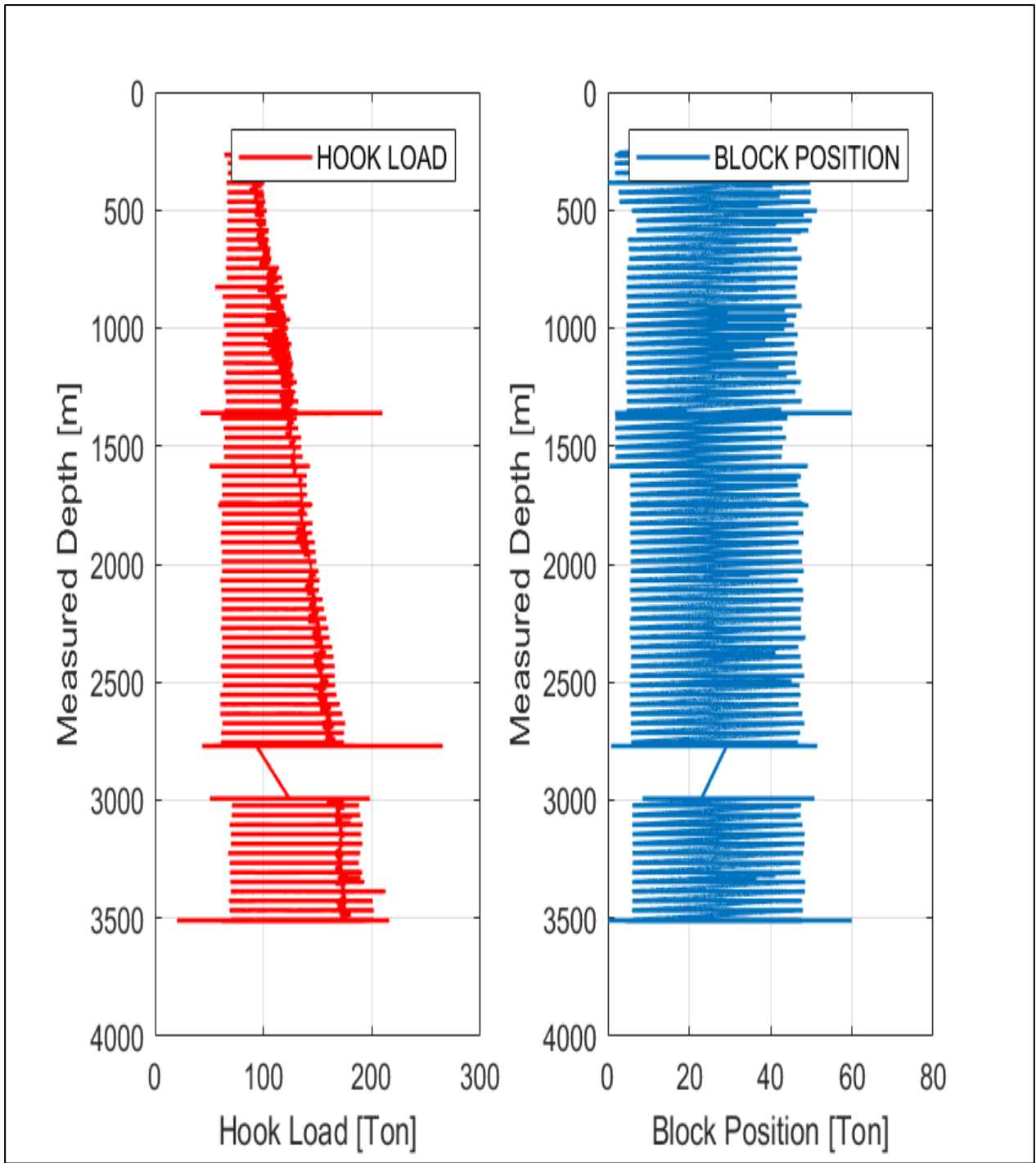
(b) HKL and BPOS for well 15/9-F-4
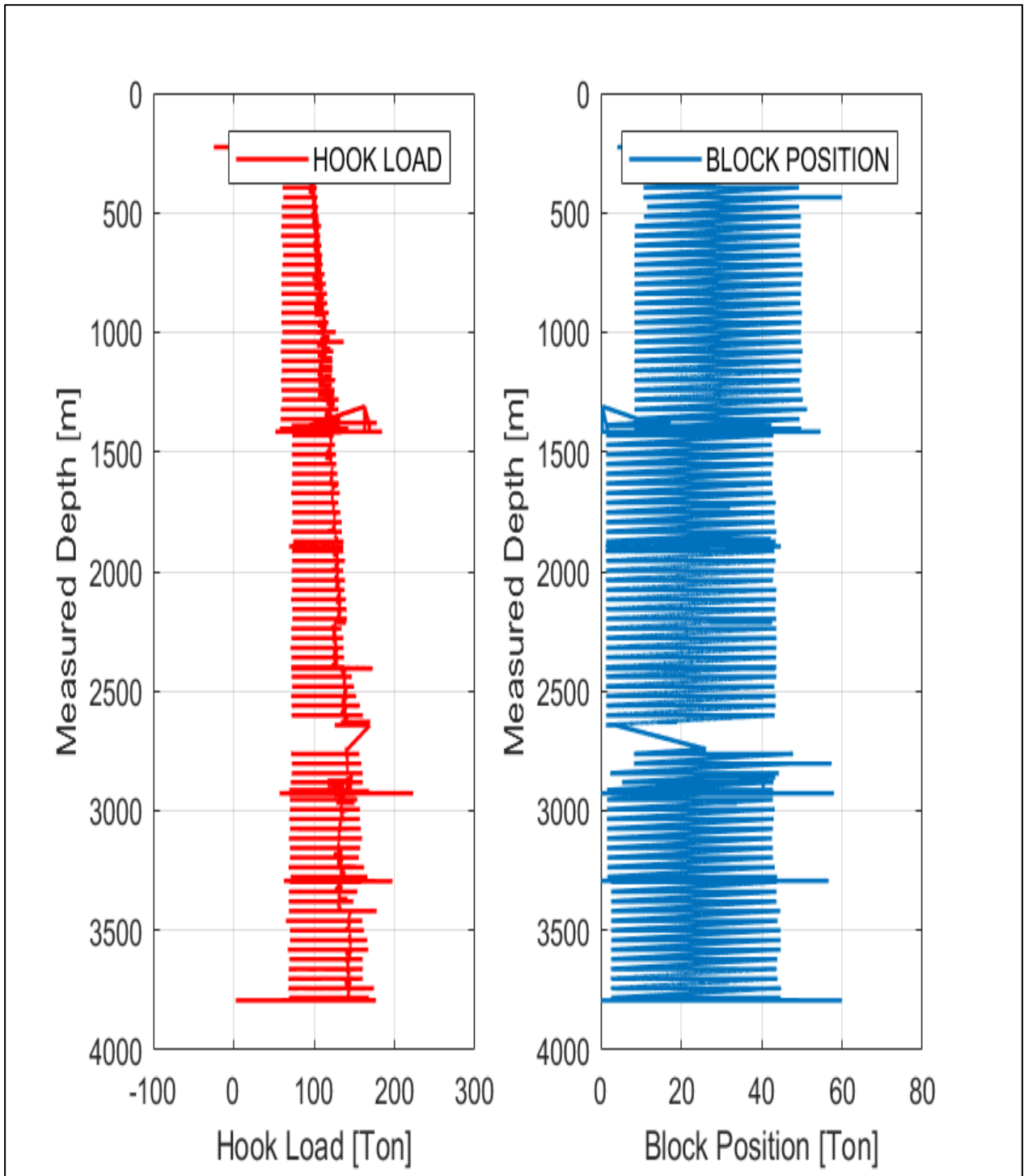
(c) HKL and BPOS for well 15/9-F-5
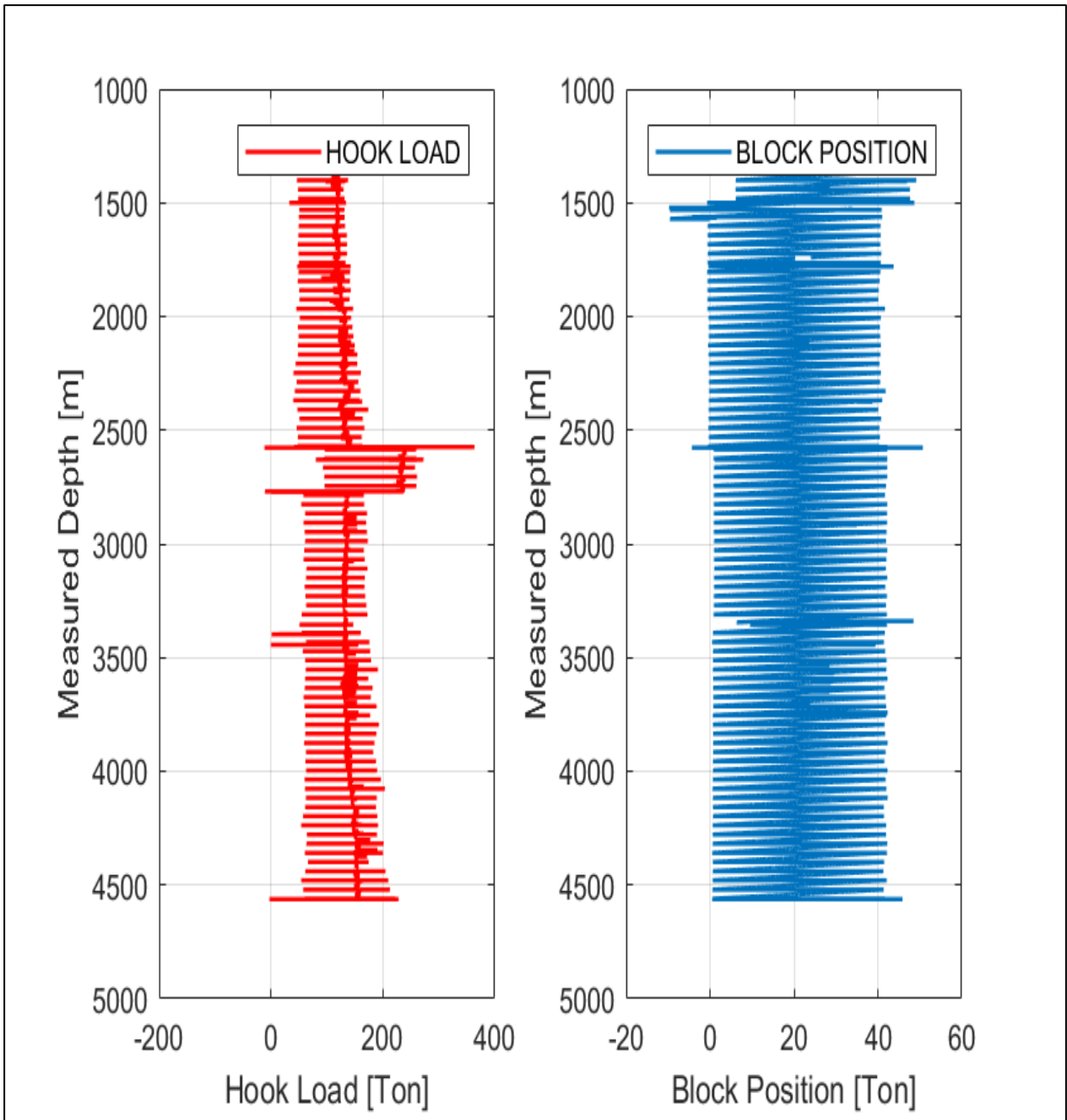
(d) HKL and BPOS for well 15/9-F-11
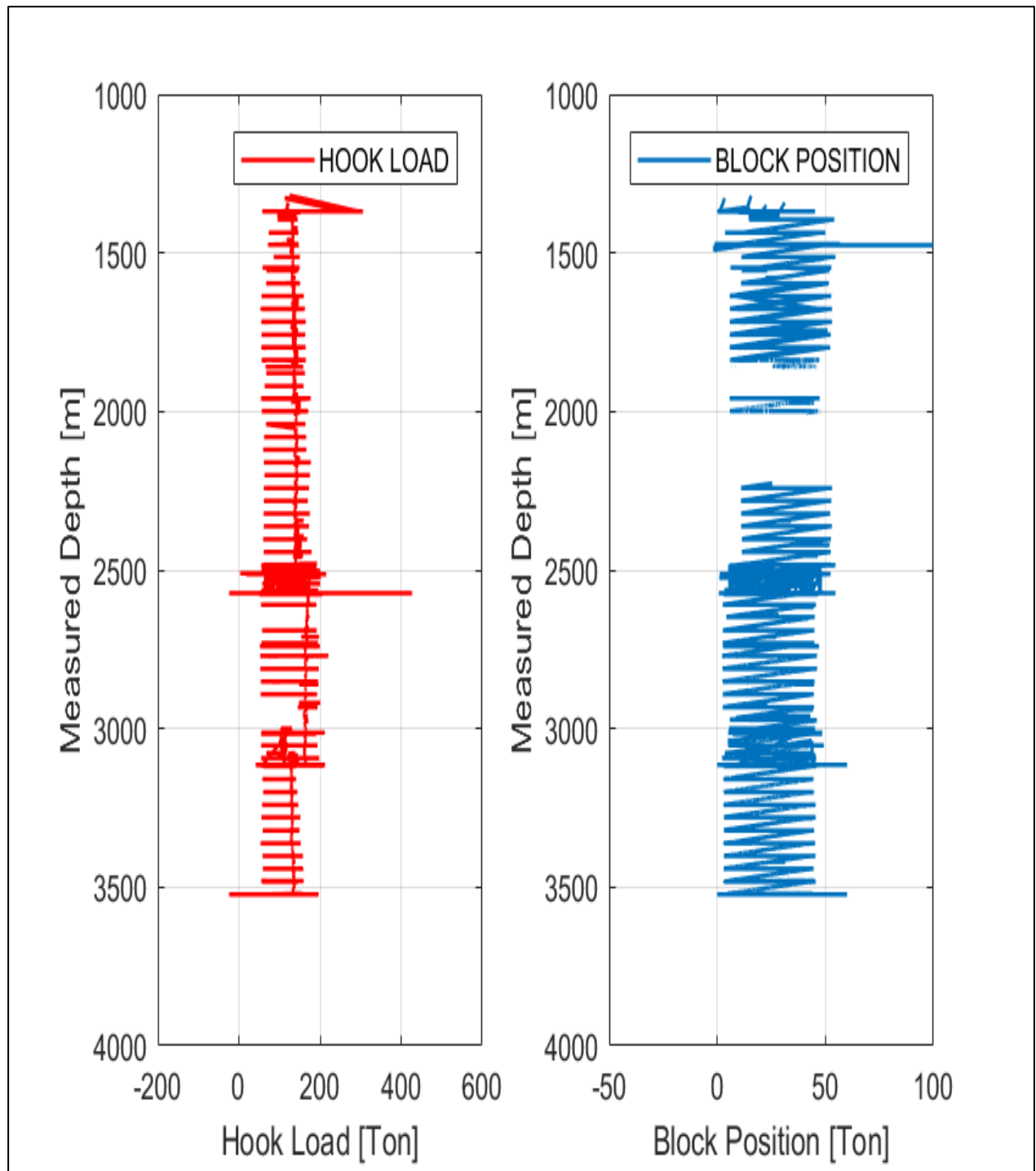
(e) HKL and BPOS for well 15/9-F-12

9.5 Appendix E: Details of Gullfaks and Volve fields

GULLFAKS FIELD		
Type	Text	Date updated
Development	Gullfaks is located in the Tampen area in the northern part of the North Sea. The water depth in the area is 130-220 meters. Gullfaks was proven in 1978, and the plan for development and operation (PDO) for Gullfaks phase I was approved in 1981. The PDO for Gullfaks phase II was approved in 1985. Production started in 1986. The field has been developed with three integrated process, drilling and home furnishings with concrete undercarriage (Gullfaks A, B and C). Gullfaks B has a simplified process plant with first-stage separation. Gullfaks A and C receives and processes oil and gas from Gullfaks South and Visund South. The Gullfaks facilities are also involved in production and transport from Tordis, Vigdis and Visund. The production from Tordis is processed in a separate plant at Gullfaks C. The PDO for Gullfaks Vest was approved in 1993, and for production from the Lunde formation in 1995. An altered PDO for Gullfaks,	04/25/2019
Reservoir	Gullfaks produces oil from Middle Jurassic sandstone in the Brent group, and from lower Jurassic and Upper Triassic sandstone in the Statfjord group and Cook and Lunde formations. There is also recoverable oil in cracked lime and slate in the overlying Shetland group and the List formation. The reservoirs are located at 1700-2000 meters deep in rotated fault blocks in the west and in a structural horst (raised fault block) in the east, with a fault zone in the middle. The reservoir quality is largely good to very good in the Jurassic reservoirs in the individual fault blocks, but poor reservoir communication is a challenge for pressure maintenance.	04/25/2019
Extraction	The drive mechanism in the main reservoirs is primarily water injection, with gas injection and water-alternating gas injection (VAG) in some areas. The drainage strategy for the Shetland / Lista reservoir has been pressure relief, but water injection has now been implemented as pressure support.	04/25/2019
Transportation	The oil is exported from Gullfaks A and C via cargo buoys to tankers. Rich gas is transported in Statpipe for further treatment at the Kårstø terminal in Rogaland.	
Status	Drilling new wells at Gullfaks has been a challenge for many years due to overpressure in some areas in the Shetland / Lista range. Production from the Shetland / Lista reservoirs gradually contributes to reducing the overpressure and making it easier to drill. Twelve new water injection and production wells were drilled in 2018, and production has been above expectations. Several wells will be drilled continuously from all facilities in 2019. The licensees carried out a pilot project in 2018 to establish water injection as a new drainage strategy in the Shetland / Lista reservoirs. Changed PDO for Shetland / List Phase II, which includes water injection and new wells, has been delivered to the government.	04/25/2019
VOLVE FIELD		
Type	Text	Date updated
Development	Volve is located in the central part of the North Sea, five kilometers north of Sleipner East. The water depth is 80 meters. Volve was proven in 1993, and the plan for development and operation (PDO) was approved in 2005. The field was	04/25/2019

	developed with a jack-up process and drilling facility, and the ship "Navion Saga" was used to store stabilized oil. Production started in 2008.	
reservoir	Volve produced oil from sandstone of middle-aged age in the Hugin formation. The reservoir is located at 2700-3100 meters deep. The western part of the structure is strongly rejected, and it is uncertain whether there is communication over the faults.	04/25/2019
Extraction	The field was produced with water injection as pressure support.	03/16/2018
Transportation	The oil was exported via tankers, and the rich gas was sent to the Sleipner A facility for further export.	03/16/2018
Status	The completion plan was presented in 2014. Production was completed in 2016, and the disposal work was completed in 2018.	04/25/2019

9.6   Appendix F: Fault evaluation encounted in well 34/10-C-47

Fault/Formation	Measured Depth [m RKB]	True Vertical Depth [m MSL]
Fault S3 (S5/S3)	3210	1975
Fault S3	3425	1999
Fault S3	3555	1998
Fault S2 (S3/S2)	3810	2000
Fault S2	4080	2005
Fault S2	4150	1999
Fault S3	4350	1985

9.7   List of figures

9.8 List of tables

10 Vita

Joseph Nkengele was born on 9th June 1990, at Bariadi District in Simiyu region-Tanzania. He is currently a registered graduate engineer by the Engineers Registration Board (ERB) of the United Republic of Tanzania. In 2016 he completed his bachelor's degree in mining engineering from the college of Engineering and Technology (CoET) at the University of Dar es Salaam (UDSM)-Tanzania. During his bachelor's degree he worked very hard and scored an overall GPA of 4.3/5.0, and soon after completion of his studies he volunteered as a graduate engineer in different small scale mine including felspar small scale mine in Tanga-Tanzania.

Basing on his good academic and social performances, he was awarded Scholarship under ANTHEI program to study for master's degree in Petroleum Engineering in Norway at NTNU. He specialized in Drilling Engineering and he prepared his master's thesis on determination and detection of DLS and side force for stuck pipe prevention in inclined wellbore under the supervision of professor Pål Skalle from NTNU and Fred Mkuyi and Godwin Nsemwa from UDSM as co-supervisors. Joseph will be completing his master's degree in August 2019 and will officially graduate and be awarded his certificate in December 2019.

Joseph Nkengele

Determination of Dogleg Severity and Side Force for Stuck Pipe Prevention

NTNU
Norwegian University of
Science and Technology